



# VCU

Virginia Commonwealth University  
VCU Scholars Compass

---

Theses and Dissertations

Graduate School

---


2014

## Novel Therapeutic Strategies for Pancreatic Cancer

Bridget A. Quinn

*Virginia Commonwealth University*

Follow this and additional works at: <https://scholarscompass.vcu.edu/etd>

 Part of the [Medical Cell Biology Commons](#), [Medical Genetics Commons](#), [Neoplasms Commons](#), [Oncology Commons](#), and the [Translational Medical Research Commons](#)

© The Author

---

Downloaded from

<https://scholarscompass.vcu.edu/etd/4671>

This Dissertation is brought to you for free and open access by the Graduate School at VCU Scholars Compass. It has been accepted for inclusion in Theses and Dissertations by an authorized administrator of VCU Scholars Compass. For more information, please contact [libcompass@vcu.edu](mailto:libcompass@vcu.edu).

# **Novel Therapeutic Strategies for Pancreatic Cancer**

A dissertation submitted in partial fulfillment of the requirements for the degree of Doctor  
of Philosophy at Virginia Commonwealth University

by

Bridget A. Quinn

Bachelor of Science, Loyola University, Maryland

Advisor: Paul B. Fisher

Professor and Chairman  
Department of Human & Molecular Genetics  
Director  
VCU Institute of Molecular Medicine  
Thelma Newmeyer Corman  
Chair in Cancer Research  
VCU Massey Cancer Center

Virginia Commonwealth University

Richmond, Virginia

November 2014

## **Acknowledgements**

I would like to take the opportunity to thank all of the people who have supported me and contributed to the successful completion of this dissertation. I would like to first thank my PhD advisor and mentor, Dr. Paul B. Fisher, for the continued encouragement and willingness to push me to achieve my very best throughout my time in the lab. I appreciate him having high goals for me and supporting me in achieving them. I also would like to thank the other members of my committee, Drs. Luni Emdad, Jolene Windle, Joyce Lloyd, Steven Grant, Paul Dent, Charles Chalfant, and Devanand Sarkar, for their words of advice and willingness to help throughout the completion of this work. I am truly grateful for the time and support offered to me.

I would also very much like to thank my friends, particularly Chadia Robinson and Tim Kegelman, for constant encouragement and friendship. I am so grateful I was able to share this journey, the ups and the downs, with all of them.

Last, but certainly not least, I would like to thank my family, for loving and supporting me always. My parents, in-laws, and siblings have been incredible in helping me through this journey. A very special thank you must be said to my husband, Ken Abrams, for being my rock throughout the completion of this work. He stood by me every single day and was a constant source of love, encouragement, and positive energy. He listened to my talks and read my papers, escorted me to the lab at 2am for time-course experiments, and always told me how proud he was of me. I am so very grateful for him.

## **Dedication**

I would like to dedicate this dissertation to my Grandmother, Isabella T. Jiras (1930-2004), to whom I shared a very special relationship. She passed away after a long battle with breast cancer. She was my initial inspiration for choosing a career in oncology and continues to this day to be my constant motivation to keep learning and keep fighting.

## Table of Contents

Acknowledgements.....	ii
Dedication.....	iii
List of Figures.....	v
List of Abbreviations.....	ix
Abstract.....	xiii
<b>Chapter 1: Introduction.....</b>	<b>1</b>
I.    Pancreatic Cancer.....	1
II.   Pancreatic Cancer Therapy.....	1
III.  Genetics of Pancreatic Cancer.....	2
a.  Major Oncogenes and Tumor Suppressors.....	3
b.  Stat3.....	7
c.  Other important contributors.....	8
IV.  Apoptosis and The Bcl-2 family of proteins.....	11
V.   Mcl-1.....	16
a.  Role of Mcl-1 in Cancer.....	18
VI.  Strategies employed in targeting Mcl-1.....	21
i.  Deubiquitinase Inhibitors.....	23
ii. Antisense oligonucleotide (ASO) treatment.....	24
iii. BH3 Mimetics.....	25
VII. Functional Redundancy Among the Bcl-2 Family.....	29
<b>Chapter 2: Sabutoclax, a novel Bcl-2 family antagonist, and its role in pancreatic cancer treatment.....</b>	<b>31</b>
I.    Introduction.....	31
II.   Methods.....	33
III.  Results:.....	39
IV.  Discussion.....	79
<b>Chapter 3: Modified Gemcitabine for the treatment of Pancreatic Cancer.....</b>	<b>83</b>
I.    Introduction.....	83
II.   Methods.....	86
III.  Results:.....	89
IV.  Discussion.....	99

<b>Chapter 4: Characterization of a novel double transgenic pancreatic adenocarcinoma mouse, ‘PanMetView (PMV) Mouse,’ to non-invasively monitor tumor development and progression.....</b>	<b>102</b>
I.    Introduction.....	102
II.   Methods.....	108
III.  Results:.....	109
IV.  Discussion.....	125
<b>Chapter 5: Summary and Future Perspectives.....</b>	<b>128</b>
<b>References.....</b>	<b>136</b>

## List of Figures

Figure 1: Genetic Progression Model of Pancreatic Cancer.....	5
Figure 2: Proposed hypothetical models of the mechanism of action of the Bcl-2 family of proteins.....	15
Figure 3: Sabutoclax inhibits cell growth and induces apoptosis in pancreatic cancer cells.....	40
Figure 4: Sabutoclax inhibits cell growth and induces apoptosis in pancreatic cancer cells.....	41
Figure 5: Sabutoclax has greater efficacy than ABT-737.....	42
Figure 6: Sabutoclax causes a G1-S phase cell cycle arrest.....	44
Figure 7: Sabutoclax causes a G1-S phase cell cycle arrest.....	45-46
Figure 8. Sabutoclax causes a G1-S phase cell cycle arrest.....	47
Figure 9: Sabutoclax causes a G1-S phase cell cycle arrest.....	48
Figure 10: Pancreatic cancer cells exhibit varying levels of sensitivity to Minocycline.....	50
Figure 11: The combination of Sabutoclax and Minocycline produce synergistic cytotoxic effects.....	51
Figure 12: The combination of Sabutoclax and Minocycline produce synergistic cytotoxic effects.....	52
Figure 13: Sabutoclax and Minocycline show synergy.....	53
Figure 14: The cytotoxicity induced by Sabutoclax and Minocycline is caspase-dependent and dependent upon loss of Stat3 activation.....	55

Figure 15: Sabutoclax and Minocycline induce cytotoxicity in PANC-1 cells that is reversed with zVAD.....	56
Figure 16: Sabutoclax and Minocycline induce cytotoxicity in PANC-1 cells that is reversed with zVAD.....	57
Figure 17: The cytotoxicity induced by Sabutoclax and Minocycline is caspase-dependent and results in loss of Stat3 activation.....	60
Figure 18: The cytotoxicity induced by Sabutoclax and Minocycline is dependent upon loss of Stat3 activation.....	61
Figure 19: The cytotoxicity induced by Sabutoclax and Minocycline is dependent upon loss of Stat3 activation.....	62
Figure 20: The cytotoxicity induced by Sabutoclax and Minocycline works through the intrinsic pathways of apoptosis.....	64
Figure 21: Sabutoclax reduces tumor growth in a subcutaneous xenograft model and is enhanced by the addition of Minocycline.....	66
Figure 22: Sabutoclax and Minocycline reduce Stat3 activation <i>in vivo</i> .....	67
Figure 23: Sabutoclax and Minocycline reduce tumor growth in a subcutaneous xenograft model of pancreatic cancer.....	68
Figure 24: Sabutoclax and Minocycline reduce tumor growth in a quasi-orthotopic xenograft model.....	71
Figure 25: KPC tumors express Mcl-1 and KPC cell lines show sensitivity to Sabutoclax and Minocycline.....	73
Figure 26: Sabutoclax and Minocycline reduce tumor growth in a syngeneic KPC model.....	74

Figure 27: Sabutoclax and Minocycline reduce proliferation in a syngeneic KPC model.....	75
Figure 28: Sabutoclax and Minocycline reduce Stat3 activation in a syngeneic KPC model.....	76
Figure 29: Sabutoclax and Minocycline enhance survival in the KPC transgenic mouse model.....	78
Figure 30: Overview model showing therapeutic effects of Sabutoclax and Minocycline in PDAC.....	82
Figure 31: Pancreatic Cancer cells express EphA2.....	91
Figure 32 : YNH-Gemcitabine inhibits tumor growth in vivo to a greater extent as compared to Gemcitabine.....	92
Figure 33 : YNH-Gemcitabine inhibits tumor growth in vivo to a greater extent as compared to Gemcitabine.....	93
Figure 34: YNH-Gemcitabine prolongs survival in a xenograft model of pancreatic cancer.....	94
Figure 35: Gemcitabine (Gem) and Paclitaxel (PTX) inhibit tumor growth in vivo to a greater extent than either single drug.....	96
Figure 36: 123B9-PTX inhibits tumor growth <i>in vivo</i> to a greater extent than PTX. ....	97
Figure 37: 123B9+PTX+Gem inhibit tumor growth <i>in vivo</i> to a greater extent than other treatment combinations.....	98
Figure 38: Development strategy for the PMV Mouse.....	107



Figure 39: KPC mouse tumors highly express CCN1.....	111
Figure 40: Characterization of PMV Mouse #41 (p53 <sup>fl/fl</sup> ).....	113
Figure 41: Characterization of PMV Mouse #51 (p53 <sup>fl/fl</sup> ).....	115
Figure 42: Characterization of PMV Mouse #48 (p53 <sup>fl/wt</sup> ).....	116
Figure 43: Characterization of PMV Mouse #225 (p53 <sup>fl/fl</sup> ).....	117
Figure 44: Characterization of PMV Mouse #247 (p53 <sup>fl/fl</sup> ).....	118
Figure 45: Characterization of PMV Mouse #271 (p53 <sup>fl/fl</sup> )(female).....	120
Figure 46: Characterization of PMV Mouse #261 (p53 <sup>fl/fl</sup> )(female).....	121
Figure 47: Characterization of PMV Mouse #249 (p53 <sup>fl/fl</sup> )(female).....	122
Figure 48: PMV-derived cells retain luciferase activity <i>in vitro</i> and when reintroduced <i>in vivo</i> .....	124

## List of Abbreviations

$\alpha$	Alpha
$\beta$	Beta
m	Milli
n	Nano
$\mu$	Micro
5-FU	5-Fluorouracil
Apaf-1	Apoptotic protease activating factor 1
ASO	Antisense oligonucleotides
BLI	Bioluminescent imaging
Bcl-2	B-cell lymphoma 2
Bcl-xL	Bcl-2-like protein 1 (BCL2L1)
Bfl-1/A1	Bcl-2 related protein A1
BH	Bcl-2 homology domain
BH3	Bcl-2 homology domain 3
BRCA2	Breast cancer type 2, early onset
Cdk	Cyclin-dependent kinase
CLL	Chronic Lymphocytic Leukemia
CHO cells	Chinese hamster ovary cells
CI	Combination index
COX-2	Cyclooxygenase 2
cm	centimeter
CNS	Central nervous system
D	Aspartic acid
DMEM	Dulbecco's modified eagle medium
DMS	Dimethyl Sulfoxide
DNA	Deoxyribonucleic Acid

DUB.....Deubiquitinase  
 EMT.....Epithelial-mesenchymal transition  
 EphA2.....Ephrin type-A receptor 2  
 ER.....Endoplasmic reticulum  
 ERK..... Extracellular signal-regulated kinase  
 F.....Phenylalanine  
 FACS.....Fluorescence-Activated Cell Sorting  
 FBS.....Fetal Bovine Serum  
 FDA.....Food and Drug Administration  
 fl.....Floxed  
 G.....Glycine  
 Gem.....Gemcitabine  
 GEMM.....Genetically modified mouse model  
 GSK3.....Glycogen synthase kinase 3  
 H.....Histidine  
 HCC.....Hepatocellular carcinoma  
 hENT1.....Human equilibrative nucleoside transporter 1  
 IC50.....Half maximal inhibitory concentration  
 IHC.....Immunohistochemistry  
 i.p.....Intraperitoneal  
 JAK.....Janus kinase  
 KPC..... *K-ras*<sup>LSL-G12D</sup>/*p53*<sup>flox/wt</sup>/Pdx-1-Cre  
 K-ras.....Kirsten rat sarcoma viral oncogene homolog  
 LDH.....Lactate dehydrogenase  
 Luc.....Luciferase  
 M.....Molar  
 MAPK.....Mitogen-activated protein kinase

Mcl-1.....Myeloid cell leukemia 1  
mg/kg.....milligram/kilogram  
Mino.....Minocycline  
miR.....microRNA  
MOMP.....Mitochondrial outer membrane permeabilization  
MTT.....4,5-dimethylthiazol-2-yl)-2,5-diphenyltetrazolium bromide  
MULE.....Mcl-1 ubiquitin ligase E3  
N.....Asparagine  
PanIN.....Pancreatic intraepithelial neoplasia  
PARP.....Poly ADP ribose polymerase  
PBS.....Phosphate Buffered Saline  
PCNA.....Proliferating cell nuclear antigen  
PDAC..... Pancreatic Ductal Adenocarcinoma  
Pdx1.....Pancreatic and duodenal homeobox 1  
PEST sequence.....Proline Glutamic acid Serine Threonine sequence  
PI3K..... Phosphatidylinositol-3-kinase  
PBMV.....Pancreatic Biomarker Metastasis View  
PMV.....Pancreatic Metastasis View/PanMetView  
PTX.....Paclitaxel  
Rb.....Retinoblastoma gene  
RNA.....Ribonucleic acid  
Sab.....Sabutoclax  
SCLC.....Small Cell Lung Carcinoma  
SD.....Standard deviation  
SEAP.....Secreted alkaline phosphatase  
SH2.....Src homology domain 2  
siRNA.....Small interfering RNA

Stat3.....Signal transducer and activator of transcription 3  
TGF-B.....Transforming growth factor beta  
TNFR.....Tumor necrosis factor receptor  
USP9X.....Ubiquitin specific peptidase 9, X-linked  
UT.....Untreated  
VEGF.....Vascular endothelial growth factor  
WT.....Wild Type  
Y.....Tyrosine

## **Abstract**

A dissertation submitted in partial fulfillment of the requirements for the degree of Doctor of Philosophy at Virginia Commonwealth University

by

Bridget A. Quinn

Bachelor of Science, Loyola University, Maryland

Advisor: Paul B. Fisher

Professor and Chairman  
Department of Human & Molecular Genetics  
Director

VCU Institute of Molecular Medicine  
Thelma Newmeyer Corman  
Chair in Cancer Research  
VCU Massey Cancer Center  
Virginia Commonwealth University

Richmond, Virginia

November 2014

Pancreatic cancer is a devastating disease that leaves patients with a very poor prognosis and few therapeutic options. Many of the treatment options available are the same that have been used for almost 2 decades. There is a dire need for both novel treatments for this disease as well as novel strategies of treatment. This body of work will introduce and provide evidence in support of a novel combination therapy for pancreatic cancer treatment, a novel strategy of modifying currently used chemotherapeutics for pancreatic cancer therapy, and a novel transgenic preclinical mouse model of pancreatic cancer. Sabutoclax, an antagonist of the anti-apoptotic Bcl-

2 proteins, and Minocycline, a commonly used antibiotic, show potent synergy when used in combination in both pancreatic cancer cells and in multiple immune-deficient and immune-competent mouse models of pancreatic cancer. Sabutoclax alone is capable of inducing cell cycle arrest and apoptosis in cells and its cytotoxicity is enhanced significantly when combined with Minocycline. This combination results in the loss of Stat3 activation both *in vitro* and *in vivo*, which is essential for its toxicity. It also inhibits tumor growth and prolongs survival in the KPC transgenic mouse model of pancreatic cancer. Also presented here are studies that demonstrate efficacy *in vivo* of modified versions of Gemcitabine and Paclitaxel. These drugs are linked to a peptide that shows specificity for the EphA2 receptor, which is overexpressed on the surface of pancreatic cancer cells and only minimally on normal cells. This peptide results in increased cellular uptake of drug, as it is bypassing its normal mechanism of entry. These normal mechanisms are often dysregulated in cancer, leading to decreased uptake and drug resistance. The use of these modified drugs show significantly increased tumor growth inhibition as compared to the parent drug alone. Finally, we provide data on the characterization of a novel transgenic mouse model of pancreatic cancer. This model, the Pan Met View (PMV) mouse, combines the commonly used KPC transgenic mouse model of pancreatic cancer and a mouse that expresses a Luciferase reporter gene under the control of the cancer-specific promoter, CCN1. Our data shows that double transgenic PMV mice can now be used to follow primary tumor and metastasis development in real time by Bioluminescent imaging (BLI) through disease progression and potentially therapy. This strategy will enhance the use of genetically engineered mouse models (GEMMS) to study cancer initiation and

progression with potential to non-invasively monitor therapy. These chapters present novel and exciting data that have the potential to open multiple avenues of translational study and result in significant advances in pancreatic cancer therapy.



## **Chapter 1: Introduction**

### **I. Pancreatic Cancer**

Pancreatic ductal adenocarcinoma (PDAC) is an extremely aggressive cancer that is estimated to result in over 39,000 deaths in the US in 2014 (NCI 2014). It is currently the fourth most commonly diagnosed cancer and holds a 5-year survival rate of about 4% (1). This poor prognosis results, in part, from a delayed diagnosis of the disease. Patients experience few symptoms and those that they may experience tend to be vague in nature. Abdominal pain, depression, weight loss, and loss of appetite are all commonly seen, though they are often overlooked until they become chronic issues. Jaundice can be a symptom of pancreatic head tumors, which is much more telling of a significant underlying problem. The consequence of this clinical presentation is that most patients have either locally advanced or metastatic disease at the time of diagnosis. Risk factors for pancreatic cancer include a history of smoking, diabetes, chronic pancreatitis, and some inherited genetic mutations/familial diseases (2).

### **II. Pancreatic Cancer Therapy**

Unfortunately, treatment options remain minimal for patients diagnosed with this aggressive disease. Surgical resection is the only potentially curative treatment, but, due to delayed diagnosis, is only an option for approximately 15% of patients (2). Because of the anatomical location of the pancreas, even tumors discovered before

metastatic spread are usually not resectable. Significant involvement of the tumor with surrounding vital organs and vessels, such as the celiac trunk, superior mesenteric artery/vein, and the hepatic artery, eliminate its ability to be surgically removed (2). This tumor involvement, which can often eventually encase organs or vessels entirely, can often be a primary cause of death in these patients, a result of the rupture of vessels or impairment of normal function.

Chemotherapy remains the most utilized option for patients with pancreatic cancer, though outcomes are still poor. Gemcitabine remains the standard of care, even though it has been almost 2 decades since it was established to have a prolonged survival benefit as compared to Fluorouracil (3). Despite this, Fluorouracil is still used in treatment regimens, as well as a number of novel combination therapies. Folfirinox, a combination of fluorouracil, irinotecan, oxaliplatin, and leucovorin, has been shown to improve survival in patients with metastatic disease and is now being evaluated in patients with locally advanced tumors. Additionally, the combination of Gemcitabine and nab-Paclitaxel (Abraxane) was also recently approved by the FDA for the treatment of metastatic pancreatic cancer after clinical trials showed significant survival advantages. These two combination therapies are now considered standard of care for patients with metastatic disease. Though radiotherapy is often incorporated into some treatment regimens and clinical trials, data regarding its efficacy remains somewhat controversial (2).

### **III. Genetics of Pancreatic Cancer**

The aggressive nature of the cancer and the resulting dismal prognosis for patients results, in part, from the vast array of molecular changes that occur during the development of pancreatic adenocarcinoma. Pancreatic tumors are known to be chemoresistant as well and this resistance to therapy is often due to the many different genetic changes seen in pancreatic tumors.

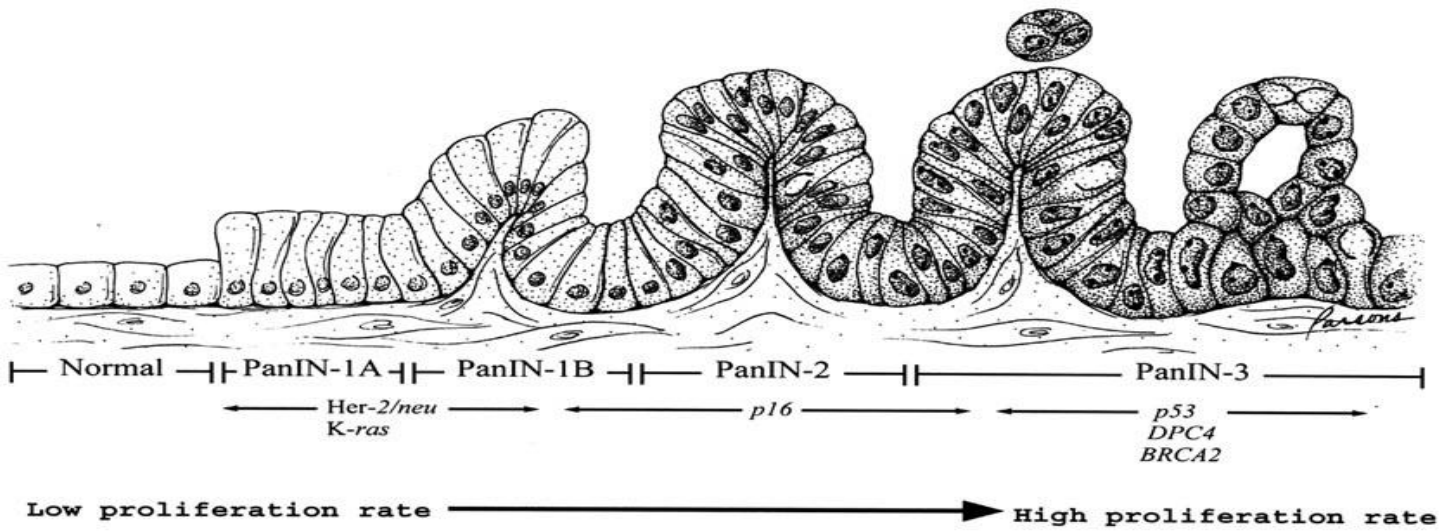
The development of a pancreatic adenocarcinoma follows a sequence of histological changes that turns a normal pancreatic epithelium into an invasive pancreatic adenocarcinoma. This process has been classified into a series of pre-invasive stages referred to as pancreatic intraepithelial neoplasia (PanIN) lesions (Figure 1). These dysplastic ductal lesions range in number from PanIN I (low-grade lesion to PanIN 3 (high grade lesion or pancreatic ductal adenocarcinoma in situ).

These progressive histological changes occur as the result of parallel underlying molecular changes. It is these molecular changes that ultimately result in an invasive pancreatic adenocarcinoma. It is also important to note that these changes occur at fairly specific time points throughout this progressive model and in a particular order. Additionally, not all pancreatic cancers will have the exact same molecular changes, further contributing to its inherent aggressive and chemoresistant nature. Different tumors will often have different combinations of genetic mutations, chromosomal losses, etc. This is why finding therapy to treat pancreatic cancers as a group remains so difficult. Despite the vast number of potential molecular changes, there are a few that occur in a large number of pancreatic cancer cases.

### **A. Major Oncogenes and Tumor Suppressors**

One of the very first changes that occur in a normal pancreatic epithelial cell is the mutation of *K-ras*. *K-ras* is part of the Ras family of proteins that is involved in signal transduction through the MAPK and PI3K/Akt pathways. *K-ras* is mutated in over 90% of pancreatic cancers and primarily responsible for the initial transformation event in normal cells. This mutation has been seen in codons 12, 13, and 61, with codon 12 being the most frequently seen site for *K-ras* mutations (4). This oncogenic, early event results in constitutive activation of *K-ras* and is seen in PanIN 1 lesions through to invasive carcinoma. *K-ras* mutation is seen in approximately 36% of PanIN-1A lesions, 44% of PanIN-1B lesions, and 87% of PanIN 2-3 lesions (5). It should also be noted that pancreatic adenocarcinomas that arise in a patients with chronic pancreatitis tend to have lower frequencies of *K-ras* mutations, though the reason is not entirely clear (4).

*In vitro* and *in vivo* studies have confirmed *K-ras* mutation as an early and initiating event in the development of PDAC. Mouse models developed that express mutant *K-ras* in the pancreas result in the generation of ductal lesions resembling PanIN lesions (6).



### Progression Model of Pancreatic Cancer

Figure 1: Genetic Progression Model of Pancreatic Cancer. Adapted from (7).

One of the next changes often seen affects the gene encoding p16, CDKN2A/INK4A. p16 is a cell cycle checkpoint protein and can initiate G1-S phase arrest. It is a very important protein in normal cell cycle function and is lost in around 90% of pancreatic cancer cases. Though p16 is lost in the majority of PDAC cases, the mechanism of its loss is not always the same. Possible mechanisms of p16 loss include homozygous deletion of the CDKN2A/INK4A gene, intragenic mutation plus the loss of the 2<sup>nd</sup> allele, and epigenetic silencing through promoter methylation (4). Loss of p16 is considered a fairly early to intermediate event in the development of PDAC. Around 30% of PanIN-1A and 1B lesions, 55% of PanIN 2 and 71% of PanIN 3 lesions show loss of p16 (4). Additionally, as seen with K-ras mutations, the frequency of loss of this tumor suppressor is decreased in cancer cases resulting from chronic pancreatitis.

The next big molecular event seen in the progression to PDAC is the inactivation of the TP53 gene. p53 function is lost in approximately 50-75% of pancreatic adenocarcinomas and occurs much later in PDAC development, with changes in p53 not usually seen until the stage of a PanIN-3 lesion. It is normally involved in cell cycle regulation and loss of it results in inappropriate cell cycle progression. It is also thought to contribute to the overall genomic instability seen in pancreatic cancer. In the majority of cases, p53 function is lost through intragenic mutation of one allele and loss of the second.

Another late event that occurs in PDAC development is the loss of the DPC4/SMAD4/MADH4 gene. The SMAD4 protein is involved in signal transduction downstream of TGF- $\beta$  and plays a role in growth inhibition. Loss of this tumor

suppressor gene therefore results in uncontrolled proliferation. This gene is lost in 50-90% of pancreatic cancers (8). SMAD4 is expressed in lower and intermediate stage PanIN lesions and lost in 31-41% of PanIN-3 lesions, supporting this as a later occurring event (4).

These four changes are the most significant and frequent molecular events seen in the development of pancreatic adenocarcinoma. Animal models developed by different groups have shown that combinations of *K-ras* mutations and loss of these tumor suppressor genes result in the development of a pancreatic adenocarcinoma in mice that closely resembles human PDAC (9).

## **B. Stat3**

Stat3 is a transcription factor that is a part of a large family of signal transducer and activator of transcription (STAT) proteins. This family consists of seven proteins and they each carry six conserved protein domains. These domains consist of a tetramerization domain, a N-terminal coil-coil domain, a DNA-binding domain, a linker domain, a SH2 domain, and a C-terminal transactivation domain (10). These domains play important roles in the normal function of Stat3 and can have clinical implications as well.

In a normal cell, Stat3 resides predominantly in the cytoplasm. When ligand binding activates tyrosine receptor kinases, they dimerize and undergo transphosphorylation. This activates a series of phosphorylation steps that can involve a variety of different intracellular kinases. These phosphorylations lead to the recruitment of proteins that are involved in signal transduction pathways. Stat3 is one

such protein. It gets recruited to the receptor complex via its SH2 domain and then it becomes phosphorylated (11). Stat3 has a tyrosine residue at position 705 and a serine residue at position 727, both of which can be phosphorylated. In most cases, it is a tyrosine kinase involved in this process and, as a result, tyrosine 705 of Stat3 is usually the phosphorylation site involved in this protein's activation. While multiple kinases are able to phosphorylate and subsequently activate Stat3, most times it is the JAK family of kinases that carry out this job (12).

Once Stat3 is phosphorylated, it forms a dimer with another Stat3 monomer through the binding of the phosphorylated tyrosine of one monomer to the SH2 domain of the second. This forms an active Stat3 dimer. This dimer is now able to translocate into the nucleus, where it functions as a transcription factor, binding DNA and regulating gene expression of its targets (10).

As a transcription factor, Stat3 can regulate the expression of its transcriptional targets. It is through the regulation of these targets that Stat3 can be responsible for the cancer supporting phenotype seen when it becomes constitutively active. Many of the transcriptional targets of Stat3 play pro-survival roles in the cell and, when Stat3 signaling goes unregulated, these targets become active players in cancer development. Some of these targets are important specifically in pancreatic cancer and include (but are not limited to) the antiapoptotic members of the Bcl-2 family, Cyclin D1, and VEGF (13).

Targeting Stat3 in pancreatic cancer has further shown the importance of this protein in this disease. Yang, et. al. showed that knocking down Stat3 via lentivirus



mediated RNAi in a pancreatic cancer cell line resulted in decreased cell growth, decreased expression of VEGF and MMP-2, and decreased invasive abilities in an in-vitro invasion assay (Yang, G. et. al. 2009). Lewis, et. al. utilized a different approach by developing oligonucleotides complementary to binding sequences of Stat3. They showed that these oligos were able to induce apoptosis in a pancreatic cancer cell line and that they could decrease expression of Stat3 target CD46. CD46 is a protein that can protect tumor cells from complement-mediated cytotoxicity (Lewis, HD, et. al. 2008).

These two methods target Stat3 expression and activity. Other methods, such as the development of peptide inhibitors and small molecule inhibitors, take a look at the activation of the Stat3 monomer and use this process to develop inhibitors. As mentioned previously, activated Stat3 monomers form dimers via their SH2 protein domains. It is this dimer that can translocate to the nucleus and carry out its transcriptional function. A strategy in targeting Stat3 has been to develop inhibitors that bind to this SH2 domain, prohibiting it from binding to another Stat3 monomer and forming a functional dimer.

This was first accomplished by Turkson, et. al. This group created the peptide, PY\*LKTK (Y\* = a phosphorylated tyrosine), that bound to the SH2 domain of a Stat3 monomer. However, like many firsts, this peptide did not exhibit good efficacy and required high doses to achieve results (Turkson, J. et. al. 2001). Further derivatives were developed by multiple groups, but, as with many peptide inhibitors, the polarity of them and the transient nature of the phosphate groups resulted in problems (Haftchenary, S. et. al. 2011). Ge, et. al. tried to address this problem by developing an unnatural amino acid meant to replace the phosphorylated tyrosine. In this amino acid,

the phosphate group was replaced by an isoxazole carboxylic acid moiety. The compound made with this new amino acid, ISS610, was a tripeptide that was shown to have moderate inhibitory effects against the SH2 domain of Stat3 and improved cell permeability (Ge, J. et. al. 2010).

Many of the small molecule inhibitors of Stat3 aim to function in the same way as the peptide inhibitors, by targeting the SH2 domain of Stat3 and preventing dimerization. However, small molecule inhibitors often have much greater efficacy than peptide inhibitors due to their more advantageous physiological properties. For example, small molecule inhibitors are able to rapidly diffuse through cell membranes, a property not exhibited by peptide inhibitors. Though there have been many Stat3 small molecule inhibitors developed, those discussed here will focus on two that have been studied in the context of pancreatic cancer, LLL12 and Cucurbitacin.

LLL12 was developed by Lin, et. al. via a structural based approach. It has been shown to bind directly to phosphorylated tyrosine 705 and exert a variety of inhibitory effects on cancer, but not on normal, cells. In pancreatic cell lines, LLL12 was shown to reduce Stat3 DNA binding, induce apoptosis, and decrease mRNA and protein expression of Stat3 targets CyclinD1, Survivin, and Bcl-2 family anti-apoptotic proteins. Additionally, it showed synergy with Gemcitabine, the current first line treatment for pancreatic cancer (Lin, L. et. al. 2010).

Cucurbitacin, unlike LLL12 and other Stat3 small molecule inhibitors, functions by targeting the JAK family of kinases. Inhibition of these proteins blocks Stat3 activation at the level of the receptor complex (Jing, N. et. al. 2005). Zhang, M. et. al. examined

the effect of Cucurbitacin B in pancreatic cancer. This group found that in addition to decreasing Stat3 activation, this compound inhibited pancreatic cancer cell growth, induced apoptosis, increased p21 levels, and decreased Stat3 targets Bcl-2 and survivin (Zhang, M. et. al. 2010).

### **C. Other Genetic Alterations**

As mentioned earlier, the aggressive nature of this cancer is due to the vast number of molecular events that occur in its development. In addition to the major genetic changes seen, there are many other alterations that occur during the development of this cancer. Examples of these include overexpression of the HER-2/NEU/ERBB2 gene, mutation of the BRCA2 gene and upregulation of the proteins Cyclin D1 and COX-2.

Overexpression of the HER-2/NEU gene is something that sometimes occurs as an early event in the development of PDAC. Reports vary as to what percentage of pancreatic cancers exhibit overexpression and range from 7-82% (14). Overexpression and therefore activation of this oncogene leads to constant proliferative signals through a multitude of pathways.

Another late event in PDAC development is mutation of the BRCA2 gene. BRCA2 is involved in DNA damage repair in cells, and loss of the normal function of the associated protein results in accumulation of DNA damage in cells. BRCA2 is mostly associated with inherited pancreatic cancer cases. Germline BRCA2 mutations predispose patients to pancreatic cancer, increasing their lifetime risk by 5-10% (15).

Despite this, there are cases of sporadic pancreatic cancer with BRCA2 mutations. Around 7-10% of pancreatic cancer cases are found to have a germline BRCA2 mutation, some of which were thought to be sporadic (4).

Cyclin D1 is another protein often overexpressed in pancreatic cancer. Cyclin D1 functions normally as part of the cell cycle in conjunction with cyclin-dependent kinases 4 and 6. Together, these proteins inactivate the retinoblastoma gene (Rb), an inhibitor of cell cycle progression, and encourage the cell cycle to proceed. Overexpression of CyclinD1, therefore, accelerates cell cycle progression. Nuclear overexpression is seen in around 33% of PanIN-2 lesions, over 50% of PanIN-3 lesions, and in between 60-80% of invasive PDAC (4). Importantly, cyclin D1 overexpression has been correlated with decreased survival in patients with pancreatic ductal adenocarcinoma (16).

Well known for its role in inflammation, Cox-2 also can be involved in the development of cancer. One study found Cox-2 to be overexpressed by immunohistochemistry in between 69 and 81% of pancreatic tumors (17). It is also increasingly expressed as lesion progresses from a PanIN-1 lesion to a PanIN-3 lesion (4).

Changes in some of genes/proteins already discussed can lead to activation of not only the individual protein, but of whole pathways as well. *K-ras* is an example of this. Interestingly, activation of some other pathways seen in pancreatic cancer includes a few normally involved in embryological signaling. The Hedgehog and Notch signaling pathways are actively involved in embryological development of different organs and are usually turned off in adult tissues. However, in pancreatic cancer, there

is evidence of activation of the components of these pathways, as well as some of their targets, like the Hes1 gene of the Notch pathway (4). As their embryological function involved regulation of cell differentiation, this activation may play a role in the abnormal differentiation and transformation seen in invasive pancreatic cancer (18).

As in many types of cancer, there is a large degree of genomic instability seen both throughout the PanIN stages and in pancreatic adenocarcinoma. The result is many chromosomal abnormalities, both numerical and structural. Loss of chromosomal material can lead to some of the changes discussed above, such as loss of the DPC4/SMAD4/MADH4 gene, which is located on frequently lost locus 18q21 (15). It is important to remember that the molecular events leading to the development of pancreatic adenocarcinoma are not necessarily isolated events and that they often represent underlying overall instability in the genome.

As mentioned previously, this genomic instability is an early event, seen in low grade PanIN lesions. Evidence of this at that stage is made apparent by shortening of telomeres seen in over 90% of PanIN lesions (4). It is thought that this early loss of telomere length initiates a state of genomic instability by leaving chromosomes vulnerable and sets the stage for future molecular events to occur.

In general, changes in *K-ras*, p53, INK4A, and SMAD4 provide a solid base for the transformation of a normal pancreatic epithelial cell into an invasive pancreatic adenocarcinoma. It is clear, however, that these changes do not solely contribute to PDAC development and that there is a vast array of molecular events that can occur in different combinations to produce an invasive cancer. The additional examples

discussed above (only a representative sample of the vast number of possible molecular changes) show how different the normal functions of these proteins can be and illustrate how the changes that contribute to PDAC development are very much widespread across the genome. Despite some of their differences of origin or function, they often work synergistically to encourage cancer development.

The correct sequence of these changes plays an important role as well. An early oncogenic mutation of *K-ras* helps to start the push of proliferative pressure on a cell. The loss of gatekeeper tumor suppressors later in development relieves any final hold on the growth of the progressing cancer. These timed events are important and, with the addition of all of the other potential molecular changes, result in the development of an invasive cancer that is aggressive, nearly impossible to treat, and ultimately and unfortunately, fatal.

#### **IV. Apoptosis and the Bcl-2 family of proteins**

Apoptosis is a biological process that is integral to normal physiological functions and maintenance of homeostasis in an organism. The cell's ability to undergo apoptosis is a consequence of a vast array of complex cellular processes that involve multiple proteins. Apoptosis can occur through two distinct, but interrelated, pathways: the extrinsic pathway of apoptosis or the intrinsic/mitochondrial pathway of apoptosis (Figure 1). The extrinsic pathway involves activation of cell surface death receptors (Fas, TNFR) by extracellular ligands such as FasL or TNF. Activation of any of the death receptors results in cleavage and activation of caspase-8, leading to a signaling cascade that culminates in death of the cell. The intrinsic pathway, which can be initiated by a variety of stress signals, involves permeabilization of the outer membrane

of the mitochondria, which leads to cytochrome c release. Once released, cytochrome c binds to Apaf-1 and forms the apoptosome, which results in cleavage and activation of caspase-9 and, ultimately, cell death (19). This mitochondrial pathway is controlled primarily by the complex interactions of the Bcl-2 family of proteins.

Bcl-2 is the founding member of this family of proteins and was discovered in studies of B-cell lymphoma. The proteins in this family share certain sequence homology via the presence of Bcl-2 homology (BH) domains. There are four BH domains that exist in this family and each member has at least one. The family is divided into two groups: one group that has pro-apoptotic effects and one group that has anti-apoptotic effects. The pro-apoptotic group is further divided into two subgroups: one group containing proteins such as Bax and Bak and a second group containing proteins including Noxa, PUMA, Bim, and Bid. The latter group is often referred to as the BH3 only proteins, as the members of this subgroup share sequence similarity to the rest of the family only through their BH3 domain. The anti-apoptotic group includes the proteins Bcl-2, Mcl-1, Bcl-X<sub>L</sub>, Bfl-1/A1 and Bcl-w (20).

Apoptosis through the intrinsic pathway is imminent when mitochondrial outer membrane permeabilization (MOMP) occurs. This process arises as the result of the formation of homo/heterodimers of the pro-apoptotic proteins Bax and Bak. The other two groups of proteins in this family ultimately regulate apoptosis by either promoting or inhibiting this dimerization. The Bcl-2 family of proteins does this through physical interactions with each other. Two different models have been proposed to describe precisely how this process might occur (Figure 2).

The first scheme is an 'indirect activation model'. In this model, the anti-apoptotic proteins bind to Bax/Bak and block dimerization. The BH3 only proteins exert their pro-apoptotic actions by binding to the anti-apoptotic proteins, thereby displacing Bax and Bak. Free Bax and Bak are now free to form dimers resulting in MOMP. The second theory is a 'direct activation model' that is somewhat more complicated. In this model, the BH3 only proteins are divided into sensitizer and activator proteins. In this model, Bax/Bak oligomerization occurs when the activator BH3 only proteins bind to and activate Bax/Bak. The goal of the anti-apoptotic proteins is to bind the activator proteins and prevent them from binding and activating Bax/Bak. Accordingly, the sensitizer BH3 only proteins bind the anti-apoptotic proteins and prevent them from interacting with the activator BH3 only proteins (21). Ultimately, it is likely that these two models may both occur, since apoptosis regulation is all about balance. At a given point in the life of a cell, the ratio of pro-apoptotic to anti-apoptotic proteins dictates whether the cell will survive or undergo apoptosis. When the pro-apoptotic proteins are expressed in greater quantity, the balance is pushed toward apoptosis. However, when the ratio favors the anti-apoptotic proteins, cell survival will be the net consequence.



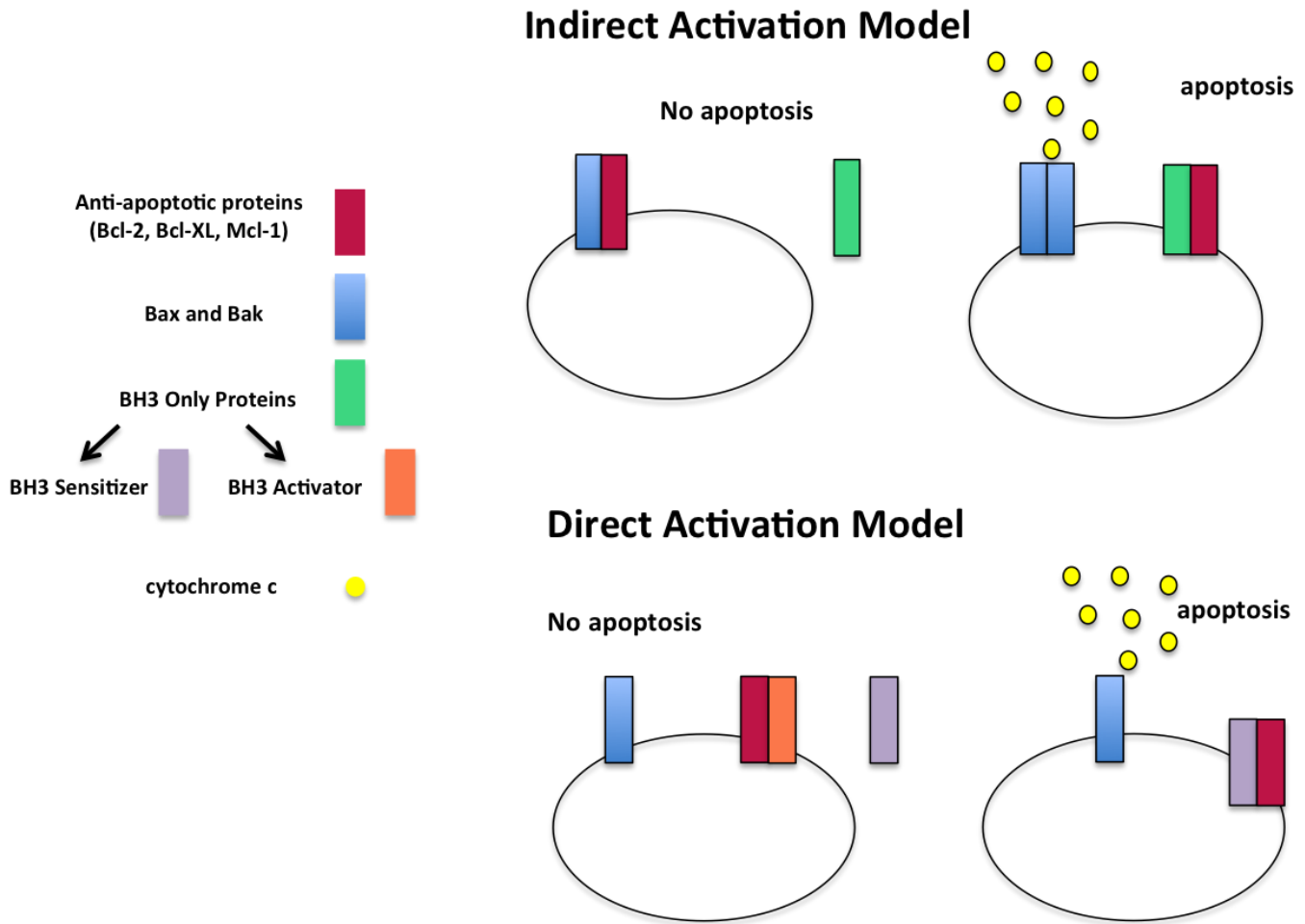


**Figure 2: Two proposed hypothetical models of the mechanism of action of the Bcl-2 family of proteins.** The “indirect activation model” describes a scenario in which the binding of anti-apoptotic proteins inhibits Bax/Bak oligomerization. Displacement of these anti-apoptotic proteins by a BH3 only protein allows dimers to form and apoptosis to occur. In contrast, the “direct activation model” holds that BH3 only proteins are divided into two classes: activators and sensitizers. The activator proteins bind to Bax or Bak, activating them and leading to apoptosis. The anti-apoptotic proteins function in this model by binding to these activator and sensitizing proteins and sequestering them. The BH3 only sensitizers bind to anti-apoptotic proteins in an attempt to displace the activator BH3 proteins. When enough activator BH3 proteins are free, they are able to activate Bax/Bak and induce apoptosis.

## V. Mcl-1 (myeloid cell leukemia-1)

Mcl-1 was the second member of the Bcl-2 family discovered. Kozopas *et al.* (22) were investigating the human myeloid leukemia cell line, ML-1. Their goal was to differentiate ML-1 cells into monocytes/macrophages and identify genes whose expression was increased during this differentiation process. One of the early induction genes identified through this strategy was named Mcl-1 (myeloid cell leukemia-1) and was shown to have sequence similarity to the previously identified protein, Bcl-2. Based on this similarity and its mode of isolation, Mcl-1 was predicted to play significant roles in cell differentiation and death (22). Future studies showed that c-myc-induced apoptosis in CHO cells was delayed by Mcl-1 overexpression, illustrating that Mcl-1 indeed contributed to the regulation of the cell death process (23).

Since its discovery in 1992, studies of Mcl-1 have revealed this to be an intriguing protein, which performs a fundamental role in cell physiology. Mcl-1 is an anti-apoptotic member of the Bcl-2 family of proteins and contains three BH domains. This is unlike the other anti-apoptotic members, which contain four BH domains. Despite this fact, it is the largest of the proteins, containing 350 amino acid residues (24). Mcl-1 is also different than other pro-survival proteins due to its N-terminus, which is larger than that of other Bcl-2 family proteins and has been shown to affect Mcl-1's function and localization (25). It also contains two proline (P), glutamic acid (E), serine (S), and threonine (T) (PEST) sequences (22) which may account for its relatively short half life (i.e., 2-3 hr), as these regions have been shown to target proteins for degradation (26).

The structural differences seen between Mcl-1 and the other prosurvival Bcl-2 proteins account for some of the differences seen in binding partners among these

proteins. The anti-apoptotic proteins all generally function in the same way as described above, but the pro-apoptotic proteins with which they specifically interact differ. For example, Mcl-1 binds with high affinity to the BH3-only protein Noxa, but does not bind to Bad. In contrast, Bcl-2 binds well with Bad, but not as well with Noxa (24).

Mcl-1 retains an alpha helical fold, similar to the other proteins, but differs in the exposed surface of its binding groove. In addition to simply having different residues, this groove is more electropositive than the other anti-apoptotic proteins. It is flanked on either side by positive electrostatic potential and contains multiple histidine residues. Proteins like Bcl-X<sub>L</sub>, however, have grooves that are almost completely uncharged. Furthermore, there are differences in the positions of some surface helices of Mcl-1, adding to the differences between this protein and its other family members (27). These structural differences become very important in the development of inhibitors of these proteins.

Mcl-1 is regulated at multiple levels, including transcriptional and translational. Transcriptionally, Mcl-1 expression can be induced by a variety of cytokines and signaling pathways, including the PI3K/AKT, Stat-3, and p38/MAPK pathways (28). Additionally, alternative splicing of Mcl-1 results in two protein isoforms, Mcl-1<sub>L</sub> and Mcl-1<sub>s</sub>. Interestingly, the Mcl-1<sub>s</sub> isoform behaves in a manner opposite to that of the normal protein, functioning to promote apoptosis, much like the BH3 only proteins (29). At the translational level, many studies have highlighted the role of microRNAs in Mcl-1 regulation. Mott *et al.* (30) identified mir29b as targeting Mcl-1 in studies comparing

cholangiocarcinoma cells to normal cholangiocytes. Additional studies have implicated this microRNA in Mcl-1 regulation in other cell types as well (31,32).

Mcl-1 also contains multiple phosphorylation sites in its PEST region. Multiple proteins resulting in different outcomes mediate the phosphorylation of these sites. Thr<sup>163</sup> can be phosphorylated by ERK leading to the increased half-life of the protein (33). Conversely, GSK-3 mediated phosphorylation of Ser<sup>159</sup> leads to increased ubiquitination and degradation of Mcl-1 (34). As previously noted, Mcl-1 has a very short half-life. This is due to its rapid degradation in the cell, primarily through the proteasome. Proteasome-mediated degradation of Mcl-1 can occur through a variety of mechanisms, GSK-3-mediated phosphorylation representing the most highly investigated of these. Mcl-1 Ubiquitin Ligase E3 (MULE) has been shown to ubiquitinate Mcl-1 on 5 different lysine residues and to be the primary mediator of normal Mcl-1 degradation (35). Additionally, Mcl-1 can be targeted for degradation through interactions with additional proteins such as Noxa and the tumor suppressor SCF<sup>FBW7</sup> (28,36).

#### **A. Role of Mcl-1 in Cancer**

Mcl-1 is highly expressed in a variety of human cancer cell lines including breast, CNS, colon, lung, ovarian, prostate, renal, and melanoma (Table 1)(37). Human melanoma cell lines express Mcl-1, though they do not show increased expression when compared to normal melanocyte controls. However, studies done in paraffin sections of benign nevi, primary melanoma, and metastatic melanoma showed an increase in Mcl-1 expression that correlated with melanoma progression (38,39).

Mcl-1 overexpression is exploited by cancer cells to evade cell death, i.e. to survive, and as a mechanism for developing resistance to diverse chemotherapeutic agents. The other anti-apoptotic members of the Bcl-2 family of proteins are also frequently overexpressed in cancers, although they will not be discussed in this review. Although overexpression of Mcl-1 does not result in increased cell proliferation, its ability to suppress apoptosis is an important contributor to the transformed state. As noted earlier, apoptosis regulation is based on the balance between pro- and anti-apoptotic proteins within cells. The ability of a cancer cell to shift the balance toward survival provides it with a major advantage in protecting itself from toxic factors. The clinical implications of this phenomenon may be manifested by chemoresistance. For example, while chemotherapeutic agents operate through a variety of mechanisms, many of them are believed to act through initiation of apoptosis in a cell. Consequently, protection from apoptosis via overexpression of Mcl-1 may represent a significant barrier to the effectiveness of chemotherapeutic agents.

Dysregulation of Mcl-1 is an important genomic change in diverse cancers, many of which become dependent upon this protein for survival as well as resistance to chemotherapy. Indeed, numerous reports have documented the importance of this protein in transformed cell survival. Thallinger *et al.* (40) reported that Mcl-1 antisense oligonucleotides (ASO) resulted in decreased Mcl-1 expression in cell lines *in vitro* and in tumors *in vivo*, and that Mcl-1 ASO treatment given by paraspinal infusion of SCID mice with melanoma subcutaneous tumors resulted in tumor sensitization to the chemotherapeutic drug, DTIC, accompanied by increased levels of apoptosis in tumor cells (40). In a study of head and neck cancer, twenty-six tumor samples from patients

with locally advanced head and neck cancer showed a 92% increase in Mcl-1 expression (41). Transfection of Mcl-1 ASO in a head and neck squamous cell carcinoma cell line promoted cytotoxic synergy when combined with chemotherapeutic agents, Paclitaxel and Cetuximab (42). Additionally, Mcl-1 is overexpressed in hepatocellular carcinoma (HCC). Sieghart *et al.* (43) showed that human tumor specimens overexpressed Mcl-1. They went on to show that the use of Mcl-1 ASO induced apoptosis in HCC cells and sensitized them to cisplatin (43). Additionally, Mcl-1 ASO decreased cell viability and induced apoptosis in multiple human myeloma cell lines as well as two primary myeloma cell lines. This result was not seen following Bcl-2 or Bcl-X<sub>L</sub> ASO treatment (44). Pancreatic adenocarcinoma is another cancer that overexpresses Mcl-1. Studies have shown that knockdown of Mcl-1 in a pancreatic cancer cell line leads to decreased cell viability and colony formation *in vitro* and decreased tumor size and weight in xenograft models. Furthermore, loss of Mcl-1 sensitized these resistant cells to the current first line treatment for pancreatic cancer, Gemcitabine (45).

Mcl-1 has been shown to play important roles in lymphomas and leukemias as well. In mantle cell lymphoma, Mcl-1 overexpression correlated with high-grade morphology, high levels of proliferation, and p53 overexpression (46). Additionally, mice expressing a Mcl-1 transgene were shown to develop B cell lymphomas at a frequency of 85% over a period of 2 years (47). In both acute and chronic leukemias, Mcl-1 has been demonstrated to be extremely important for cancer survival, with siRNA knockdown of Mcl-1 leading to apoptosis in cell lines. Furthermore, patients who show resistance to Rituximab, an anti-CD20 antibody used to treat B-cell malignancies,

exhibit increased levels of Mcl-1. Mcl-1 knockdown has also been demonstrated to sensitize cells to Rituximab treatment (48).

## **VI. Strategies employed in targeting Mcl-1**

There have been numerous approaches designed to target Mcl-1. Some of these schemes focus primarily on Mcl-1, but the majority of strategies target multiple anti-apoptotic proteins in the Bcl-2 family. Here we review the most significant inhibitors developed to date.

### **A. Drugs that result in Mcl-1 Downregulation**

There are multiple drugs that, despite not being designed to specifically target Mcl-1, display a mechanism of action that involves downregulation of Mcl-1. Studies with these drugs provide continued evidence of the importance of this protein in maintenance and progression of the cancer phenotype.

#### **1. Cyclin-dependent kinase inhibitors**

##### **Flavopiridol**

Flavopiridol is a semisynthetic flavonoid that functions as a cyclin-dependent kinase inhibitor by competing for the kinase active site. It is able to inhibit the activity of multiple CDKs and results in G<sub>1</sub>/S and G<sub>2</sub>/S cell cycle arrest (49). Flavopiridol also globally decreases transcription levels in the cell *via* inhibition of P-TEFb and it can also bind double stranded DNA (50). However, one of the more interesting observations seen with Flavopiridol was its ability to downregulate Mcl-1 protein levels in B-cell chronic lymphocytic leukemia cells (51). Notably, significant activity was observed in

patients with high-risk CLL treated with a hybrid infusional flavopiridol schedule. This new dosing regimen included a 30-minute loading dose prior to 4 hours of infusion given weekly for 4-6 weeks. A group of 42 patients with refractory CLL were studied and of those 42, 45% showed a partial response. Importantly, genetically high-risk patients with del(17p13.1) showed a 42% response rate and those with del(11q22.3) a 72% response rate (52).

Further studies in breast cancer showed that Flavopiridol treatment synergistically enhanced the toxicity of the ERBB1/ERBB2 inhibitor Lapatinib in a Mcl-1-dependent manner. The combination of Lapatinib and Flavopiridol increased the rate of reduction of Mcl-1 protein compared to Flavopiridol alone. Moreover, overexpression of Mcl-1 induced resistance to this combination (53). In studies involving human leukemia cells, Flavopiridol interacted synergistically with the HDAC inhibitor Vorinostat through a mechanism involving Mcl-1 down-regulation (54).

Flavopiridol is the first cyclin-dependent kinase inhibitor to enter clinical trials. It has been studied in a variety of cancer types and has shown moderate effects in some neoplastic diseases. Dose-related toxicities, which include neutropenia and diarrhea, have limited some studies (50,55). Interestingly, one study looking at a combination of Flavopiridol and Cisplatin/Carboplatin in solid tumors suggested that the lack of significant activity seen may be the result of the failure to achieve decreases in Mcl-1 levels in tumors (50). Nevertheless, there is preclinical evidence of synergism between Flavopiridol and proteasome inhibitors associated with Mcl-1 down-regulation (56,57).

### **SNS-032**



Another cyclin-dependent kinase inhibitor, SNS-032 was originally identified in a screen developed to identify specific inhibitors of Cdk2. This compound has since been shown to also inhibit Cdk7 and Cdk9 as well. SNS-032, like Flavopiridol, also shows strong cytotoxic effects *in vitro* and results in decreases in anti-apoptotic proteins such as Mcl-1 (58). Unfortunately, this compound exhibited disappointing results when evaluated in clinical trials (59).

## **2. Sorafenib**

Sorafenib is a multi-kinase inhibitor that was originally developed as an inhibitor of B-Raf, but was subsequently shown to inhibit multiple other kinases, including PDGFR, FLT, Kit, and VEGFR. In human leukemia cells, pharmacologically achievable concentrations of sorafenib induced apoptosis through a mechanism involving Mcl-1 down-regulation (60-62). This has been found to be due to inhibition of translation resulting from sorafenib-induced ER stress (60).

## **3. Deubiquitinase Inhibitors**

### **WP1130**

As discussed previously in this review, Mcl-1 is degraded rapidly in the cell via a proteasome-dependent pathway. Blocking the proteasome can lead to increased levels of Mcl-1 protein. Mcl-1 can also be rescued from degradation by deubiquitinases (DUBs), which are able to remove ubiquitin from ubiquitinated Mcl-1. In a study investigating interactions between Mcl-1 and other proteins in the cell, Schwickart *et. al.* (63) found that one of the proteins that co-immunoprecipitates with Mcl-1 is the DUB

USP9X. This group hypothesized that this interaction might lead to increased stability of Mcl-1 and play an important role in cancers that overexpress Mcl-1. Indeed, they showed that USP9X, in addition to Mcl-1, was overexpressed in samples of ductal adenocarcinoma, colon adenocarcinoma, and small cell lung cancer. Additionally, USP9X overexpression was found to correlate with poor prognosis in multiple myeloma. Knockdown of USP9X via siRNA resulted in decreased Mcl-1 protein levels, but not RNA levels, supporting the suggestion that USP9X knockdown results in increased Mcl-1 degradation. This knockdown also led to increased sensitivity of colon carcinoma and leukemia cells lines to ABT-737, a compound discussed later in this review, which are usually resistant to this agent (63).

WP1130 is a small molecule that has multiple anti-cancer effects. It has been shown to induce removal of Bcr-Abl from the cytoplasm into aggresomes, where it is not able to facilitate oncogenic signaling. Additionally and most interesting for this review, it directly inhibits USP9X. When used as a treatment in CML, WP1130 results in decreased levels of Mcl-1, compartmentalization of Bcr-Abl, and the induction of apoptosis (64).

## **B. Antisense oligonucleotide (ASO) treatment**

Despite the fact that there are many studies looking at the effects of Mcl-1 ASO treatment on cancer *in vitro* and in animal models *in vivo*, there is no report of a Mcl-1 ASO treatment being effectively translated into the clinic. This is likely due to the issues that can arise with the use of ASO treatment in patients. In the human body, ASO have an extremely short half-life, which makes achieving sufficient blood concentrations

difficult. This is partly due to the ability of DNases to degrade them. Delivery of ASO is also an issue, as it is difficult to direct ASO to their specific cellular target (65).

### **C. BH3 Mimetics**

The concept of BH3 mimetics has been one of the most promising translational strategies. As discussed, pro-apoptotic or anti-apoptotic effects arise, ultimately, as a result of physical interactions between the anti-apoptotic Bcl-2 protein and the BH3 proteins. The anti-apoptotic proteins contain a hydrophobic binding pocket made from the folding of their BH1, BH2, and BH3 domains. The BH3 domain of the BH3 only proteins fits into and binds this hydrophobic pocket (66). Based on this modeling prediction, small molecules have been developed that mimic the BH3 domain and therefore are able to fit into the hydrophobic pocket of the anti-apoptotic proteins and block their ability to bind pro-apoptotic proteins, inhibiting their function. Some of these mimetics have been developed through structural studies and others through screening studies. Regardless of how these drugs were discovered, they represent a novel and exciting new strategy in cancer therapeutic development.

#### **1. ABT-737**

One of the most successful and well studied BH3 mimetics, ABT-737, was discovered using NMR-based screening and demonstrated strong binding affinity to the Bcl-2 family anti-apoptotic proteins Bcl-2, Bcl-XL, and Bcl-w. ABT-737 does not bind to Mcl-1 or Bfl-1. This difference in affinity is due to differences in the structures of these proteins as was described previously in this review. Initial studies showed that ABT-737 was effective in inducing cytotoxicity as a single agent in follicular lymphoma and small

cell lung carcinoma (SCLC) cell lines. Additionally, it was found to enhance the lethality of paclitaxel in NSCLC (non small cell lung carcinoma) (67). Subsequently, ABT-737 has been widely studied in a variety of cancers. It has been shown to induce cytotoxicity both *in vitro* and *in vivo* in leukemia and lymphoma, glioblastoma, multiple myeloma, and SCLC (68-72). Despite many promising studies in these cancer types, there remain a large percentage of cancers that are resistant to ABT-737. This resistance has been shown to stem from an overexpression of Mcl-1, one of the anti-apoptotic proteins to which ABT-737 does not bind. Even within cancers that are sensitive to ABT-737, specific cell lines that express higher levels of Mcl-1 display increased resistance to this compound (68). Mcl-1-dependent ABT-737 resistance has been consistently shown in the literature and multiple studies document that downregulation of Mcl-1 through a variety of mechanisms is able to induce sensitivity to ABT-737 (73-76). Notably, the CDK inhibitor roscovitine dramatically increased ABT-737 lethality in human leukemia cells through a mechanism involving Mcl-1 down-regulation (77).

Phase I/II clinical trials with ABT-263, an orally available form of ABT-737 with a longer half-life, are in progress in patients with SCLC, leukemia, and lymphoma. Thus far, studies in chronic lymphocytic leukemia (CLL) and SCLC have shown this drug to be well tolerated, with some potentially manageable toxicities including back pain, nausea/vomiting, diarrhea, and thrombocytopenia (78). More advanced clinical trials, however, have shown limited efficacy of this drug as a single agent in SCLC (79).

## **2. Obatoclox (GX15)**

Obatoclax is another example of a BH3 mimetic. This mimetic differs from ABT-737 in that in addition to targeting Bcl-2, Bcl-XL, and Bcl-w, it also binds to and inhibits Mcl-1 and Bfl-1. Studies have shown that this compound induces cytotoxicity in a number of cancer types including, but not limited to, NSCLC and a variety of leukemias. Additionally, it has shown synergy when combined with various conventional chemotherapeutic agents (53,80-83). Obatoclax also serves to again illustrate the importance of Mcl-1 in cancer. Studies have shown that this compound's cytotoxic effects are partially mediated through specific effects on Mcl-1. Obatoclax can disrupt the constitutive Bak-Mcl-1 interaction on the outer mitochondrial membrane (84). This compound has advanced to clinical trials and Phase I studies in a variety of cancer types have shown it to be fairly well tolerated, with neurologic toxicities being the most common adverse event seen. Some evidence of efficacy was seen in these studies, though ongoing Phase II trials will ultimately determine the effectiveness of this agent (85-87).

### **3. Gossypol**

Gossypol is a polyphenolic aldehyde derived from cottonseed. Original studies with this extract focused on its ability to function as a male contraceptive (88). However, it has also been shown to have potent anti-cancer activity. Gossypol functions as a typical BH3 mimetic and binds to and inhibits the Bcl-2 anti-apoptotic proteins Bcl-2, Bcl-XL, and Mcl-1 (89). Many groups have shown Gossypol to exhibit anti-carcinogenic effects toward a wide variety of cancer types both *in vitro* and *in vivo*, including, but not limited to, breast, prostate, glioma, and colon cancer (88,90-93). LeBlanc *et al.* (94) also demonstrated Gossypol's ability to inhibit growth of adrenal

gland carcinoma cells, medullary thyroid carcinoma cells, ovarian carcinoma cells, and endometrial carcinoma cells. Compared to ABT-737, Gossypol displays toxicity against a much wider array of cancer types, possibly due to its ability to target Mcl-1. This compound has been evaluated in Phase II clinical trials as a single-agent in patients with advanced malignancies as well as in clinical trials that evaluated Gossypol in combination therapy with conventional chemotherapeutics (95-98).

The presence of two reactive aldehyde groups on Gossypol, combined with initial clinical trial results that showed difficulty in achieving sufficient Gossypol blood concentrations, prompted groups to create Gossypol derivatives. Apogossypol was the first derivative designed and showed better efficacy and less toxicity than its parent compound (99). To date, there have been many such derivatives created with varying binding affinities to the Bcl-2 anti-apoptotic proteins.

#### **4. Sabutoclax (BI-97C1)**

Sabutoclax (BI-97C1) is one of the newest Apogossypol derivatives developed by Wei *et al.* (89,100). This novel compound binds to the Bcl-2 anti-apoptotic proteins Bcl-2, Mcl-1, Bcl-X<sub>L</sub>, and Bfl-1. It was originally identified for its ability to bind Bcl-X<sub>L</sub> with low to submicromolar binding affinity. Competitive fluorescence polarization assays showed that BI-97C1 inhibited Bcl-X<sub>L</sub> with an IC<sub>50</sub> value of .31 mM. Further assays showed that this compound also had displacement activity against Bcl-2 (IC<sub>50</sub> = 0.32 mM), Mcl-1 (IC<sub>50</sub> = 0.20 mM), and Bfl-1 (IC<sub>50</sub> = 0.62 mM) (100).

Sabutoclax induced apoptosis in the large B-cell lymphoma cell line, BP3, which expresses high levels of Mcl-1 and Bfl-1 and is resistant to ABT-737. Furthermore,

while toxic to wild type mouse embryonic fibroblasts, this compound showed only slight toxicity against BAX/BAK double knockout MEF cells. This provided evidence that Sabutoclax only has minimal off-target effects. Additionally, as Sabutoclax showed efficacy against a cell line that overexpressed Mcl-1, unlike some earlier compounds like ABT-737, it was evaluated in the context of a prostate cancer xenograft involving M2182 cells, which rely on Mcl-1 for survival. A dose of 3 mg/kg induced nearly 60% tumor inhibition, while a dose of 5 mg/kg nearly eliminated the tumors (100).

## **5. BH3-M6**

This BH3 mimetic is a very new compound designed to inhibit Bcl-2, Bcl-X<sub>L</sub>, and Mcl-1. It has been shown to disrupt the interactions between these proteins and the pro-apoptotic BH3 only proteins. In the lung adenocarcinoma cell line, A549, this compound induced apoptosis through cytochrome c release from the mitochondria. Preliminary studies, however, showed high doses of this compound (doses of 25 and 50 mM) were needed to induce apoptosis. Additional studies with this compound in other cancer types will be useful in determining the efficacy of this new BH3 mimetic (101).

## **VII. Functional Redundancy Among the Bcl-2 Family**

As discussed previously, the majority of compounds that target Mcl-1 also affect other members of the anti-apoptotic Bcl-2 family of proteins. This reflects structural and functional redundancy in many protein members of this gene family. While some cancers rely more heavily on Mcl-1 (44), others rely on alternate anti-apoptotic members of the family for survival and progression (100). Accordingly, one might try to identify and employ therapies for a particular cancer based on such reliance. Indeed,

there have been compounds, such as ABT-737, that do not target all of the anti-apoptotic Bcl-2 proteins. This compound is most effective in cancers that rely on proteins targeted by ABT-737. However, the limitations observed with ABT-737 highlight why targeting of specific anti-apoptotic proteins alone may not promote optimal therapeutic outcome.

In addition to a lack of efficacy against cancers reliant on Mcl-1 and Bfl-1, multiple studies have now shown that, over time, cells sensitive to ABT-737 begin to develop resistance to the drug by upregulating the anti-apoptotic proteins that it does not target, i.e., Mcl-1 and Bfl-1. Yecies *et al.* (102) showed that lymphoma cells subjected to long-term exposure of ABT-737 developed resistance via transcriptional upregulation of Mcl-1 and Bfl-1. They further demonstrated that decreasing Mcl-1 protein levels via multiple mechanisms resulted in restored sensitivity to ABT-737 (102). Previously, a similar phenomenon was also seen in acute myeloid leukemia (AML) cells. This group noticed a positive correlation between Mcl-1 expression and ABT-737 resistance (101). These studies indicate that the Bcl-2 family of anti-apoptotic proteins may provide overlapping compensatory functions when one of the proteins is lost. This supports strategies involving compounds that target all of the anti-apoptotic proteins, as this approach may help prevent the development of resistance mechanisms to BH3 mimetics.



## **Chapter 2: Novel combinatorial therapy for pancreatic cancer: a BH3 mimetic and a synthetic tetracycline**

### **Introduction:**

Pancreatic ductal adenocarcinoma (PDAC) is an extremely aggressive cancer that is predicted to cause almost 40,000 deaths in the US this year (NCI 2014). PDAC is fairly resistant to most standard therapies and results in a 5-year survival rate of about 4%(1). These dire statistics, combined with the fact that there have been minimal new therapies developed for PDAC over the last decade, highlight the need for new approaches to effectively treat this invariably fatal disease.

The aggressive nature and dismal prognosis of patients with pancreatic cancer results partly from the plethora of molecular changes that occur during PDAC development, one of which is overexpression of the anti-apoptotic proteins of the Bcl-2 family (103-106). Cancer cells exploit this overexpression to evade cell death and as a mechanism promoting resistance to diverse chemotherapeutic agents. Apoptosis reflects a balance between pro- and anti-apoptotic proteins within cells. The ability of a cancer cell to shift the balance toward survival promotes resistance to toxic factors (107).

Consequently, the anti-apoptotic Bcl-2 proteins have emerged as a novel therapeutic target. While multiple strategies have attempted to target these molecules, BH3 mimetics have shown significant promise. Pro-apoptotic or anti-apoptotic effects in cells arise, ultimately, as a consequence of physical interactions between anti- and pro-

apoptotic Bcl-2 proteins (66,72). Based on modeling predictions of these interactions, small molecules have been developed that mimic the BH3 domain of pro-apoptotic proteins and bind to the anti-apoptotic proteins, thereby impeding their ability to inhibit apoptosis. These drugs represent a novel and exciting new strategy in cancer therapeutic development (107).

Sabutoclax (BI-97C1) is a novel Apogossypol derivative BH3 mimetic developed by Wei *et al.* (89,99,100,108). This compound binds to the Bcl-2 anti-apoptotic proteins Bcl-2, Mcl-1, Bcl-X<sub>L</sub>, and Bfl-1. It was originally identified based on its ability to bind Bcl-X<sub>L</sub> with low to submicromolar binding affinity (100). We have previously shown that Sabutoclax shows efficacy against prostate and colorectal cancers, two cancers that also overexpress anti-apoptotic Bcl-2 proteins (109,110).

Minocycline is a synthetic tetracycline antibiotic that displays marginal activity against multiple cancers (111-115). However, less than stellar outcomes have diminished enthusiasm for using these drugs in cancer research. The marginal single agent effects of Minocycline against cancer may be due to the fact that it also impedes cell death in the face of toxicity or injury by inhibiting mitochondrial apoptosis and upregulation of Bcl-2 (116-118). In an attempt to develop a unique therapeutic strategy for PDAC, we hypothesized that Sabutoclax and Minocycline might show therapeutic efficacy against this disease when used in combination because of both the reliance of PDAC on the Bcl-2 proteins for survival as well as the theoretical ability of Sabutoclax to counteract the anti-apoptotic effects of Minocycline, thereby uncovering the true therapeutic potential of this previously overlooked drug.

## **Materials and Methods**

### ***Human Cell Lines***

MIA PaCa-2, PANC-1, BxPC-3, AsPC-1, and HPNE cells were all obtained from the American Type Culture Collection (ATCC). LT2 cells were purchased from Millipore. MIA PaCa-2 and PANC-1 were maintained in DMEM plus 10% FBS. BxPC-3 and AsPC-1 cells were maintained in RPMI plus 10% FBS. HPNE and LT2 cells were maintained with media according to distributor's instructions. Cell lines were expanded and cryopreserved at early passages and new vials were thawed out and used for experiments approximately every 3 months.

### ***Creation of KPC Mouse Cell Lines***

Cell lines were derived from the ascites of tumor bearing KPC mice. At the time of necropsy, ascitic fluid was collected from the mice and centrifuged to pellet tumor cells. The pellet was repeatedly washed in PBS and centrifuged before being resuspended in RPMI supplemented with 4% FBS and placed in culture. This media was used to maintain these cell lines.

### ***Drugs and Drug Administration***

For all *in vitro* studies, Sabutoclax (produced by Dr. Maurizio Pellecchia) was diluted in DMSO and Minocycline (Sigma) in PBS. For combination treatments, Sabutoclax and Minocycline were administered to cells simultaneously. zVAD-FMK (20  $\mu$ M, Promega) was incubated with cells for 1 hour prior to treatment with Sabutoclax and Minocycline.

Caspase 8 specific inhibitor, z-IETD-FMK (20  $\mu$ M, BD Pharmingen) was also incubated with cells for 1 hour before treatment with Sabutoclax and Minocycline.

### ***Proliferation Studies***

5 x 10<sup>3</sup> cells were plated in 96-well plates and treated with Sabutoclax and/or Minocycline for 72 hours. Proliferation was assessed by MTT assay as previously described (119). All data were normalized to the control.

### ***Cell Death Assays***

For Trypan Blue exclusion assays, 5 x 10<sup>5</sup> cells were plated in 6-cm dishes, treated as indicated for 48 hours, and then assayed as previously described (120).

### ***LDH Cytotoxicity Assays***

5 x 10<sup>5</sup> cells were plated in 6-cm dishes and treated as described. After 48 hours, media was collected from each dish and assayed according to the manufacturer's instructions (Cytotoxicity Detection Kit (LDH), Roche).

### ***Cell Cycle Studies***

1 x 10<sup>6</sup> cells were plated in 10-cm dishes and cultured in normal media with 0.5% serum for 48 hours. Cells for the zero hour time point were collected and fixed at this point. Remaining plates were kept in either normal media or 750 nM Sabutoclax for indicated time points. Once all cells were collected and fixed, they were incubated with propidium iodide and FACS was used for cell cycle analysis. Cell cycle studies were done as previously described (121).

### ***Colony Forming Assay***

MIA PaCa-2 cells were treated with Sabutoclax (500 nM), Minocycline (50  $\mu$ M), or a combination of both for 24 hours. Cells were then trypsinized and 1,000 cells were plated into 6-cm plates in triplicate. Cells were allowed to grow and form colonies in normal media for approximately 14 days. Plates were then fixed and stained with Giemsa.

### ***Western Blotting***

$5 \times 10^5$  cells were plated in 6-cm dishes and treated as described. After 48 hours, whole cell lysates were prepared and western blotting analysis was carried out as previously described (120). Primary antibodies used for these studies are PARP (1:1,000), Stat3 (1:1,000), pStat3 (1:750), Mcl-1 (1:1,000), Survivin (1:750), p21 (1:750), p27 (1:1,000), Cyclin D1(1:500), Caspase 2 (1:1,000), Caspase 3 (1:1,000), Caspase 6 (1:1,000), Caspase 7 (1:1,000), Caspase 8 (1:1,000), Caspase 10 (1:1,000), Caspase 12 (1:1,000), AIF (1:1,000), pRB (1:750) (Cell Signaling), EF1- $\alpha$  (1:1,000, Millipore), and Actin (1:5,000, Sigma). Densitometric analysis was done using ImageJ software (National Institutes of Health).

### ***Constructs and Transfection***

*Stat3Y705F Clones:* MIA PaCa-2 or PANC-1 cells were transfected with a plasmid expressing a mutated form of Stat3 (pRc.CMV.Stat3Y705F, Addgene). Clones were selected with Neomycin for approximately 2 weeks and then picked and grown up individually. Whole cell lysates were made and samples were used for western blotting to characterize clones. *Luciferase Clones:* MIA PaCa-2 or PANC-1 cells were

transfected with pGL3.CMV.luc (Promega). Transfections used Lipofectamine 2000 (Invitrogen, Carlsbad, CA) according to the manufacturer's protocol.

### ***Immunohistochemistry***

Tumors were fixed in formalin, embedded in paraffin, and sectioned for staining. Staining was done as previously described (122) with anti-p-Stat3 (1:100, Abcam), anti-PCNA (1:100, Abcam), and anti-Mcl-1 (1:100, Abcam) per the manufacturer's instructions.

### ***Combination Index Calculation***

Combination index (CI) values were determined for the combination of Sabutoclax and Minocycline in MIA PaCa-2 cells. Values were calculated using CompuSyn software (ComboSyn, Inc.) according to the Chou-Talalay method.

### ***In vivo studies***

#### ***Subcutaneous Xenograft Studies***

$5 \times 10^6$  MIA PaCa-2 and  $3.5 \times 10^6$  PANC-1 cells were used to establish bilateral subcutaneous tumors on the flanks of 8-10 week old male athymic nude mice. Studies were done as previously described (109). Treatment began when tumors reached  $\sim 100\text{-mm}^3$ . Sabutoclax was given at a dose of 1 mg/kg for both studies and was dissolved in a 10:10:80 solution of 100% ethanol:Cremophor:PBS. Minocycline was given at a dose of 20 mg/kg and dissolved in PBS. Both drugs were given via IP injection 3 times per week.  $n = 5$  mice/group

## ***Quasi-Orthotopic Xenograft Studies***

### **Low Tumor Burden**

In this model, we injected  $1 \times 10^6$  MIA PaCa-2-luc cells IP into 8-10 week old male athymic nude mice. We allowed 1 week for tumor cells to attach and grow and then began treatment with PBS, 1 mg/kg Sabutoclax, 20 mg/kg Minocycline, or both Sabutoclax and Minocycline. Sabutoclax and Minocycline were given via IP injection 3x/week. Mice were imaged by BLI at 3 weeks after treatment was initiated and then sacrificed at 4 weeks. At time of sacrifice, mice were imaged pre-necropsy. After necropsy, organs from a few mice/group were imaged to determine tumor specificity. n = 7 mice/group

### **High Tumor Burden**

$5 \times 10^6$  MIA PaCa-2-luc cells were injected IP into 8-10 week old male athymic nude mice. We allowed 1 week for tumor cells to attach and grow and then began treatment with PBS, 1 mg/kg Sabutoclax, 20 mg/kg Minocycline, or both Sabutoclax and Minocycline. Sabutoclax and Minocycline were given via IP injection 3x/week. Mice were sacrificed at 4 weeks. The pancreas from each mouse was removed and weighed during necropsy. n = 10 mice/group

### ***BLI of Mice***

During imaging, mice were placed in the imaging chamber and maintained with 2% isoflurane gas anesthesia at a flow rate of approximately 0.5-1 L/min per mouse. Anesthetized mice were injected IP with 150mg/kg body weight D-Luciferin (Xenogen Corporation, Alameda, CA). After approximately 10 min, mice were imaged using a

charge-coupled-device (CCD) camera coupled to the Xenogen *in vivo* imaging (IVIS) imaging system (Caliper Life Sciences, Inc., Hopkinton, MA). The positive signal from background-subtracted images was analyzed by Living Image software for integrated density.

### ***Syngeneic Mouse Study***

KPC (Pdx-1-Cre/K-*ras*<sup>LSL-G12D</sup>/*p53*<sup>flox/wt</sup>) mouse cell line 48 was injected subcutaneously into both flanks of non-tumorigenic KPC mice (Pdx-1-Cre negative/K-*ras*<sup>LSL-G12D</sup>/*p53*<sup>flox/wt</sup>). Tumors were inoculated 1 week prior to initiation of treatment. Mice were treated with PBS, 1.5 mg/kg Sabutoclax, 10 mg/kg Minocycline, or both Sabutoclax and Minocycline. Sabutoclax was dissolved in a 10:10:80 solution of 100% ethanol:Cremophor:PBS. Minocycline was dissolved in PBS. Mice were treated with Sabutoclax, Minocycline, or both drugs every 2-3 days via IP injection for a total of 6 injections. Tumors were measured with calipers to obtain tumor volumes. n = 5 mice/group

### ***Survival Study***

KPC mice (Pdx-1-Cre/K-*ras*<sup>LSL-G12D</sup>/*p53*<sup>flox/flox</sup>) were started on a Sabutoclax and Minocycline treatment regimen at 1 month of age. Mice were treated with a combination of Sabutoclax (1.5 mg/kg) and Minocycline (10 mg/kg) via IP injection 3 times per week. Mice were kept on this treatment until reaching a moribund status. At this point, mice were sacrificed and necropsied. Tumor sections were obtained from these mice and subjected to immunohistochemistry. n = 12 mice (control group); n = 10 mice (Sabutoclax + Minocycline group).



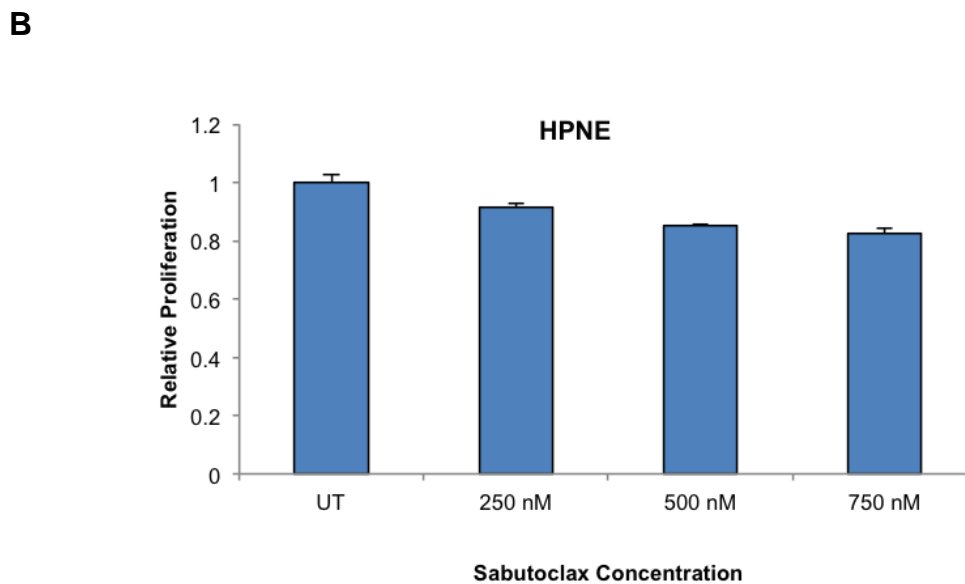
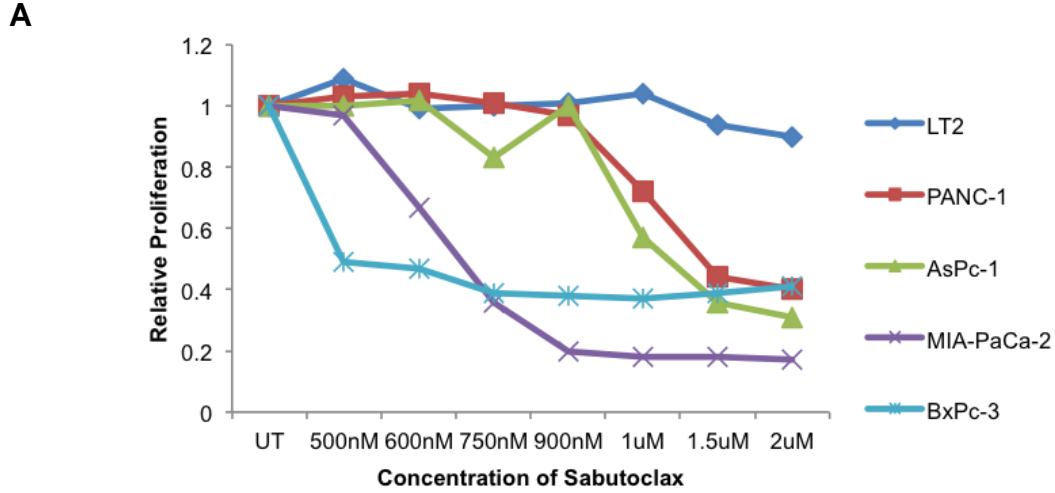
## ***Statistical Analysis***

The data presented are the mean  $\pm$  S.D. of the values from three independent experiments. For *in vivo* studies, data shown are the mean  $\pm$  95% confidence interval. Significance was determined using the Student's t-test.  $p < 0.05$  was considered statistically significant.

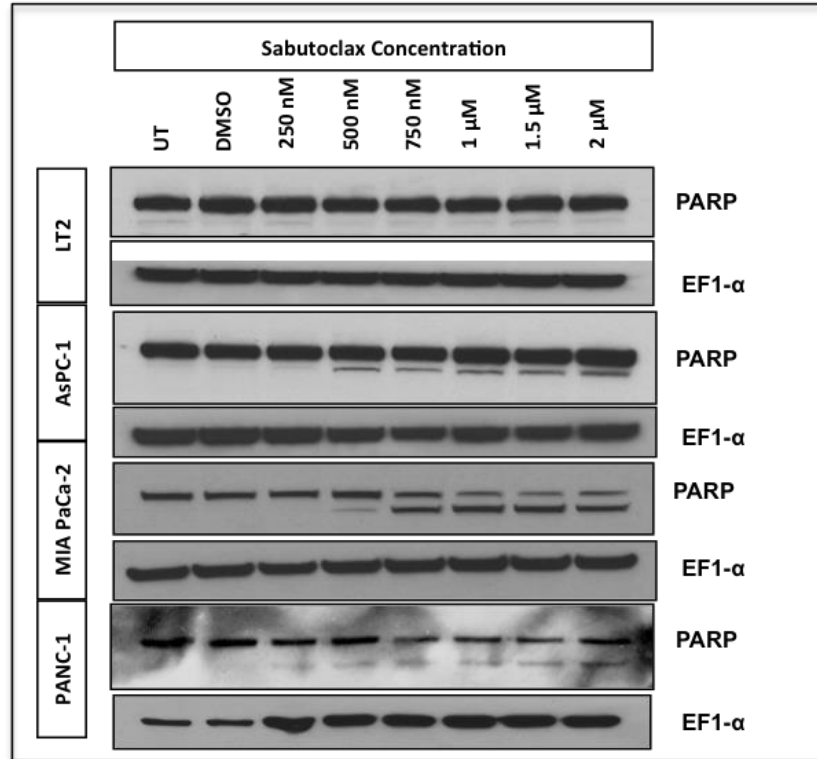
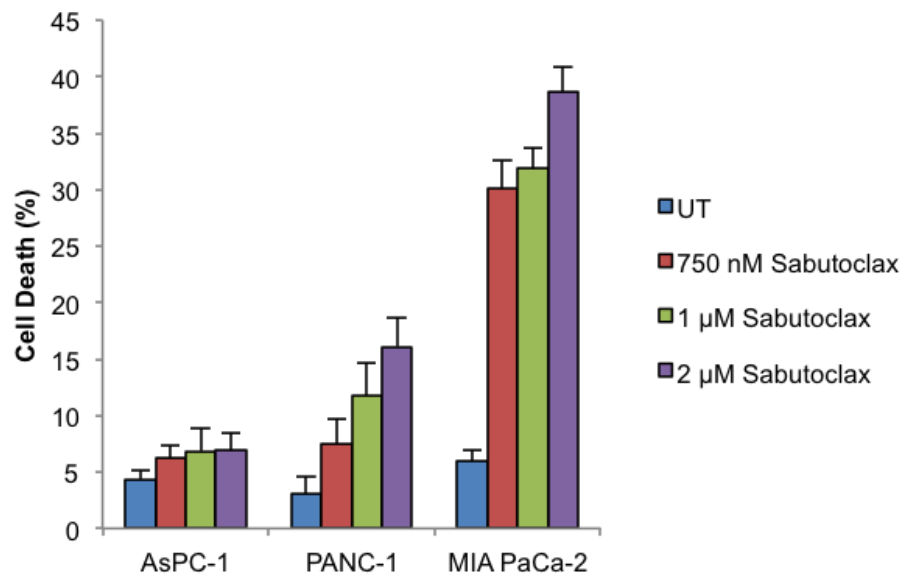
## **Results:**

### **Sabutoclax inhibits cell growth and induces apoptosis in PDAC**

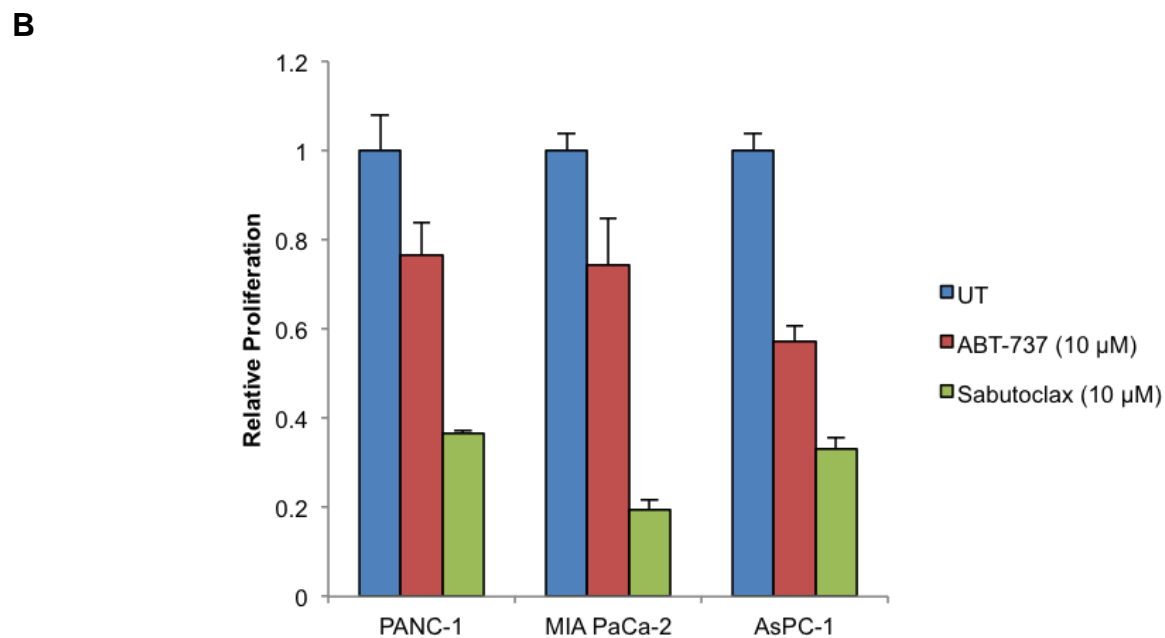
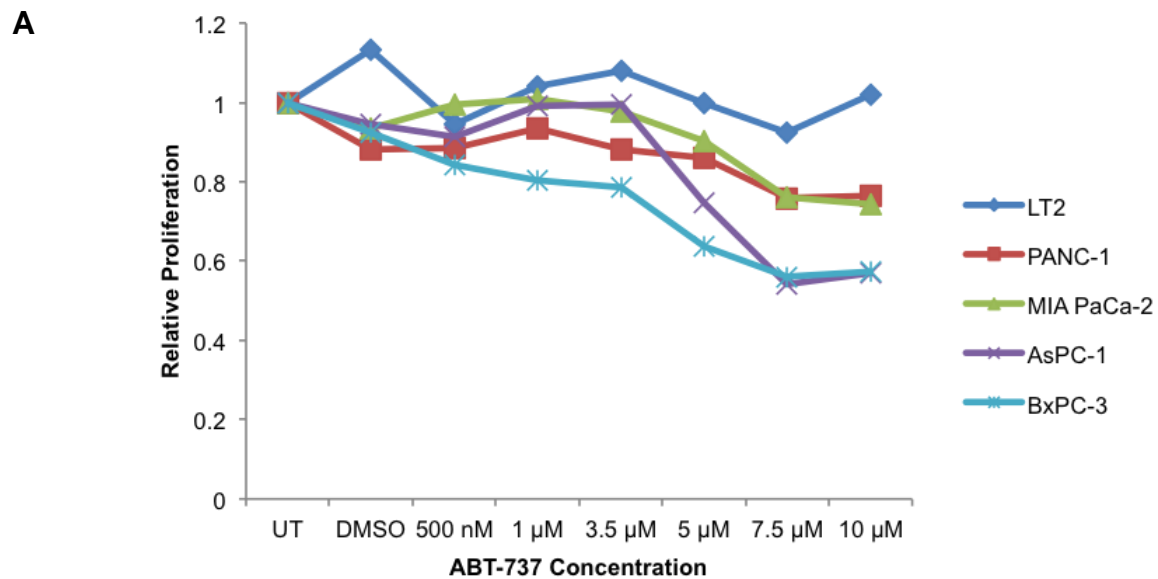
Multiple PDAC cell lines, one immortalized pancreatic fibroblast cell line (LT2), and one immortalized pancreatic epithelial cell line (HPNE) were treated with increasing doses of Sabutoclax and assessed for effects on proliferation. The normal cell lines displayed little change in cell growth (Fig. 3A-B), while all of the cancer cell lines were growth inhibited. Interestingly, the sensitivity of the cancer cell lines varied, with some being very sensitive to Sabutoclax (MIA PaCa-2) and others more resistant (AsPC-1) (Fig. 3A). The ability of Sabutoclax to induce cell death and apoptosis was also evaluated through Trypan Blue assays and detection of the cleavage of PARP, a protein cleaved by caspases during apoptosis (Fig. 4A-B). Again, MIA PaCa-2 was most sensitive to Sabutoclax. However, despite not showing a potent cell death phenotype, cells like AsPC-1 still showed profound growth inhibition following Sabutoclax treatment at higher doses. Furthermore, Sabutoclax displayed greater growth inhibitory effects than the BH3 mimetic ABT-737 (Fig. 5A-B).



**Figure 3: Sabutoclax inhibits cell growth and induces apoptosis in pancreatic cancer cells. (A)** Sabutoclax dose response curves via MTT proliferation assays in pancreatic fibroblast cell line, LT2, and pancreatic cancer cell lines PANC-1, AsPC-1, MIA PaCa-2, and BxPC-3. Experiments done in triplicate and independently repeated three times. **(B)** Sabutoclax dose response curve via MTT proliferation assay in pancreatic epithelial-derived cell line, HPNE. Experiments done in triplicate and independently repeated three times.

**A****B**

**Figure 4: Sabutoclax inhibits cell growth and induces apoptosis in pancreatic cancer cells.** (A) Western blotting for PARP and EF1- $\alpha$  (loading control). Data representative of three independent experiments. (B) Trypan Blue assays in AsPC-1, PANC-1, and MIA PaCa-2. \*\* $p < 0.001$  as compared to UT sample. Experiments done in triplicate and independently repeated three times.

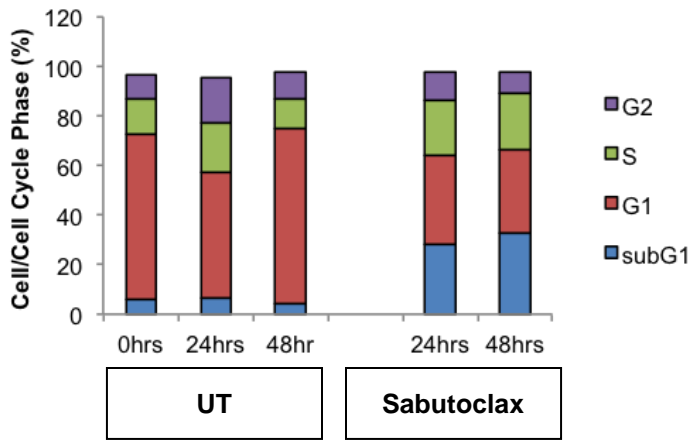
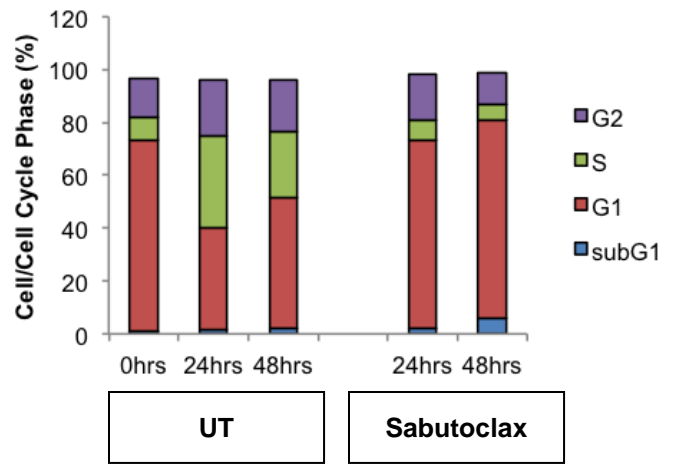
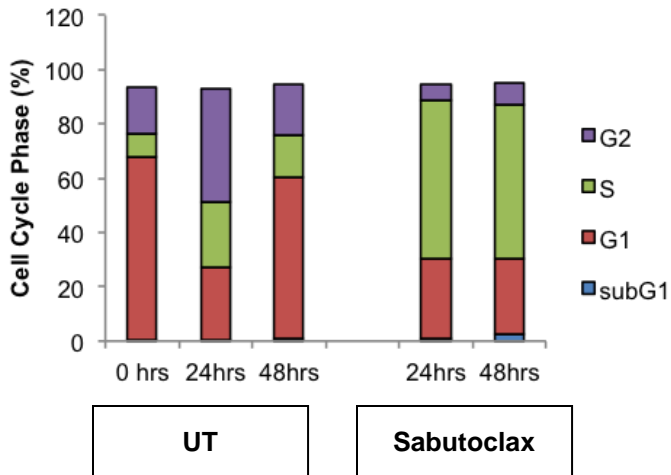
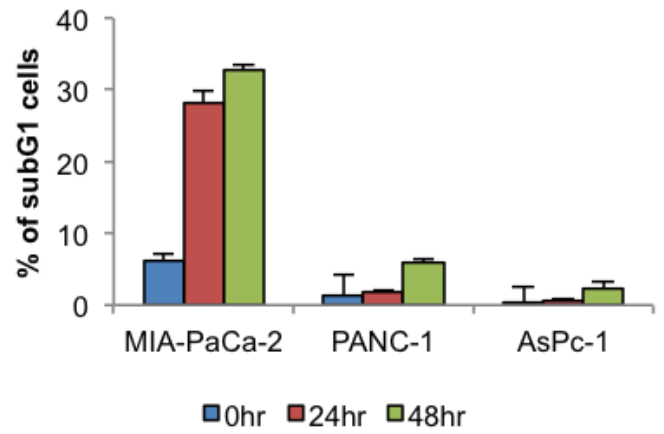


**Figure 5: Sabutoclast has greater efficacy than ABT-737. (A)** MTT proliferation assays 72 hours post treatment. **(B)** MTT proliferation assay comparing ABT-737 to Sabutoclast. \* $p < 0.001$ . Experiments done in triplicate and independently repeated three times.

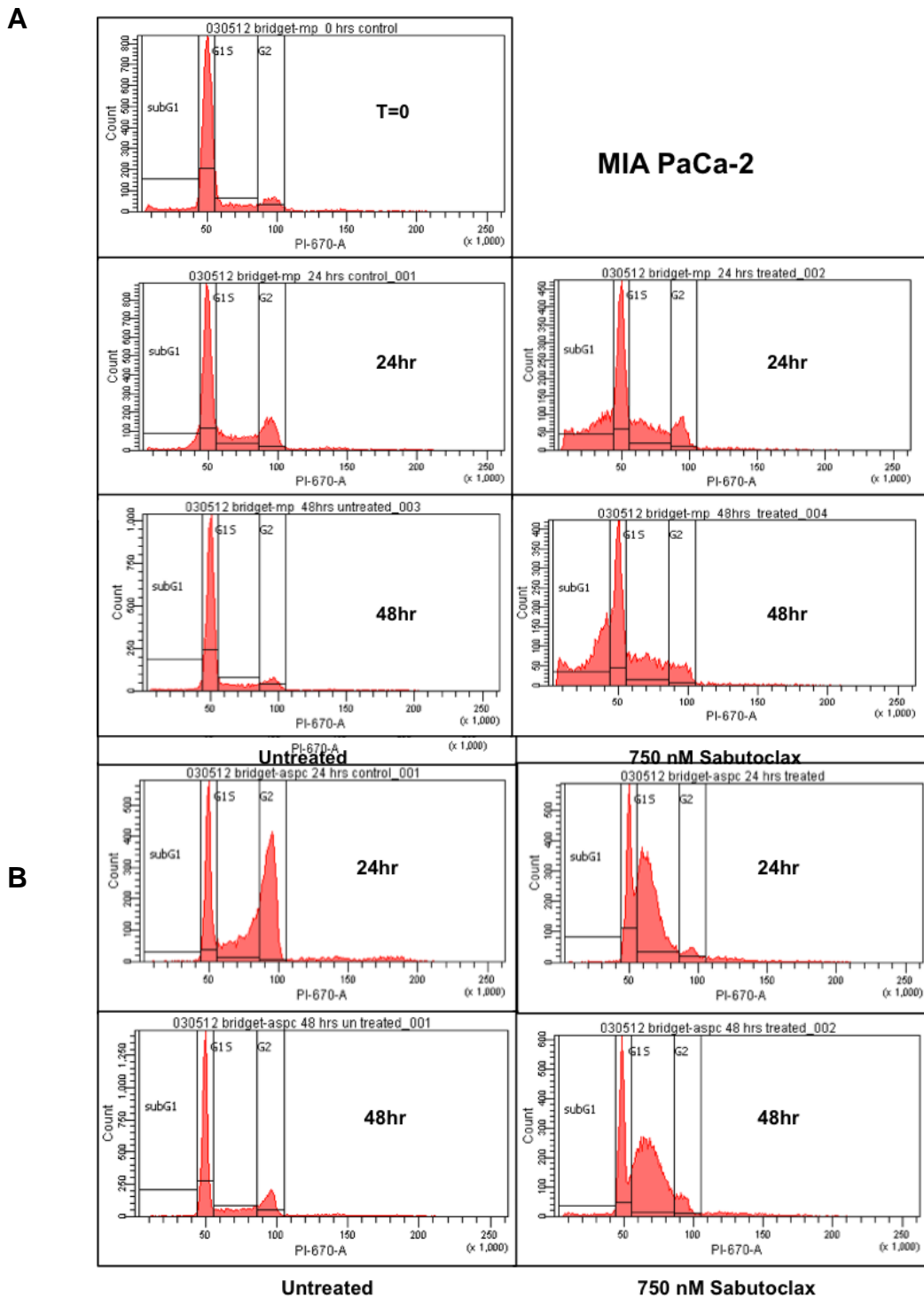
## **Sabutoclax induces G1-S phase arrest**

Sabutoclax induces cell death in MIA PaCa-2 cells, without promoting potent cell death in either AsPC-1 or PANC-1. Despite this, there is still a dramatic reduction in cell growth after drug treatment in these cell lines. To interrogate the mechanism of growth suppression in these cell lines, we performed cell cycle analysis via FACS analysis (Fig. 6-7). Sabutoclax increased the percentage of MIA PaCa-2 subG1 phase cells, which have a DNA content less than 2n and are indicative of dead cells, after 24 and 48 hours, without affecting cell cycle, which is consistent with our previous data (Fig. 6A,D). In PANC-1 and AsPC-1 cells, however, potent G1-S phase cell cycle arrest was evident (Fig. 6B-C). These experiments only evaluated cells up to 48 hours post-treatment. A second set of experiments also included 72 and 96 hour time points (Fig. 8-9) to determine if longer drug incubations promoted cell cycle arrest or resulted in a switch to apoptosis. In AsPC-1, the G1-S phase arrest was sustained throughout all time points evaluated (Fig. 8B). However, at 72 and 96 hours, PANC-1 showed an increase in the subG1 population of cells, indicating that there is an initial cell cycle arrest in these cells that later switches to apoptosis (Fig. 8A,C). These results emphasize the complexity of responses observed in PDAC to a single agent, such as Sabutoclax.

Evaluation of cell cycle protein markers (Fig. 8D) confirmed decreased Cyclin D1 and increased p27 expression in AsPC-1 and PANC-1 cells. Additionally, there was a dramatic decrease in levels of phosphorylated Rb (Ser780). This corresponded with the observed G1-S phase arrest. Interestingly, while levels of p21 in AsPC-1 cells increased, p21 levels decreased in PANC-1 cells. This difference may account for the switch from growth arrest to apoptosis in these cells (123,124).

**A****MIA PaCa-2****B****PANC-1**UT  
UT**C****AsPC-1****D**

**Figure 6: Sabutoclastax causes a G1-S phase cell cycle arrest.** (A-C) Cell cycle analysis. (D) Percentage of cells analyzed in the subG1 phase, indicating cell death. Data representative of three independent experiments.



C

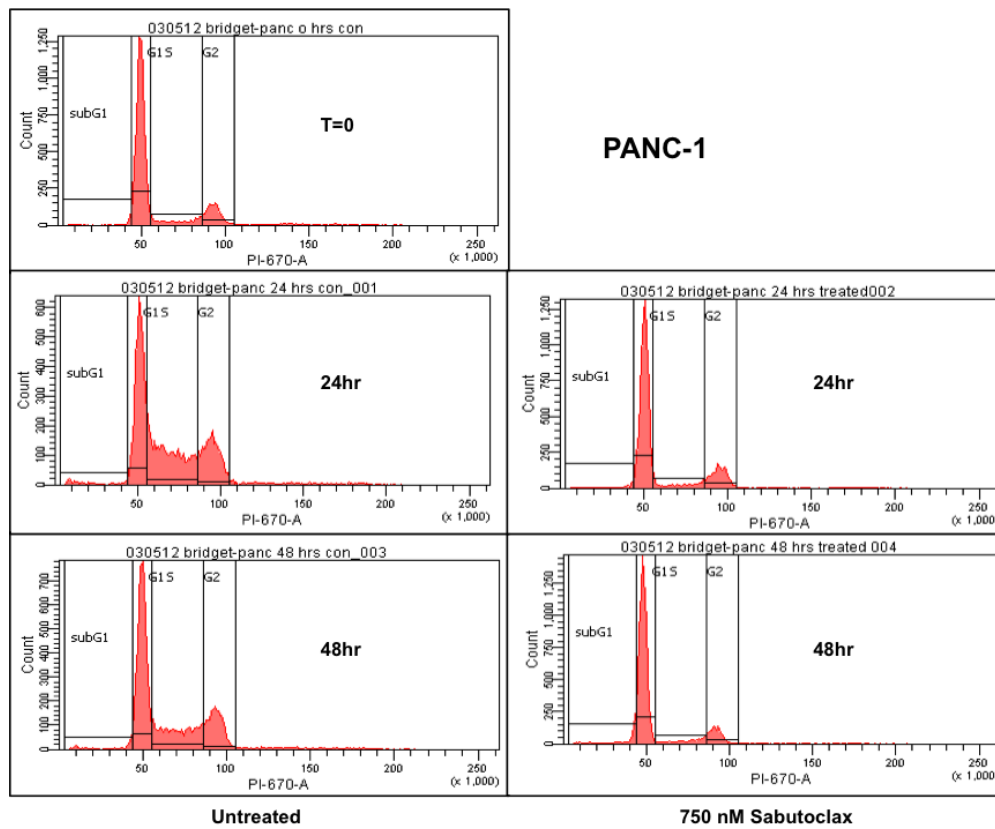


**Figure 7: Sabutoclox causes a G1-S phase cell cycle arrest. (A-C)** FACS analysis data of graphs presented in Figure 6. Data representative of three independent experiments.



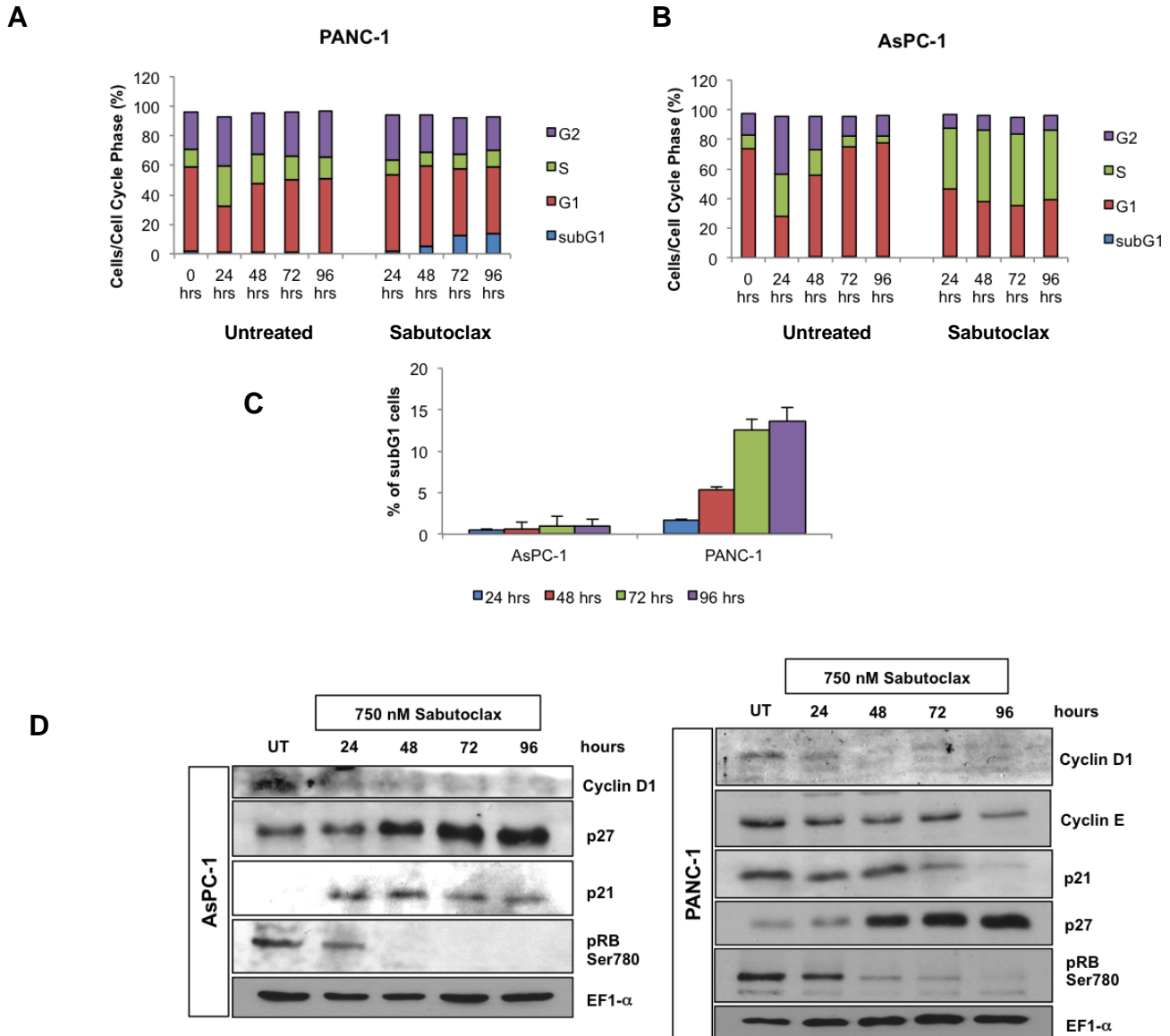


**Figure 8. Sabutoclax causes a G1-S phase cell cycle arrest.** (A-B) Cell cycle analysis. (C) Percentage of cells analyzed in the subG1 phase, indicating cell death. (D) Western blotting of whole cell lysates for Cyclin D1, Cyclin E, p27, p21, and phospho-Rb. EF1- $\alpha$  was used as a loading control. Data representative of three independent experiments.

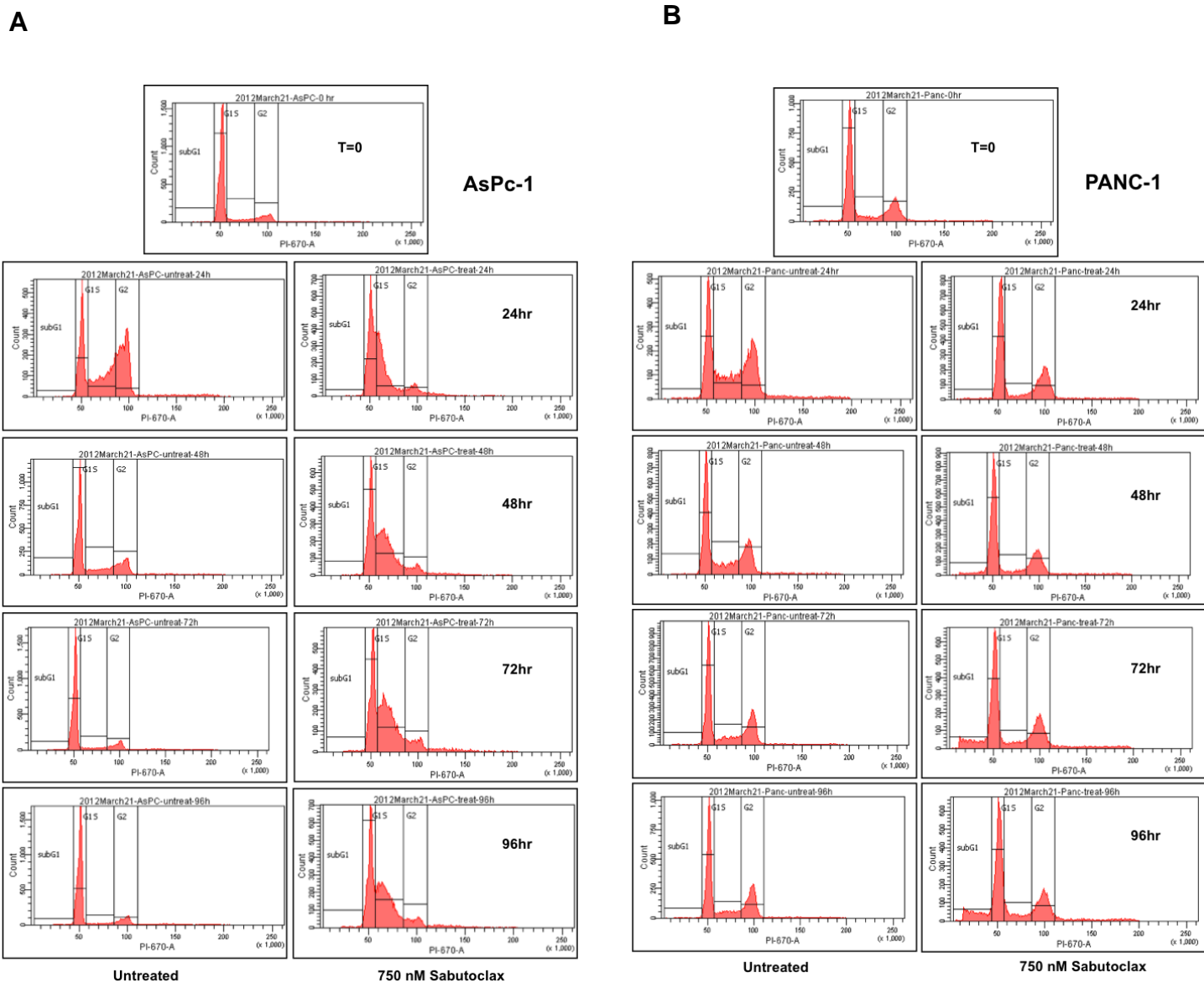


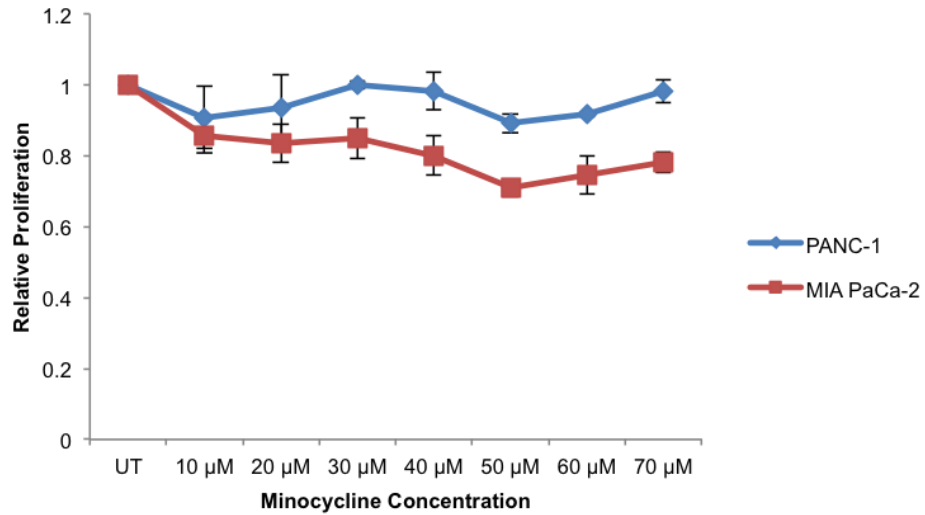
**Figure 9: Sabutoclax causes a G1-S phase cell cycle arrest. (A-B) FACS analysis data of graphs presented in Figure 8. Data representative of three independent experiments.**

## **Sabutoclax synergizes with synthetic tetracycline, Minocycline, in PDAC**

It is now almost axiomatic that to successfully combat cancer multiple targeting strategies used in combination will be necessary. Cancer cells develop resistance to initially effective treatments and acquire avoidance mechanisms preventing toxicity. Accordingly, combinatorial approaches attacking multiple pathways in a cancer cell can increase drug efficacy, reduce toxicity, and increase the time to resistance. Based on this concept, we sought to identify an agent that would promote synergy when combined with Sabutoclax. Minocycline, a commonly used antibiotic, can negatively impact cancer growth and survival (111-115). Despite this, it paradoxically also protects cells in the face of an insult through inhibition of mitochondrial apoptosis and upregulation of Bcl-2 (116-118). For these reasons, we hypothesized that these drugs might work well in combination, given their cancer-selective toxicities as single agents and the potential of Sabutoclax to counteract the pro-survival effects of Minocycline.

Minocycline is fairly nontoxic to several PDAC cells (MIA PaCa-2 and PANC-1), but is inhibitory in others (AsPC-1 and BxPC-3) (Fig. 10). In resistant cells, the combination of Sabutoclax and Minocycline is very toxic and significantly reduces cell proliferation and overall cell number, and induces cell death to a much greater extent than either agent alone in MIA PaCa-2 (Fig. 11) and PANC-1 cells (Fig. 15-16). Combination index values also demonstrate synergy between these two compounds (Fig. 13). It also promotes increased apoptosis and reduced colony formation in PDAC cells. Importantly, this synergistic effect is not evident in the non-cancerous cell line, HPNE (Fig. 12).

**A**



**B**

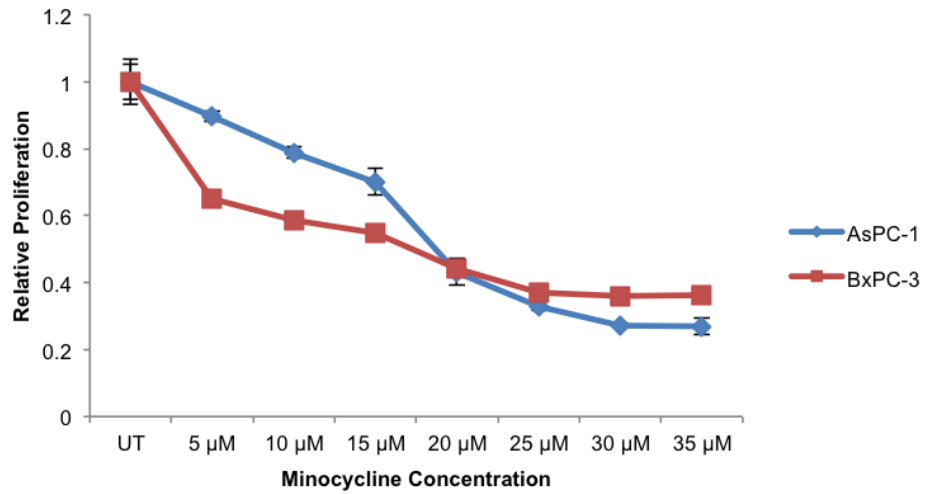


**Figure 10: Pancreatic cancer cells exhibit varying levels of sensitivity to Minocycline.** MTT proliferation assay in MIA PaCa-2 and PANC-1 cells (**A**) and AsPC-1 and BxPC-3 cells (**B**) 72 hours post treatment. Experiments done in triplicate and independently repeated three times.

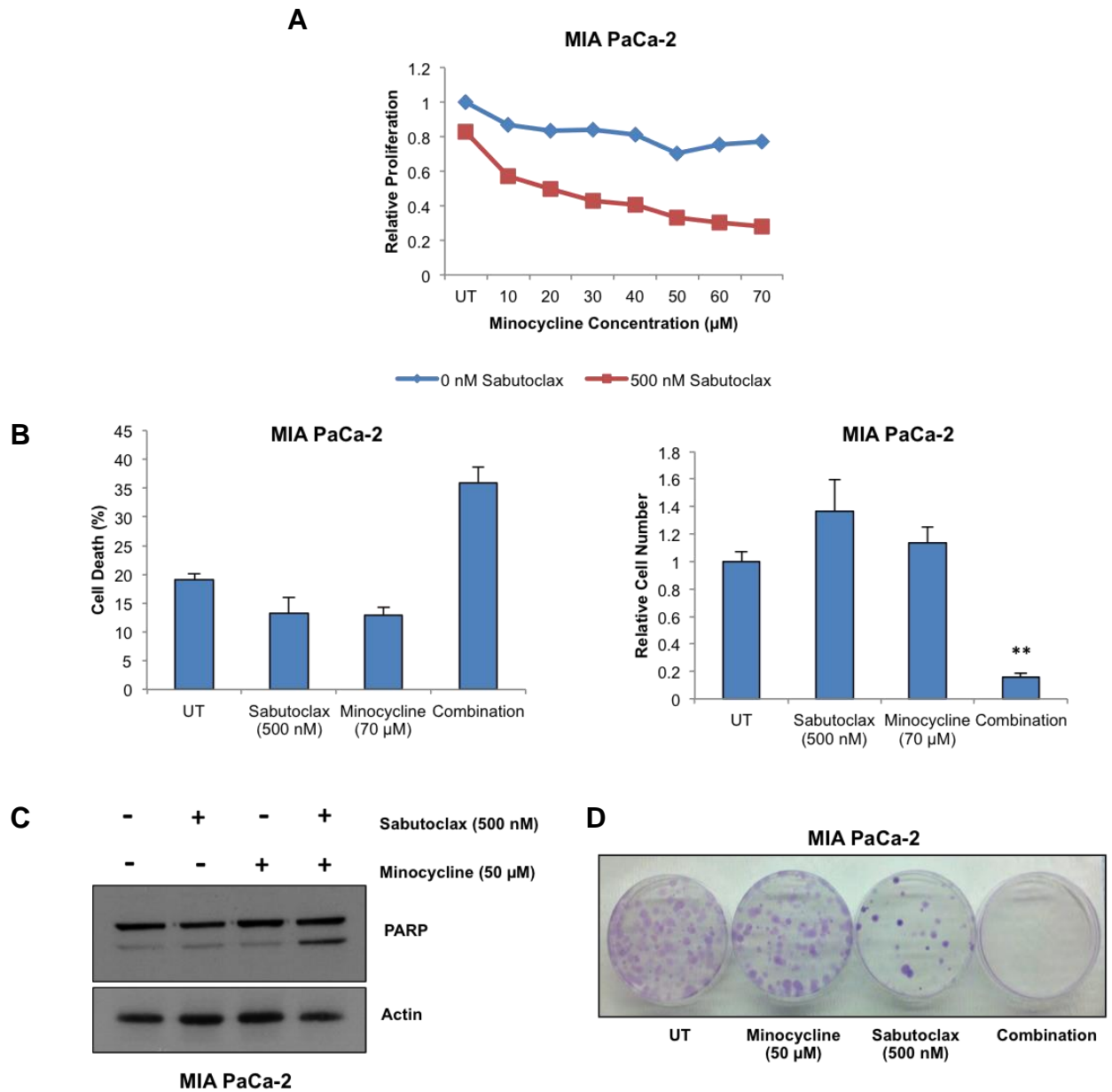


**Figure 11: The combination of Sabutoclax and Minocycline produce synergistic cytotoxic effects.** (A) MTT proliferation assay in MIA PaCa-2 cells 72 hours post treatment. Experiments done in triplicate and independently repeated three times. (B) Trypan blue assays evaluating cell death and cell numbers in MIA PaCa-2 cells 48 hours post treatment. \*\* $p < 0.0001$ . Experiments done in triplicate and independently repeated three times. (C) Western blotting of whole cell lysates for PARP expression in MIA PaCa-2 cells 48 hours post treatment. Actin was used as a loading control. Data representative of three independent experiments. (D) Colony forming assay in MIA PaCa-2 cells. Experiments done in triplicate and independently repeated three times.

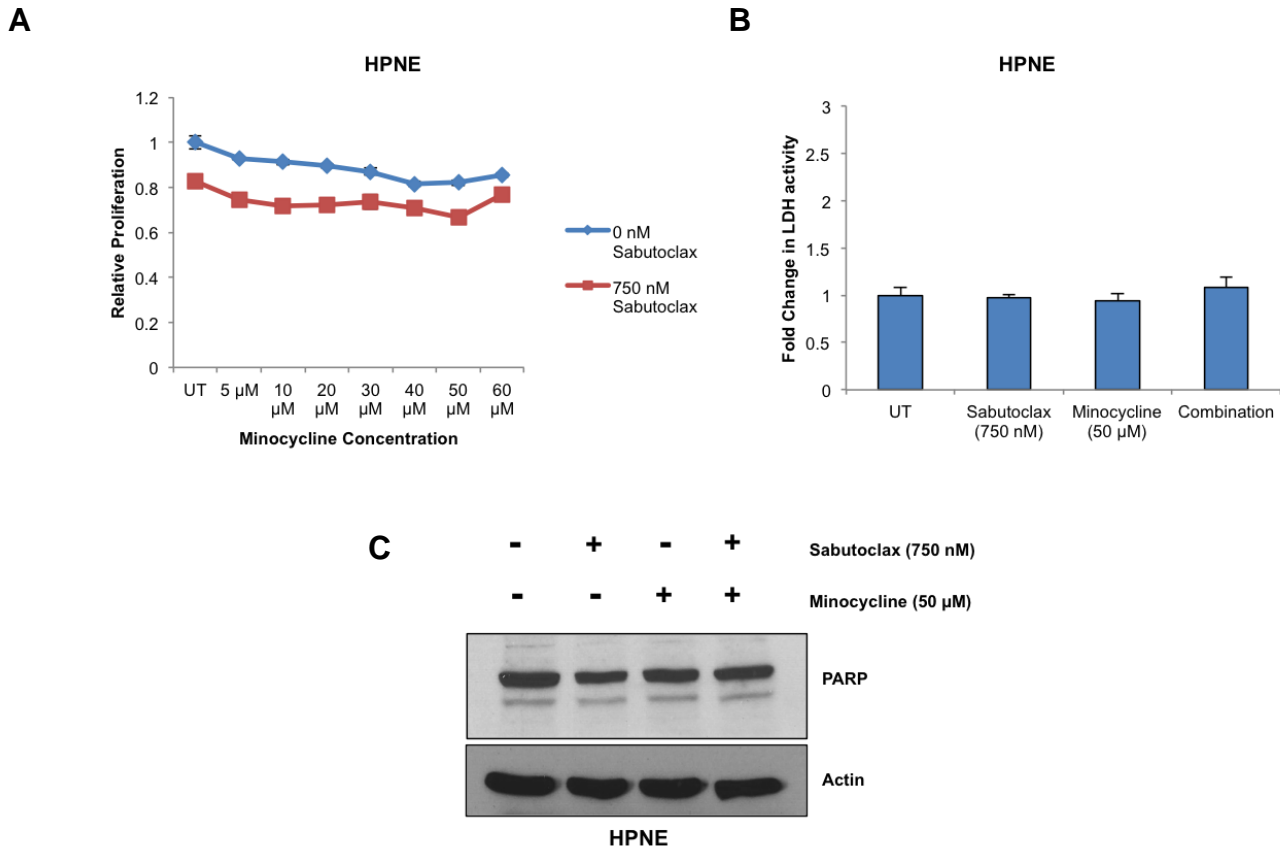
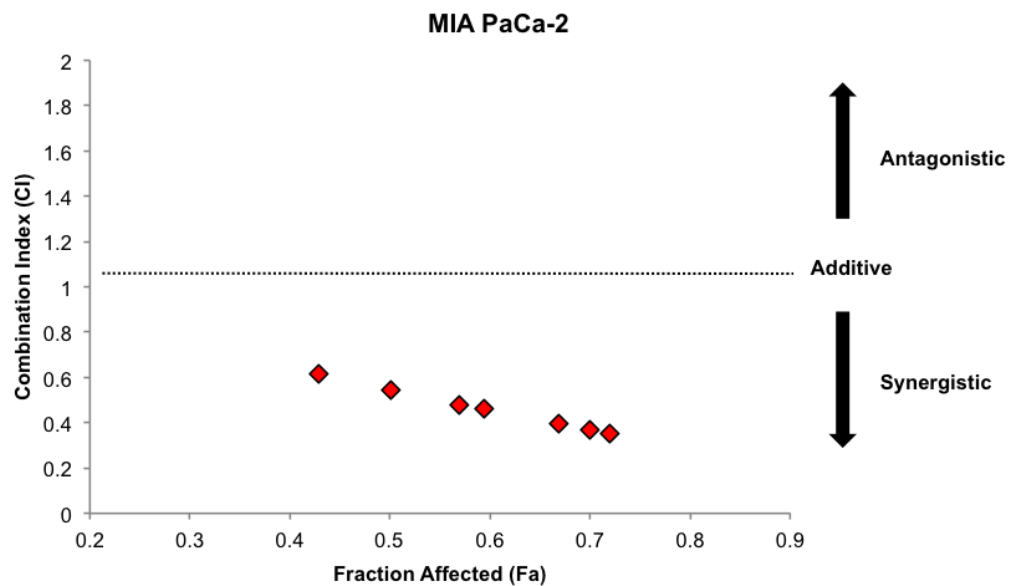


**Figure 12: The combination of Sabutoclax and Minocycline produce synergistic cytotoxic effects.** (A) MTT proliferation assays in HPNE cells 72 hours post treatment. Experiments done in triplicate and independently repeated three times. (B) LDH cytotoxicity assay in pancreatic epithelial cell line, HPNE. Experiments done in triplicate and independently repeated three times. (C) Western blotting for PARP using whole cell lysates from HPNE cells 48 hours post treatment. Data representative of three independent experiments.



Dose Sab ( $\mu\text{M}$ )	Dose Mino ( $\mu\text{M}$ )	Effect	CI
0.5	10.0	0.42828	0.61389
0.5	20.0	0.50104	0.54367
0.5	30.0	0.5698	0.47955
0.5	40.0	0.59384	0.46144
0.5	50.0	0.66856	0.39513
0.5	60.0	0.69918	0.37046
0.5	70.0	0.71933	0.35468

**Figure 13: Sabutoclax and Minocycline show synergy.** Combination index (CI) values for the combination of Sabutoclax and Minocycline in MIA PaCa-2 cells.

We next sought to define the mechanism underlying this synergy. The combination of subtoxic doses of Sabutoclax and Minocycline induced potent cell death that was partially abrogated by pretreatment with zVAD, indicating that this toxic effect is, in part, caspase-mediated. This rescue phenotype is evident in the morphology of treated cells (Fig. 14A, 16) and through reductions in LDH activity, indicating lower levels of cell death (Fig.14B, 15B). Furthermore, PARP cleavage was reduced in cells pretreated with zVAD (Fig. 14C, 15A). When specific caspases were evaluated, the combination treatment showed caspase-3 cleavage and loss of full-length caspase-8. In zVAD-treated samples, caspase-3 cleavage was not seen at all and levels of full-length caspase-8 were partially restored.



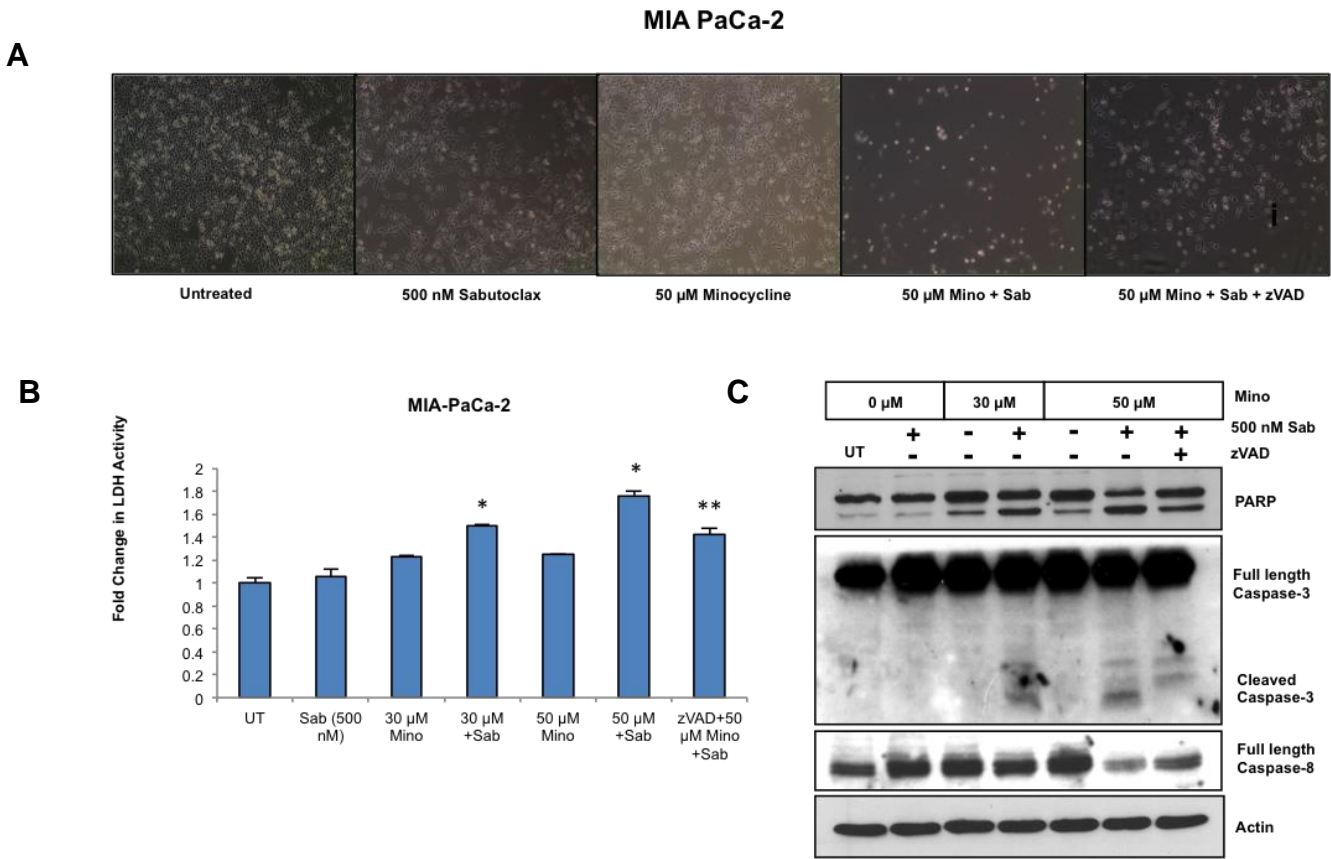


**Figure 14: The cytotoxicity induced by Sabutoclax and Minocycline is caspase-dependent and dependent upon loss of Stat3 activation. (A)** Phase contrast images showing MIA PaCa-2 cells 48 hours post Sabutoclax and/or Minocycline treatment. Experiments done in triplicate and independently repeated three times. **(B)** Media from

plates photographed in panel A was collected and used for LDH activity assays. \* $p < 0.005$  as compared to single drug treated samples. \*\* $p = 0.006$  as compared to 50  $\mu\text{M}$  Minocycline + Sabutoclax-treated samples. Experiments done in triplicate and independently repeated three times. (C) Western blotting of whole cell lysates for expression of PARP, caspase-3, and caspase-8. Actin was used as a loading control. Data representative of three independent experiments.

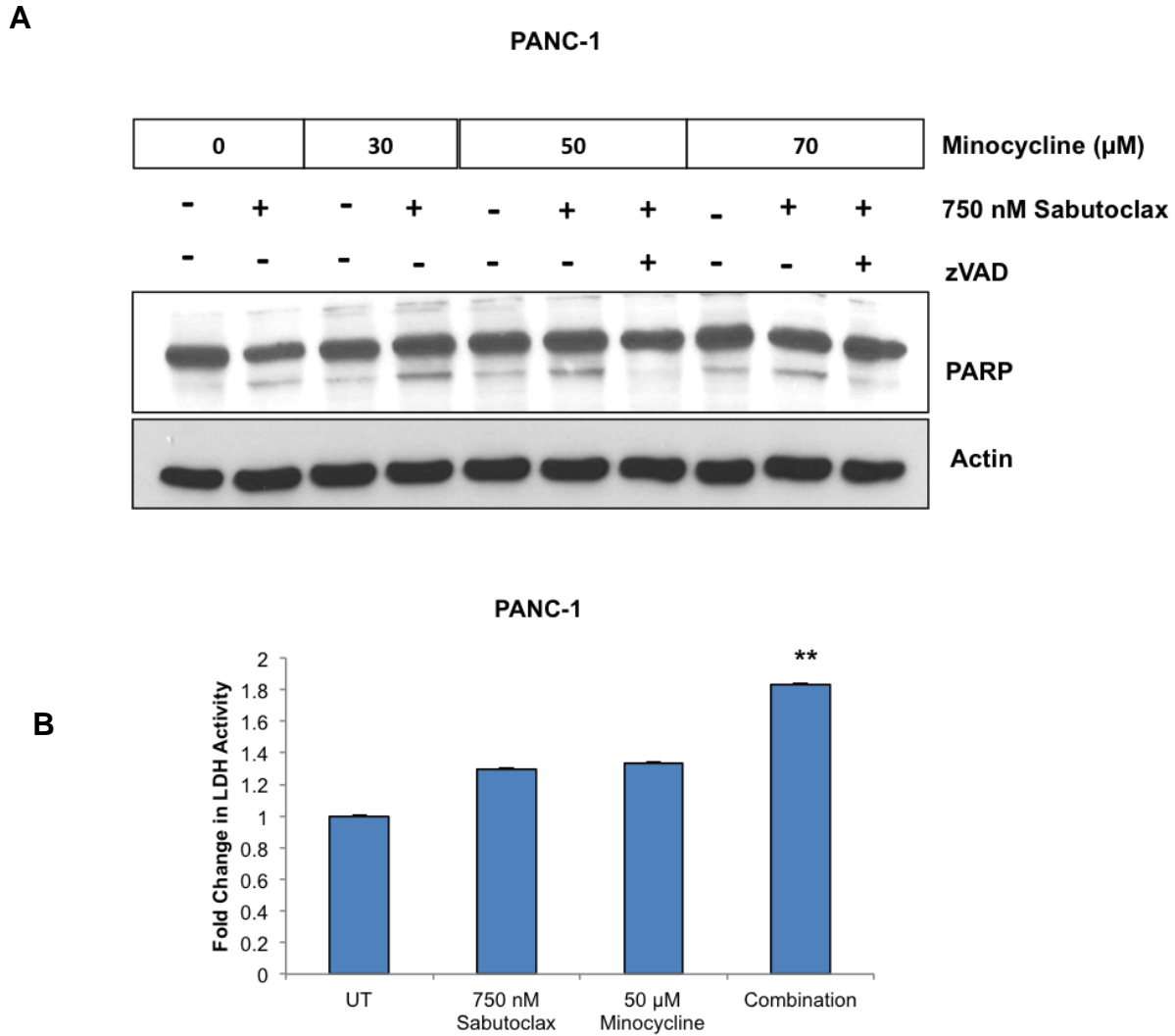


**Figure 15: Sabutoclax and Minocycline induce cytotoxicity in PANC-1 cells that is reversed with zVAD. (A) Western blotting of whole cell lysates for expression of PARP**

48 hours post treatment. Actin was used as a loading control. Cells treated with zVAD were incubated with the inhibitor for 1 hour prior to combination treatment. Data representative of three independent experiments. (B) Media from plates used for western blots in panel A was used for LDH activity assays. \*\*p=0.01.

**A**

PANC-1

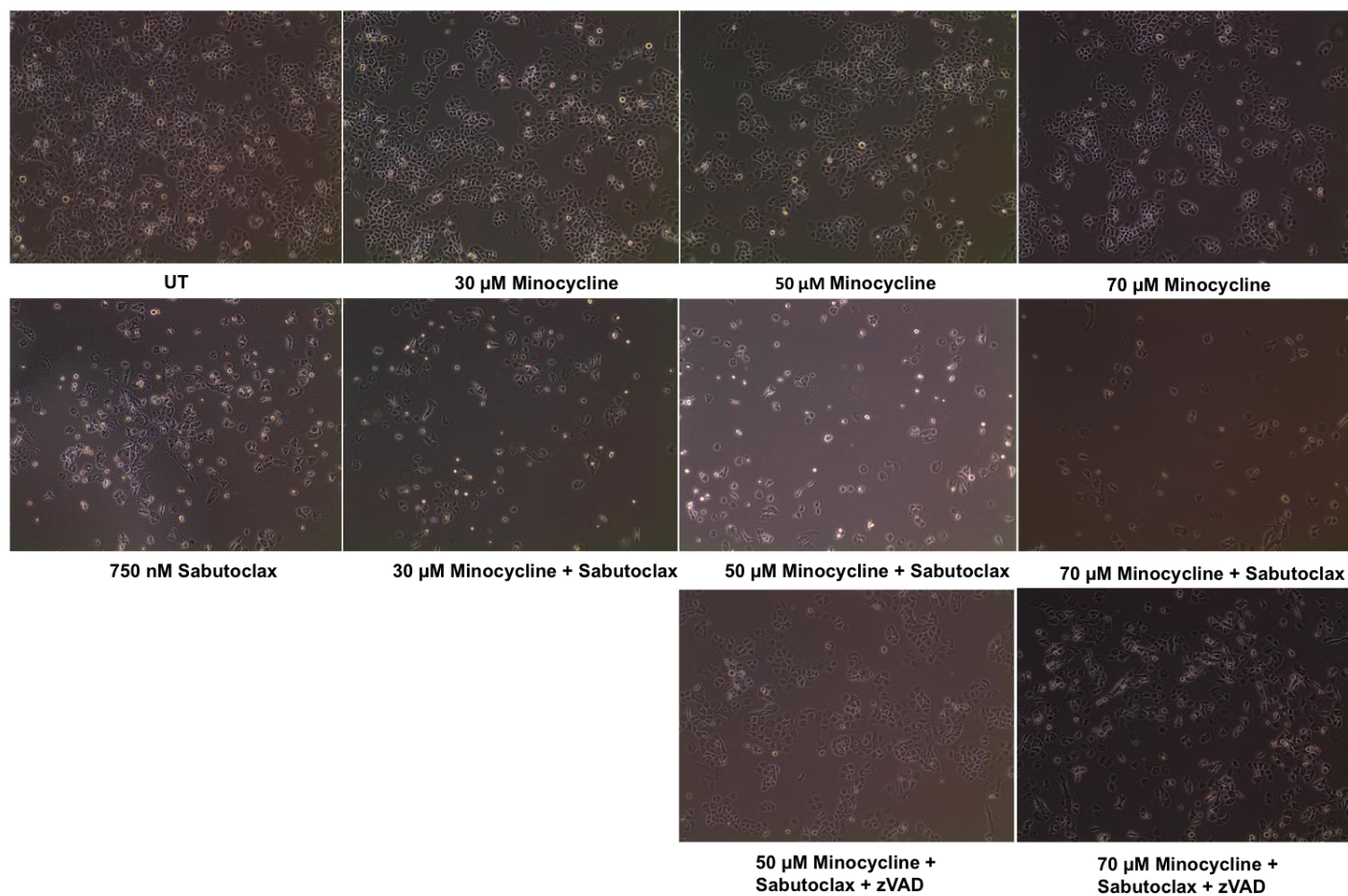


**Figure 16: Sabutoclax and Minocycline induce cytotoxicity in PANC-1 cells that is reversed with zVAD.** (A) Phase contrast images showing PANC-1 cells 48 hours after treatment. Data representative of three independent experiments.

### **The cytotoxic effect of Sabutoclax and Minocycline is Stat3-dependent**

Stat3 activation is clinically relevant for PDAC as constitutive activation of Stat3 has been reported in 30-100% of human tumor specimens, and is crucial for PDAC initiation, progression, and maintenance (125). Sabutoclax treatment resulted in a potent loss of Stat3 phosphorylation (Tyr 705), as well as a loss of downstream Stat3 targets, such as survivin (Fig. 17A). Minocycline alone induced similar changes (Fig. 17B). Subtoxic doses of each drug lowered Stat3 activation, but the combination of both drugs almost completely eliminated pStat3 expression (Fig. 17C). To determine whether this would affect the cytotoxicity of the combination, we created MIA PaCa-2 clones stably expressing an activated Stat3 mutant, Stat3 Y705F, e.g. C 13 (Fig. 18A). As compared to the parental cell line, C 13 showed enhanced resistance to combination treatment (Fig. 18B). A similar elevated resistance was observed in other Stat3 Y705F overexpressing MIA PaCa-2 clones (data not shown). Because pretreatment with zVAD partially rescued cells from Sabutoclax and Minocycline-induced cell death, we evaluated expression of a variety of caspases to determine their potential involvement not only in death induced by the combination, but which ones might be affected in C 13 cells (Figure 18C). In parental MIA PaCa-2 cells, caspases 3, 7, and 8 were cleaved.

Loss of full-length caspases 2 and 6 was evident, whereas AIF, caspase 12, and caspase 10 (caspase 10 data not shown) were not significantly altered. In C 13 cells, however, we did not see any significant changes in any caspase examined, supporting the observation that loss of Stat3 activation is necessary for caspase-dependent cell death by Sabutoclax and Minocycline. We also created stable cell lines overexpressing Stat3 Y705F in PANC-1 cells. Similar to what we observed in MIA PaCa-2 cells, constitutive Stat3 activation in these clones protected them from cytotoxicity induced by the combination of Sabutoclax and Minocycline (Fig. 19).

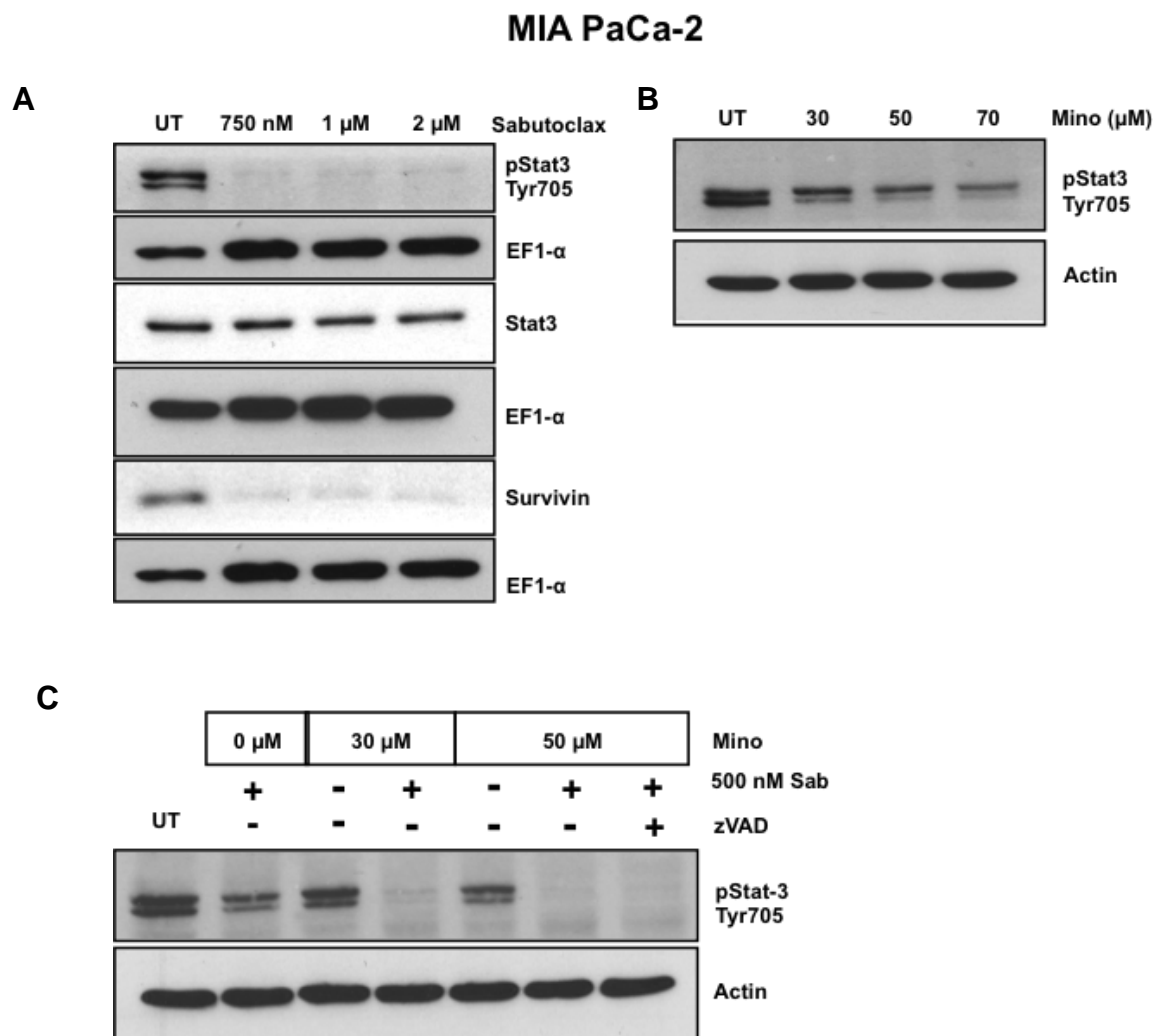


**Figure 17: The cytotoxicity induced by Sabutoclax and Minocycline is caspase-dependent and results in loss of Stat3 activation. (A-B)** Western blotting of whole cell lysates for pStat3 Tyr705, Stat3, Survivin, Actin (loading control) and EF1- $\alpha$  (loading

control) 48 hours post treatment. Data representative of three independent experiments. **(C)** Western blotting of whole cell lysates for pStat3 Tyr705 48 hours post treatment. Actin was used as a loading control. Cells were incubated with zVAD for 1 hour prior to Sabutoclax and Minocycline treatment. Data representative of three independent experiments.

**A**

**B**

**C**

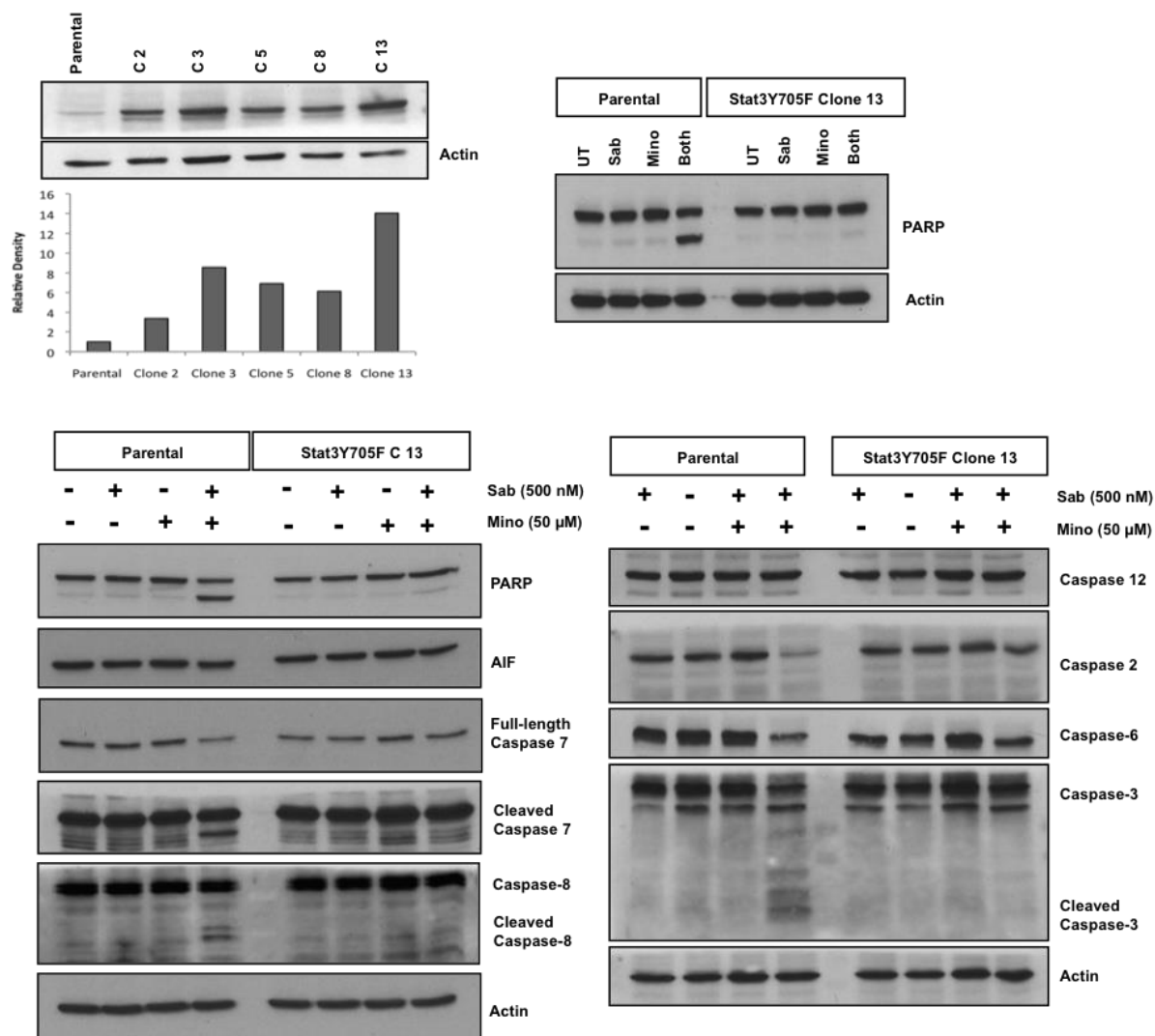


**Figure 18: The cytotoxicity induced by Sabutoclox and Minocycline is dependent upon loss of Stat3 activation.** (A) Western blotting of whole cell lysates from MIA-PaCa-2-Stat3Y705F stable clones for pStat3 Tyr705. Actin was used as a loading control. Graph below blot shows quantification. Data representative of three independent experiments. (B) Western blotting of whole cell lysates for PARP in parental MIA PaCa-2 and Stat3Y705F stable clone 13. Actin was used as a loading control. Sab = 500 nM Sabutoclox, Mino = 50 μM Minocycline. Data representative of three independent experiments. (C) Western blotting of whole cell lysates 48 post treatment for PARP, AIF, Caspase-7, Caspase-8, Caspase-12, Caspase-2, Caspase-6, and Caspase-3. Actin was used as a loading control. Data representative of three independent experiments.



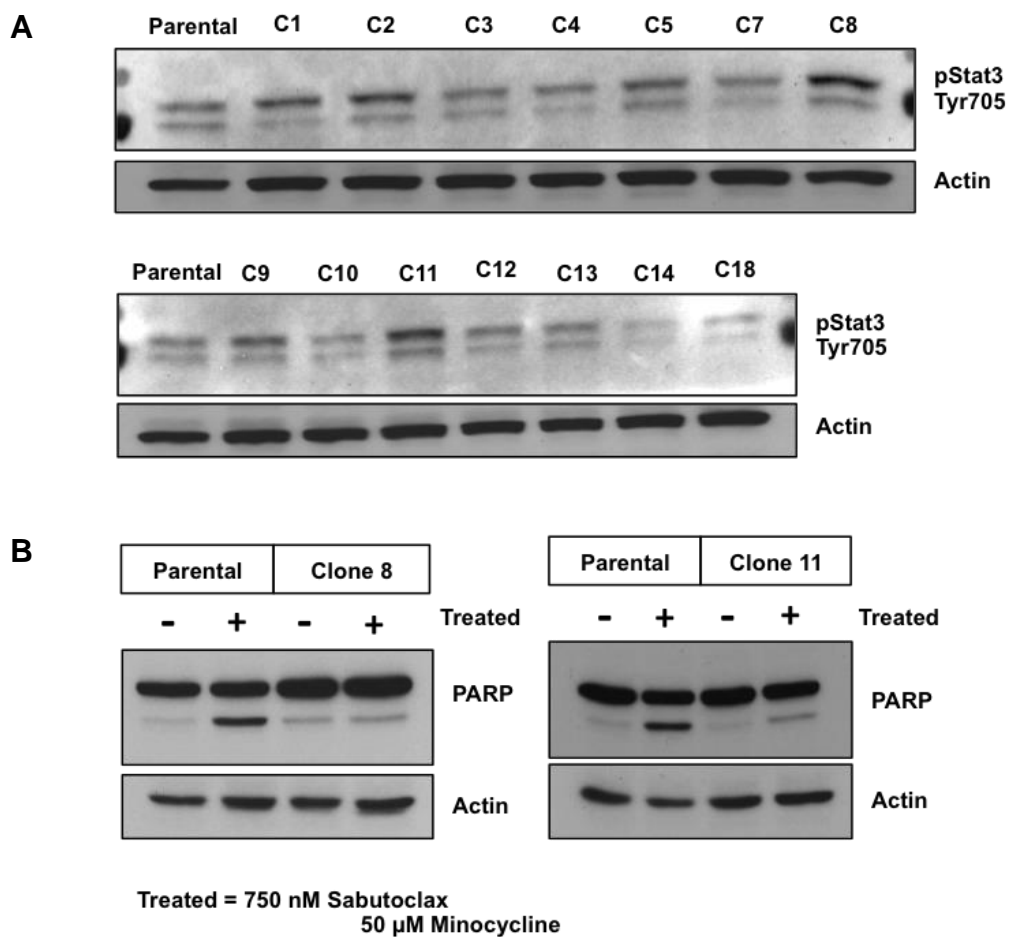


**Figure 19: The cytotoxicity induced by Sabutoclax and Minocycline is dependent upon loss of Stat3 activation.** (A) Western blotting of whole cell lysates from PANC-1-Stat3Y705F stable clones for pStat3 Tyr705. Actin was used as a loading control. (B) Western blotting of whole cell lysates for PARP in parental PANC-1 cells and Stat3Y705F stables clones 8 and 11. Actin was used as a loading control. Data representative of three independent experiments.

**Sabutoclax and Minocycline induce cytotoxicity through the intrinsic pathway of apoptosis**

Caspase-8 activation is an integral part of the extrinsic pathway of apoptosis. However, it can also be activated independent of this pathway by other caspases (126). To determine if caspase-8 involvement was due to extrinsic pathway activation or downstream intrinsic pathway activation, we used Z-IETD-FMK to specifically inhibit caspase 8 before drug treatment. Unlike the pan caspase inhibitor, zVAD, pretreatment with Z-IETD-FMK did not protect cells from Sabutoclax and Minocycline-induced cell death (Fig. 20). This indicates that caspase-8 activation is dispensable for Sabutoclax and Minocycline-induced cell death and is most likely a secondary effect of other caspases. Therefore, our data support the hypothesis that Sabutoclax and Minocycline induce a cytotoxic phenotype through activation of the intrinsic pathway of apoptosis.

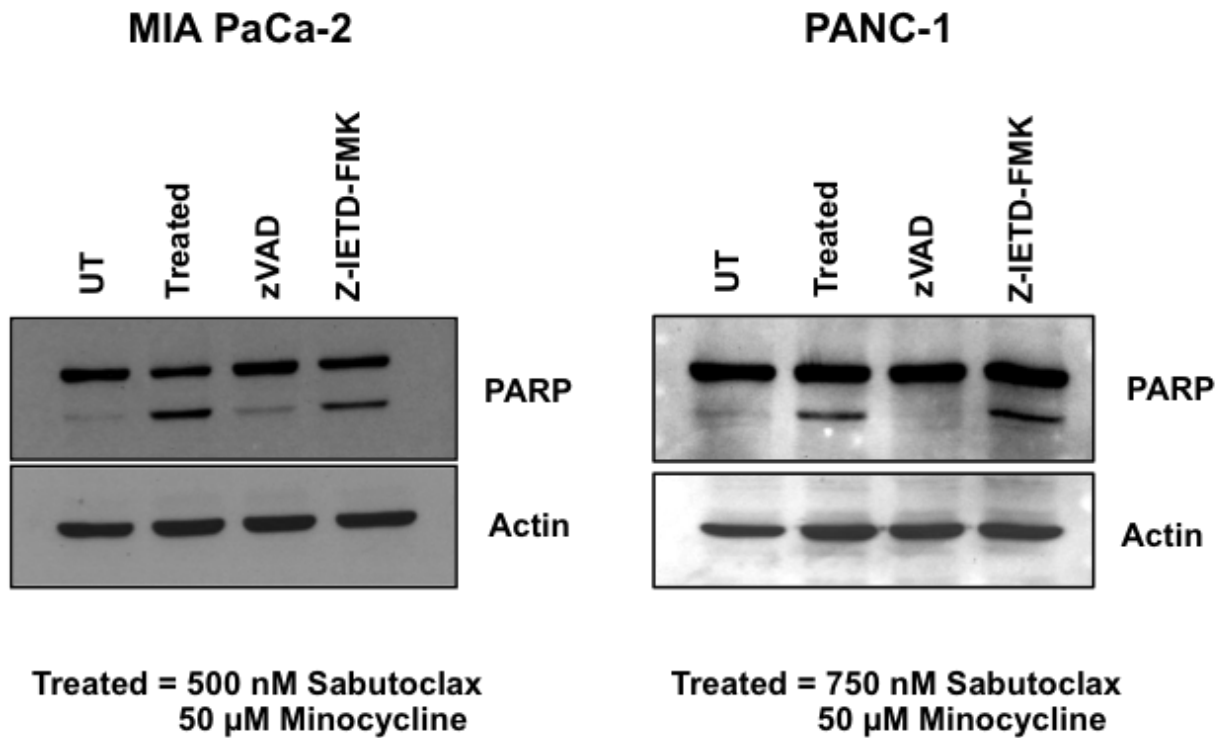
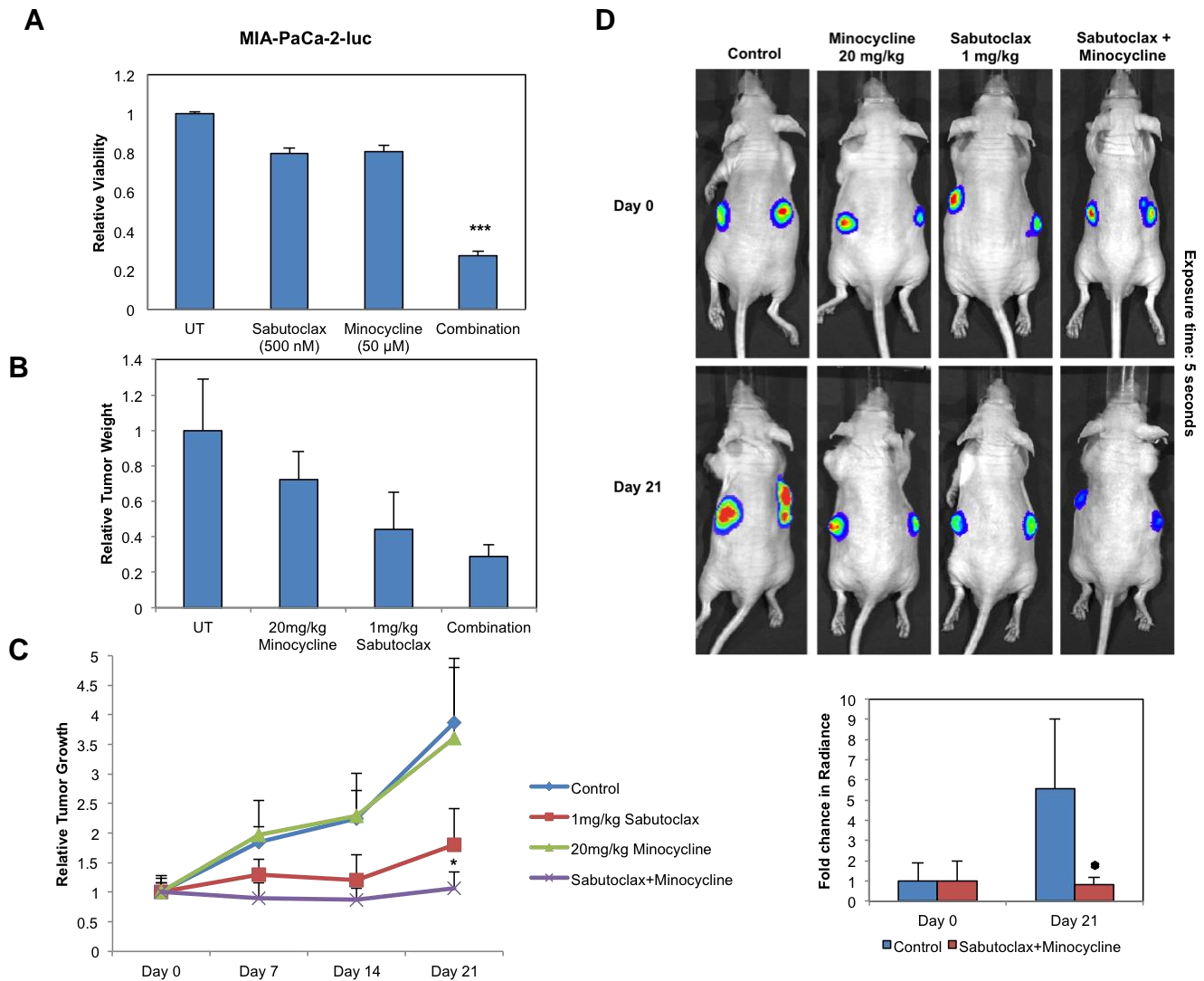


**Figure 20: The cytotoxicity induced by Sabutoclax and Minocycline works through the intrinsic pathways of apoptosis.** Western blotting 48 hours post treatment for PARP and Actin (loading control). Cells were incubated with zVAD or z-IETD-FMK for 1 hour prior to treatment with Sabutoclax and Minocycline. Data representative of three independent experiments.

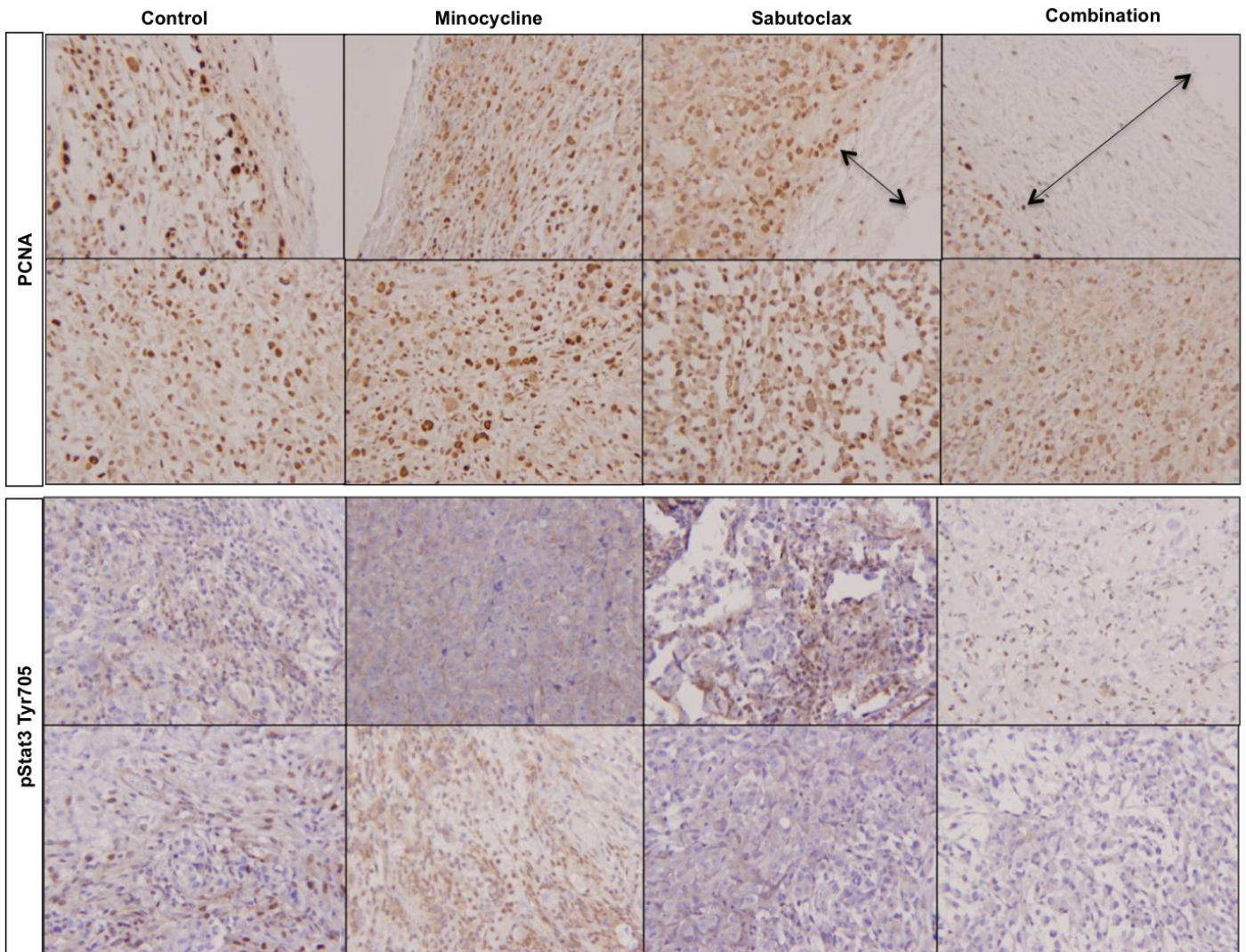
### **Sabutoclax alone reduces tumor growth in a xenograft model of pancreatic cancer and this effect is enhanced with the addition of Minocycline**

Luciferase-expressing MIA PaCa-2 cells, displaying a similar phenotype as parental cells (Fig. 21A), were established as subcutaneous xenografts in athymic nude mice, which were then treated with Sabutoclax (1 mg/kg), Minocycline (20 mg/kg), or both agents. Both drugs were given via IP injection 3x/week. Minocycline treatment alone showed minimal effects, while Sabutoclax alone showed greater reductions in tumor weight and growth (Fig. 21B-C). Despite this, animals treated with a combination of Sabutoclax and Minocycline showed a synergistic reduction in tumor growth, with a significantly smaller tumor growth rate, even as compared to Sabutoclax alone (Fig. 21C). This was confirmed with bioluminescence imaging (BLI) (Fig. 21D). A similar experiment was conducted using PANC-1-luc cells resulting in the same trend, with the combination group showing significant inhibition of tumor growth (Fig. 23).

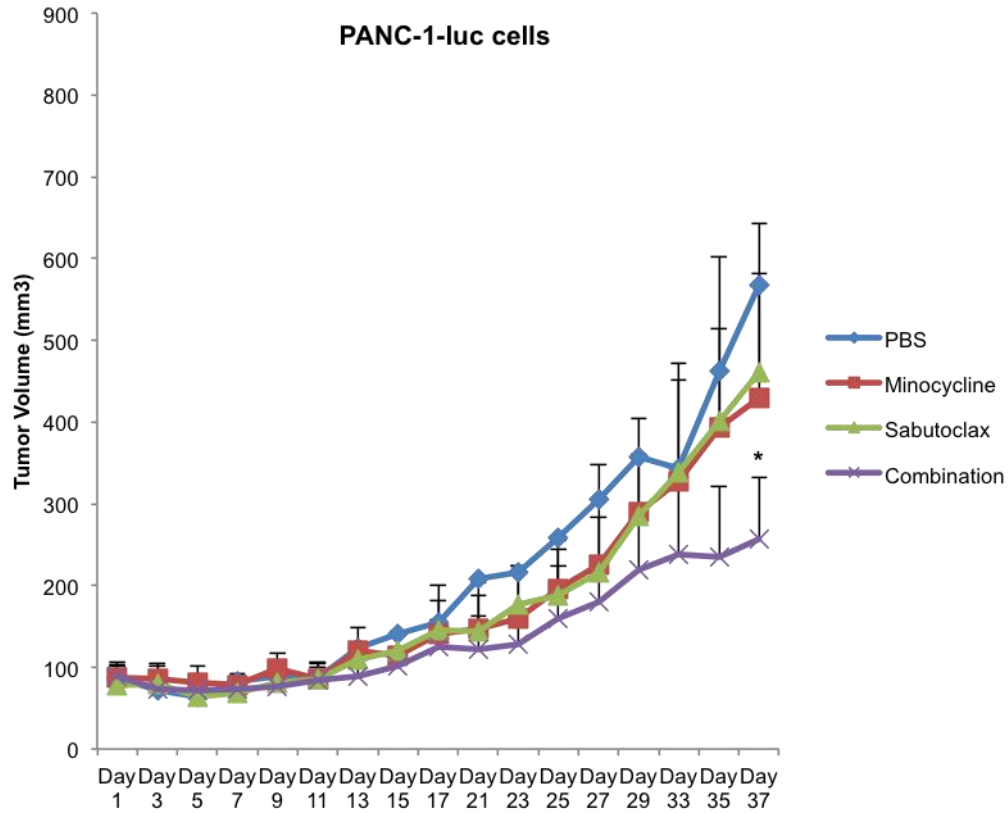
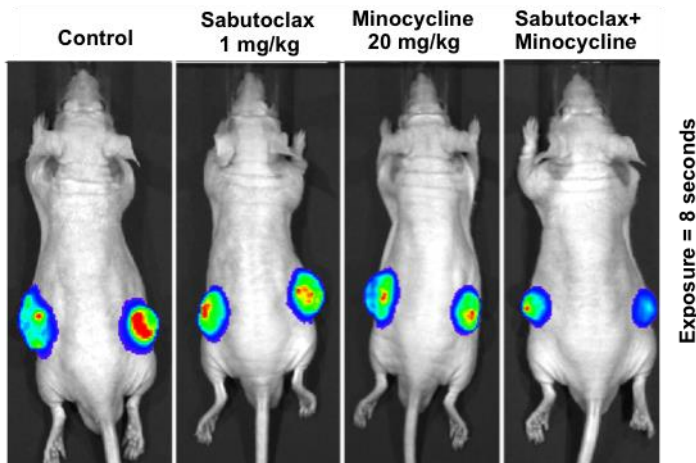
Immunohistochemistry of tumor sections (Fig. 22) demonstrated higher intensity proliferation marker PCNA staining in control, Sabutoclax, and Minocycline-treated groups as compared to the combination-treated group. Furthermore, combination-treated tumors showed significantly less phosphorylated Stat3 expression, consistent with *in vitro* observations.



**Figure 21: Sabutoclax reduces tumor growth in a subcutaneous xenograft model and is enhanced by the addition of Minocycline.** (A) MTT proliferation assay of MIA PaCa-2 cells stably expressing luciferase after treatment with Sabutoclax and/or Minocycline. \*\*\* $p < 0.0001$ . Experiments done in triplicate and independently repeated three times. (B) Tumor weight as normalized to the control animals at the end of the experiment. (C) Tumor growth kinetics of MIA PaCa-2-luc cell subcutaneous tumors on the flanks of athymic mice. \* $p < 0.04$  as compared to all other groups. (D) Bioluminescence imaging (BLI) of tumors and image quantification. Exposure time = 5 seconds.  $n = 5$  mice/group.



**Figure 22: Sabutoclax and Minocycline reduce PCNA expression and Stat3 activation *in vivo*.** Tumors were fixed in formalin, embedded in paraffin, and sectioned for staining. Representative images of immunohistochemistry (IHC) stained with p-Stat3 Y705 and PCNA. Arrows in PCNA images show margin of negatively stained tumor area at the periphery of each tumor. Data representative of three independent experiments.

**A****B**

**Figure 23: Sabutoclax and Minocycline reduce tumor growth in a subcutaneous xenograft model of pancreatic cancer. (A)** Tumor growth kinetics of PANC-1-luc cell subcutaneous tumors on the flanks of athymic mice. \* $p < 0.04$  as compared to all other groups. **(B)** Bioluminescence imaging (BLI) of tumors. Exposure time = 8 seconds.  $n = 5$  mice/group

## Quasi-orthotopic xenograft mouse model

While subcutaneous xenograft studies are useful in evaluating *in vitro* observations in an *in vivo* setting, flank tumors do not accurately mimic natural disease states. To study the effect of our drugs in a more natural setting, we used a quasi-orthotopic model of PDAC (127). We found that MIA PaCa-2-luc cells, when injected intraperitoneally, specifically homed to the pancreas, with the majority of tumors or tumor nodules found in this organ. Other locations in which we found tumors (liver, peritoneal lining) are common places for this cancer to metastasize and more closely mimic the clinical picture of this disease.

In an initial set of experiments, we injected  $1 \times 10^6$  cells i.p. and allowed 1 week for tumor establishment before treating mice with Sabutoclax and Minocycline, alone or in combination. Consistent with our previous data, Minocycline as a single agent did not have any effect and mice presented similarly to control animals. Sabutoclax showed a potent single-agent effect, with fewer animals showing evidence of disease. The combination group showed even more promise (Fig. 24C), with only 1/7 mice showing tumors by BLI (Fig. 24A-B). Pancreas weight did not show significant differences, though the trend supported our other observations (data not shown).

A second quasi-orthotopic study was conducted using similar drug dosing parameters. Tumors, though, were initiated with the injection of  $5 \times 10^6$  cells as opposed to  $1 \times 10^6$ . In our first study, the use of fewer cells allowed testing whether Sabutoclax and Minocycline could prevent tumor formation. However, the use of fewer cells also means that the overall tumor burden was less when therapy was initiated,



which prevented determining the true magnitude of the effect Sabutoclax and Minocycline would have in the context of a greater tumor burden, which might more closely imitate the clinical setting.

As anticipated, injecting a greater number of cells resulted in a larger overall tumor burden in the animals. Mice from all groups developed tumors or tumor nodules in the pancreas. However, the weight of the pancreas from mice treated with both Sabutoclax and Minocycline was significantly less than those from animals in all 3 other groups and visually showed fewer gross nodules (Fig. 24D).

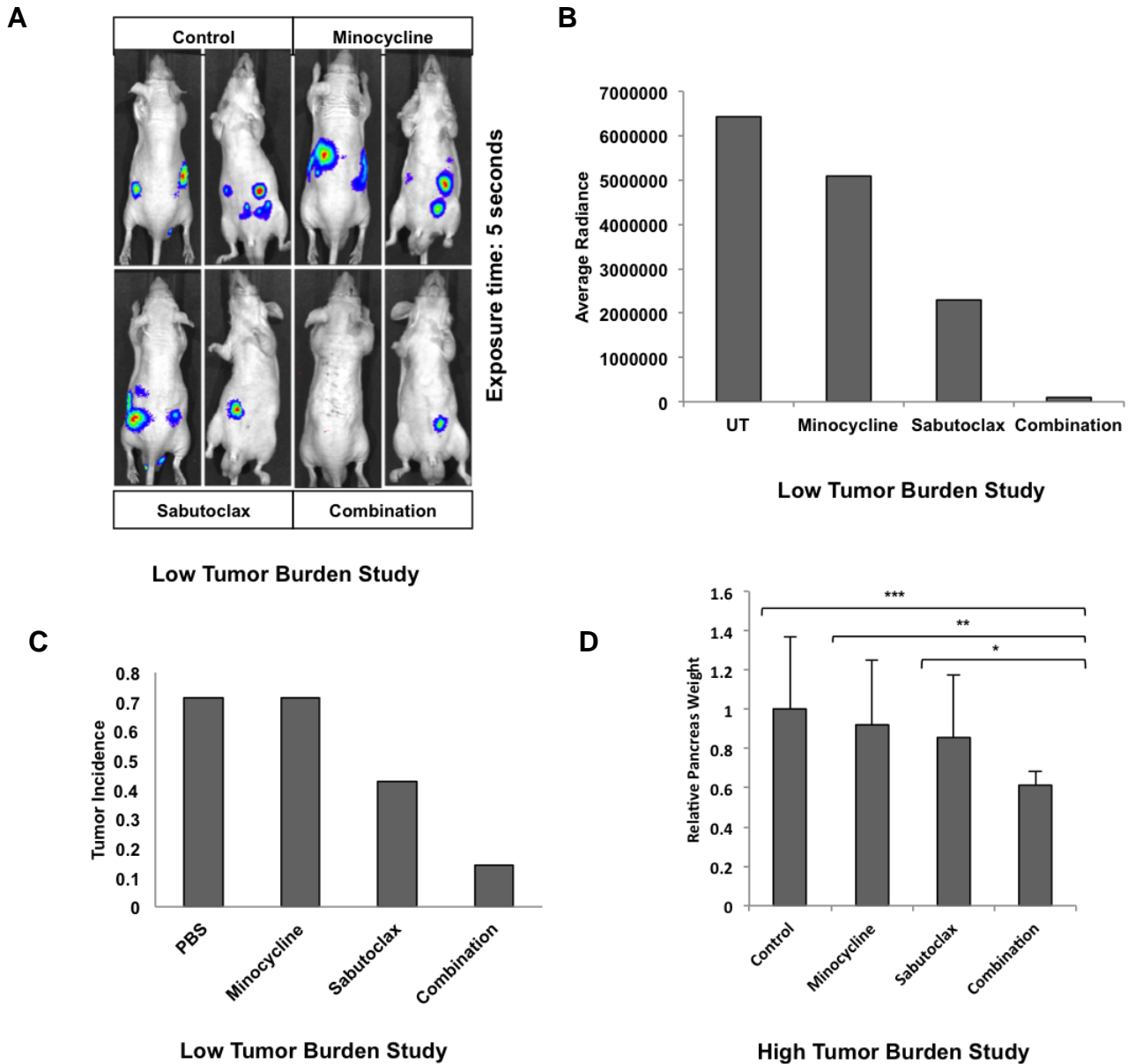


**Figure 24: Sabutoclox and Minocycline reduce tumor growth in a quasi-orthotopic xenograft model. (A)** Low Tumor Burden study: BLI images of mice post treatment. Exposure time = 5 seconds. **(B)** Image quantification of panel A. **(C)** Tumor incidence in pancreas – measured by imaging and by gross examination of animals at necropsy. n= 7 mice/group. **(D)** High Tumor Burden study: pancreas weight at necropsy. Treatment groups normalized to the control. \*p=0.03, \*\*p=0.01, \*\*\*p=0.004. n= 10 mice/group

## **Sabutoclax and Minocycline in a transgenic mouse model of PDAC (KPC)**

The KPC transgenic PDAC mouse model is used frequently in PDAC research (128-132). This animal spontaneously develops precursor pancreatic lesions, PanINs, which progress and eventually develop into invasive disease. Tumors form as a result of activated *K-ras* and functional loss of *p53* in the pancreas, genetic changes also seen in a high percentage of human tumors. Histological analysis shows extensive local invasion as well as metastasis in a subset of animals (133).

Pancreatic tumors from these mice overexpress Mcl-1 as shown by immunohistochemistry (Fig. 25A). This is consistent with the disease observed in humans (103-106) and provides a rationale for using Sabutoclax in these animals. Additionally, cell lines derived from these animals show combination effects with Sabutoclax and Minocycline (Fig. 25B). These cells were injected subcutaneously into the flanks of control KPC mice (*Pdx-1-Cre-negative/K-ras<sup>LSL-G12D</sup>/p53<sup>fllox/wt</sup>*) and allowed to grow for approximately one week. Mice were treated with Sabutoclax, Minocycline, or both drugs every 2-3 days via i.p. injection for a total of 6 injections. Sabutoclax or Minocycline alone did not significantly affect tumor growth. The combination of drugs, however, significantly inhibited tumor growth as compared to controls (Fig. 26). Immunohistochemistry of tumor sections demonstrated decreased staining for PCNA and pStat3 in combination-treated tumors (Fig. 27-28).

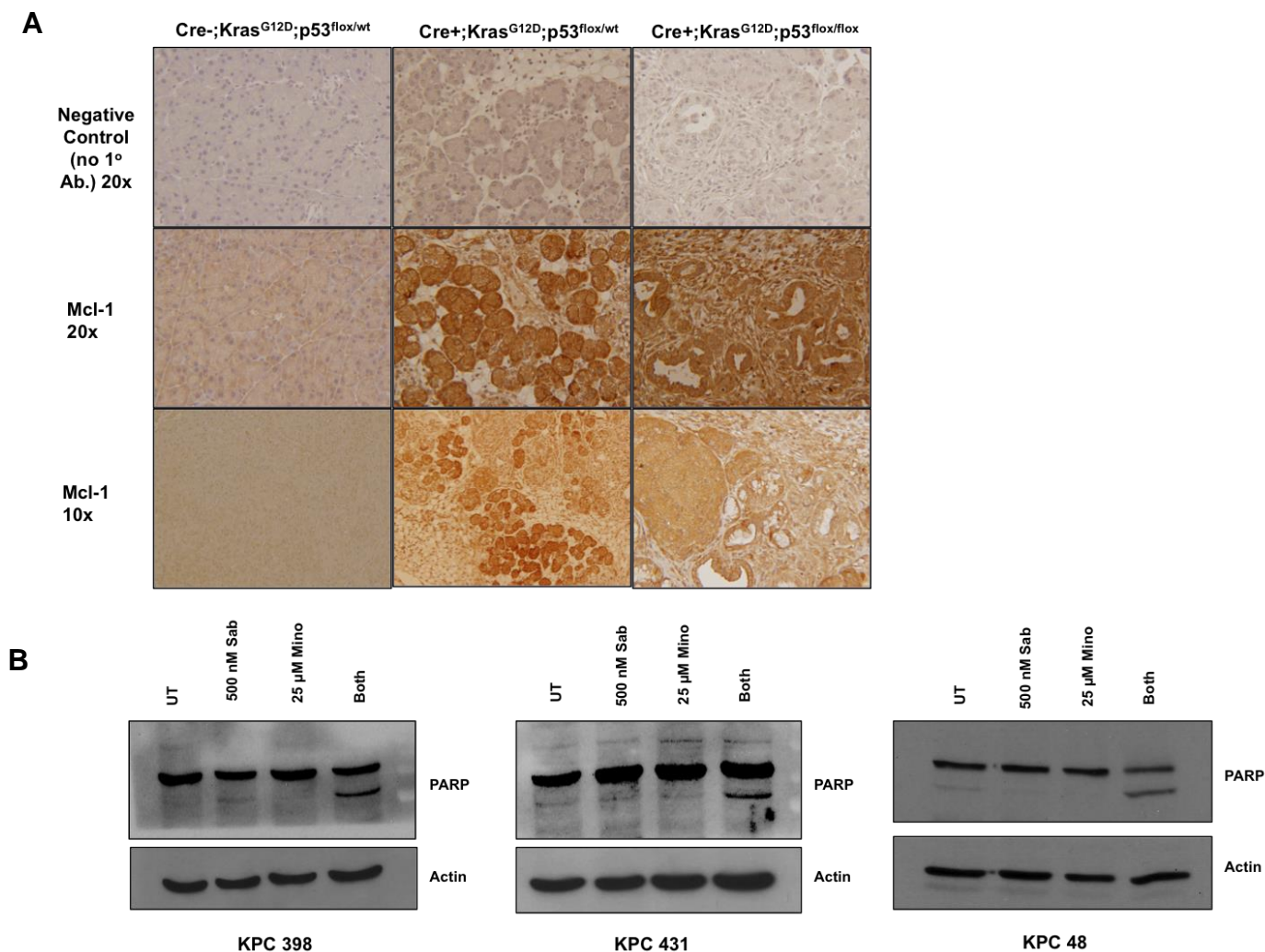


**Figure 25: KPC tumors express Mcl-1 and KPC cell lines show sensitivity to Sabutoclax and Minocycline.** Tumors from Pdx-1-Cre/*K-ras*<sup>LSL-G12D</sup>/*p53*<sup>flox/wt</sup> and Pdx-1-Cre/*K-ras*<sup>LSL-G12D</sup>/*p53*<sup>flox/flox</sup> mice overexpress Mcl-1 and show sensitivity to Sabutoclax and Minocycline. **(A)** IHC for Mcl-1 in sections of pancreas from control, Pdx-1-Cre/*K-ras*<sup>LSL-G12D</sup>/*p53*<sup>flox/wt</sup> and Pdx-1-Cre/*K-ras*<sup>LSL-G12D</sup>/*p53*<sup>flox/flox</sup> mice. **(B)** Western blotting of whole cell lysates for PARP 48 post treatment in cell lines derived from Pdx-1-Cre/*K-ras*<sup>LSL-G12D</sup>/*p53*<sup>flox/wt</sup> mice. Data representative of three independent experiments.

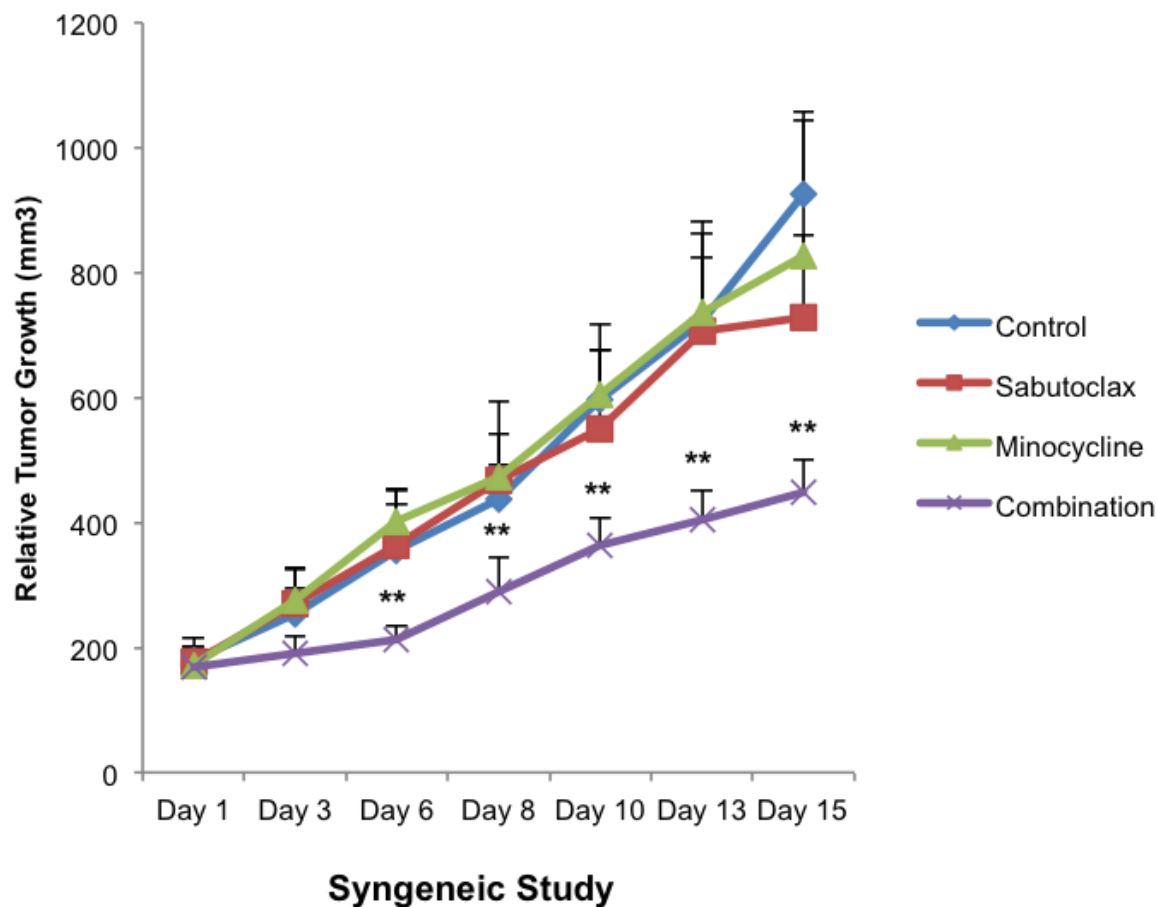


**Figure 26: Sabutoclax and Minocycline reduce tumor growth in a syngeneic KPC model.** Syngeneic study: Tumor growth kinetics of control Pdx-1-Cre negative/*K-ras*<sup>LSL-G12D</sup>/*p53*<sup>flox/flox</sup> mice bearing subcutaneous Pdx-1-Cre/*K-ras*<sup>LSL-G12D</sup>/*p53*<sup>flox/wt</sup>-derived tumors. \*\*p<0.01 as compared to all other groups. n= 5 mice/group.

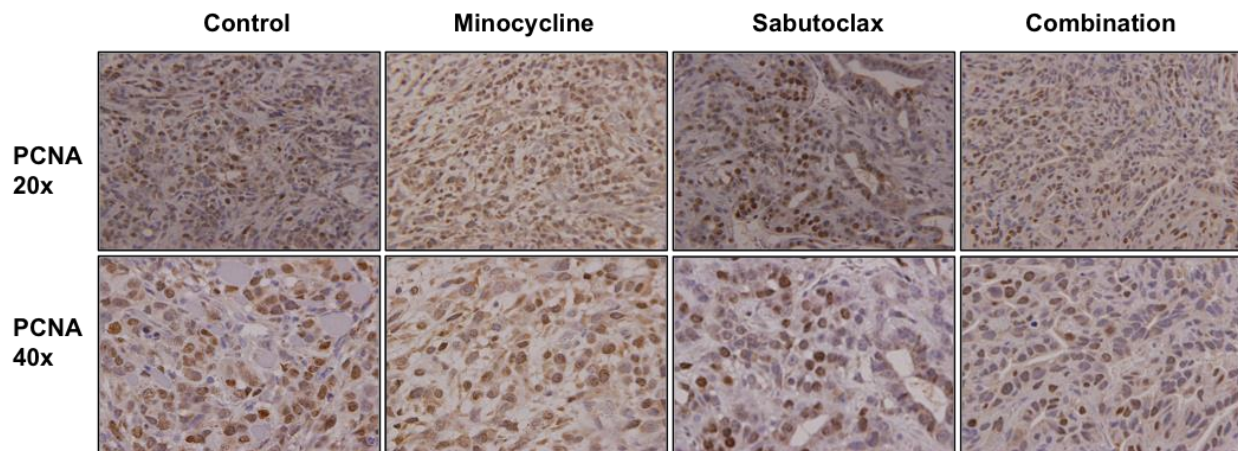


**Figure 27: Sabutoclax and Minocycline reduce proliferation in a syngeneic KPC model. IHC for PCNA. Data representative of three independent experiments.**

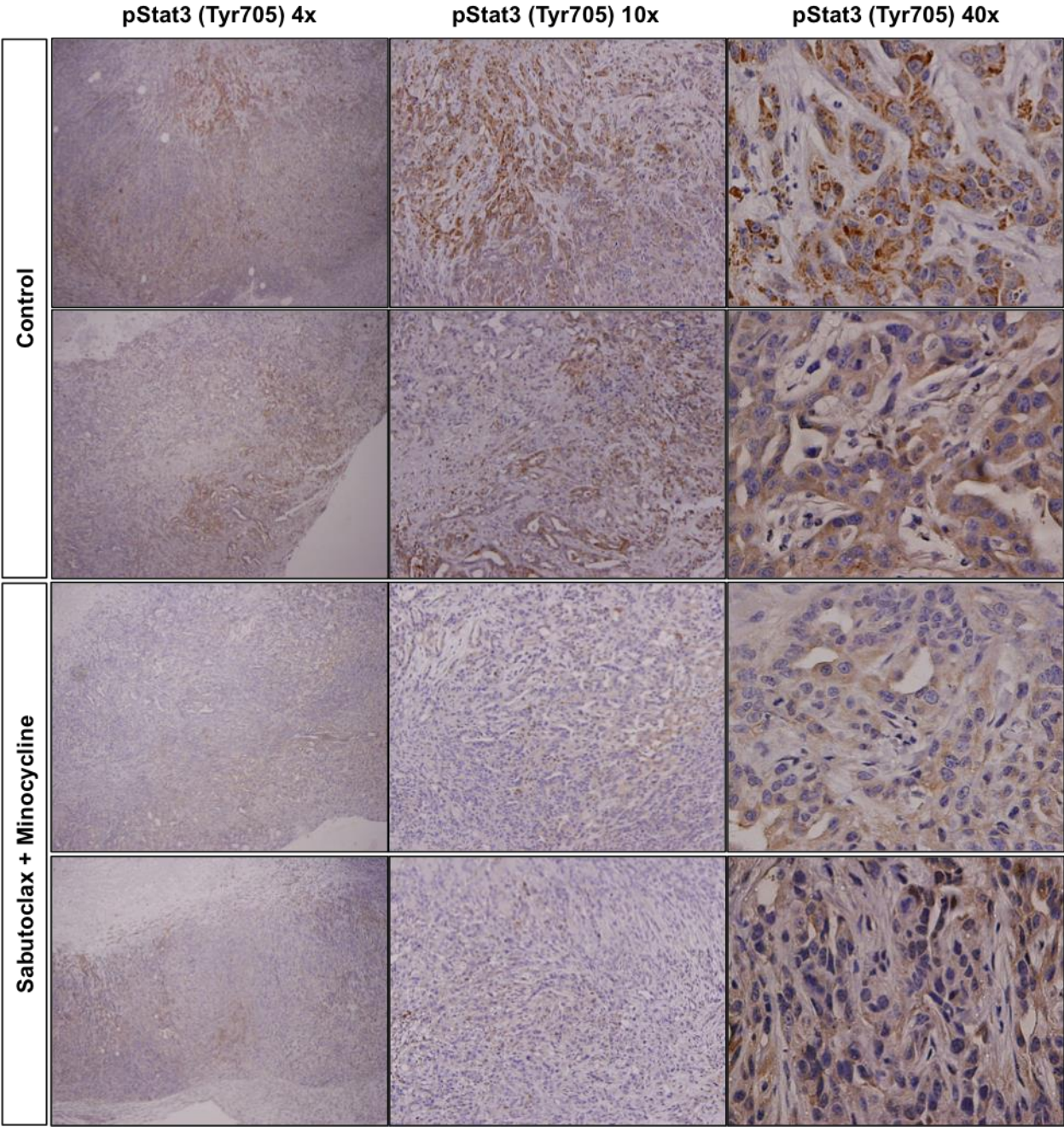
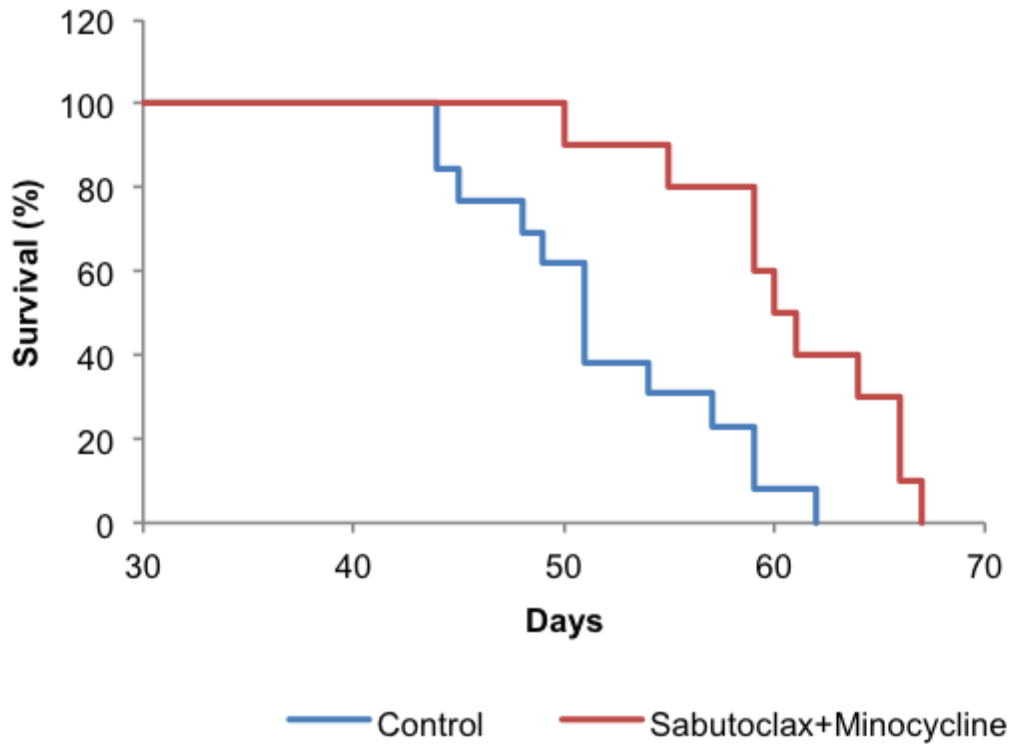


**Figure 28: Sabutoclax and Minocycline reduce Stat3 activation in a syngeneic KPC model.** IHC for pStat3 Y705. Data representative of three independent experiments.

Additionally, a survival study was done using KPC mice (Pdx-1-Cre/K-*ras*<sup>LSL-G12D</sup>/*p53*<sup>flox/flox</sup>) to determine the effects of Sabutoclax and Minocycline. Mice were treated with Sabutoclax (1 mg/kg), Minocycline (10 mg/kg), or a combination of both three times a week via i.p. injection starting at around 1 month of age and continuing until animals reached a moribund state. Mice receiving combination treatment showed a significant survival advantage as compared to control mice (Fig. 29). Importantly, no toxicity was seen from either drug in any of the animal studies conducted.





### KPC Transgenic Study

**Figure 29: Sabutoclax and Minocycline enhance survival in the KPC transgenic mouse model.** Kaplan-Meier survival curve for Pdx-1-Cre/*K-ras*<sup>LSL-G12D</sup>/*p53*<sup>fllox/fllox</sup> mice treated with Sabutoclax and Minocycline. \* $p=0.001$ .  $n = 12$  mice (control group);  $n = 10$  mice (Sabutoclax + Minocycline group).

## **Discussion:**

Pancreatic cancer is one of the most lethal cancers, remaining largely untreatable. Moreover, advances in therapy have been minimal over the last 15 years, due in part to the aggressive nature of PDAC and the difficulty in developing selective and effective therapeutics. We presently describe an efficacious novel drug combination for PDAC that uses a new BH3 mimetic and uncovers the hidden therapeutic potential of Minocycline as an anti-cancer agent.

Considering overexpression of the anti-apoptotic Bcl-2 proteins in PDAC, we initially evaluated the efficacy of Sabutoclax, a BH3 mimetic that targets these anti-apoptotic proteins, inhibiting their function. Sabutoclax was effective as a single agent. It induced cancer-inhibitory effects in multiple genetically diverse PDAC cell lines. Potent apoptosis-inducing activity was evident in some PDAC cell lines and in those that only showed minor increases in death, we found instead a potent cell cycle arrest. Tumor heterogeneity is a problem manifested to some degree in all cancers, but is especially relevant in PDAC, contributing to the global resistance seen in this cancer to conventional chemotherapeutics. A beneficial aspect of Sabutoclax is its anti-cancer activity in multiple PDAC cell lines, irrespective of genetic background.

Despite the potential of Sabutoclax as a single-agent, there is a pressing need for combination therapy in the clinical setting. Cancer is an adaptive disease and effectively combatting it requires a multifaceted approach. Because of this, we sought to find a second drug that would potentially synergize with Sabutoclax to further promote its clinical applicability. We focused on the antibiotic, Minocycline, which has a small literature base supporting a novel role for this drug in the field of cancer (111-

115). Despite these reports, translational cancer research using tetracyclines never expanded as only minor efficacy was evident with these drugs. In addition to its classical role as an antibiotic, Minocycline has also been studied extensively as a neuroprotective agent. Zhu, et. al. showed that this neuroprotection develops, in part, through the inhibition of caspase-9 and caspase-3 activation after exposure to death-inducing stimuli due to the inhibition of cytochrome c release from mitochondria (118). Minocycline has also been shown to lead to increases in the expression of anti-apoptotic Bcl-2 proteins like Bcl-2 (116,117). We hypothesized that these properties might actually mask the true potential of Minocycline as a cancer therapeutic and contribute to the disappointing results seen in the past. However, we hypothesized that these properties might make it an ideal combination partner for Sabutoclax. Sabutoclax works by directly acting at the level of the mitochondria, specifically inducing apoptosis driven by cytochrome c release. In combination with Sabutoclax, the block on apoptosis in cells treated with Minocycline may be released, thereby leading to synergistic anti-cancer properties.

Our study has shown that Sabutoclax plus Minocycline is exceptionally effective against pancreatic cancer (Fig. 30). Subtoxic individual doses of each drug produced a dramatic synergistic cytotoxic effect. Furthermore, we found that this combination resulted in a loss of Stat3 activation. Reintroduction of a constitutively active Stat3 mutant into cells rendered them resistant to the combination of Sabutoclax and Minocycline. This combination shows promise *in vivo* using multiple mouse models, both immune-compromised and immune-competent transgenic models of PDAC, showing significant anti-cancer activity without any signs of gross toxicities.

In summary, we describe an innovative combinatorial therapeutic approach with remarkable activity against pancreatic cancer cells *in vitro* and *in vivo* in three animal PDAC models. Considering the paucity of effective therapies for PDAC, it is clear that new approaches are mandatory to impact clinically on this invariably fatal cancer. The ability to target the Bcl-2 family for inactivation, using Sabutoclax, and combining this with a simple synthetic tetracycline antibiotic, such as Minocycline, opens up new areas of research with the potential to lead to an effective therapy for pancreatic cancer.

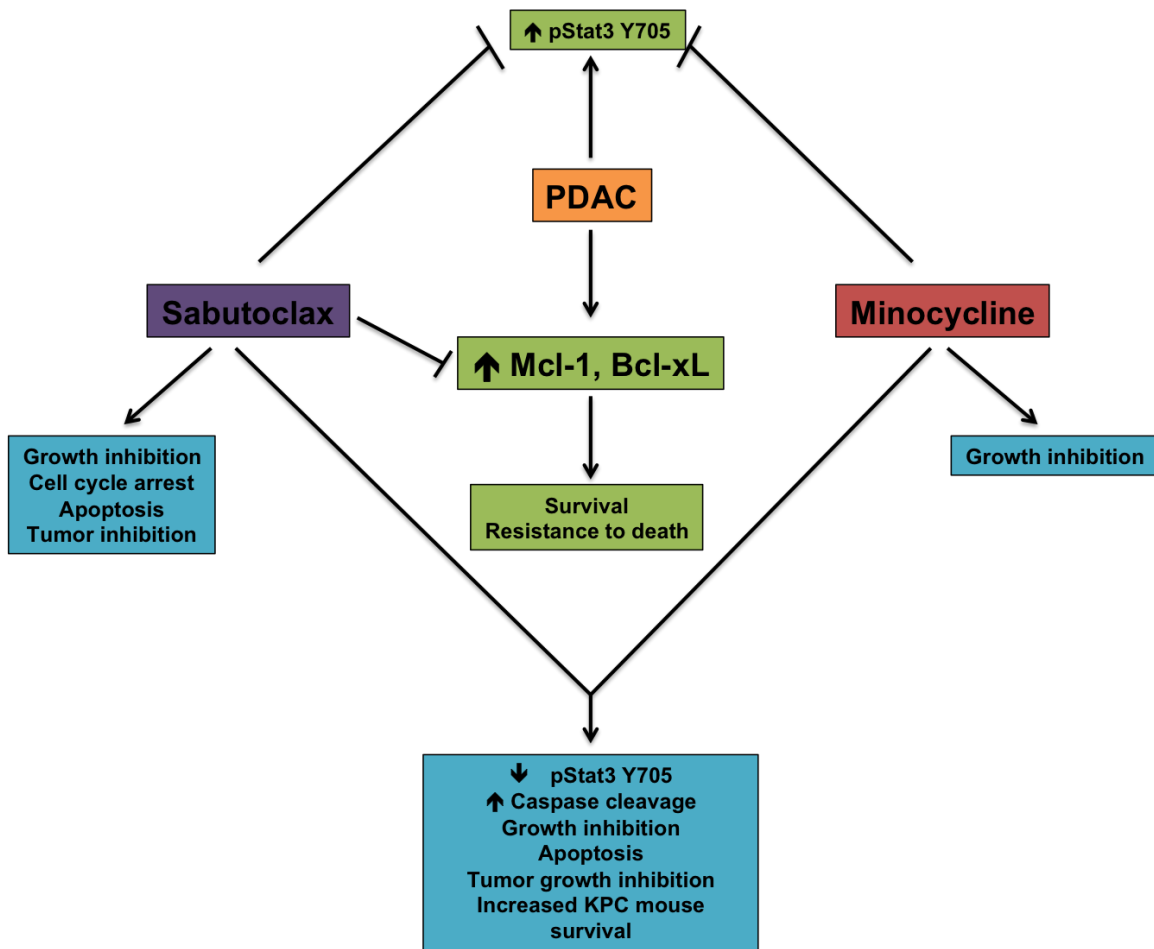


**Figure 30: Overview model showing therapeutic effects of Sabutoclax and Minocycline in PDAC.**

## **Chapter III: Gemcitabine Chemotherapy Modification for the Treatment of Pancreatic Cancer**

### **Introduction:**

Pancreatic cancer is an extremely deadly disease, with a 5-year survival rate of less than 5%. Most tumors are either locally advanced or metastasized at the time of diagnosis and, intrinsically, this cancer is extremely resistant to chemotherapy and radiation. Currently, first line treatment for pancreatic cancer consists of surgical resection, if possible, and a subsequent course of chemotherapy. This chemotherapy usually consists of treatment with Gemcitabine (2).

In 1997, Burris, et al. published a clinical study comparing Gemcitabine to 5-Fluoruracil for the treatment of pancreatic cancer. In this study, 126 patients were enrolled with 63 per treatment group. 23.8% of patients showed clinical benefit with Gemcitabine, as compared to only 4.8% of 5-FU-treated patients. The median survival was shown to be 5.65 months for Gemcitabine and 4.41 months for 5-FU. Finally, 18% of patients treated with Gemcitabine were alive at 12-month time point, while survival at this time point for patients treated with 5-FU was only 2% (3). This trial helped encourage the FDA to approve Gemcitabine for the treatment of pancreatic cancer in 1998. Gemcitabine is currently a standard treatment used for patients with pancreatic cancer. Despite this, the drug only provides minimal benefit to patients.

Gemcitabine's cytotoxic effects are due to its ability to act as a pyrimidine analog. Gemcitabine triphosphate acts as an analog for deoxycytidine triphosphate, which allows it to be incorporated into DNA during replication. After Gemcitabine is

incorporated, another nucleotide may be added to the chain, but inhibition of chain elongation subsequently occurs. DNA damage repair is not able to remove the drug and, consequently, apoptosis occurs (134).

Gemcitabine enters the cell through multiple cell membrane transporters, though the sodium-independent transporter, hENT1, has been shown to preferentially transport Gemcitabine (134). Though there are multiple mechanisms of Gemcitabine resistance, one important mechanism revolves around expression of this protein. Giovannetti, et al. showed that patients with tumors that express high amounts of hENT1 have a greater survival advantage with Gemcitabine treatment as compared to those with lower hENT1 expression (Giovannetti, et al. 2006). Patients with higher hENT1 expression have tumors that can more readily take up Gemcitabine, leading to an increased clinical benefit. However, in many tumors, low expression of Gemcitabine transporters translates to a need for the drug to be administered frequently and at high doses, two things that can add significantly to drug toxicity.

Toxicity is a major issue with many chemotherapeutic agents and, as a result, the creation of more targeted therapies that have a lower risk of toxicity has become an attractive strategy in developing cancer therapeutics. Many conventional chemotherapeutic drugs work well in killing cells, but because they also target normal cells, often lead to high levels of toxicity. Targeted therapies focus on attacking cancer cells specifically and sparing normal cells to reduce ill side effects. One specific strategy of targeted therapy involves modifying currently used drugs to make them cancer specific. This often involves identifying a biomarker on cancer cells that the modified drug can target. One such target is the Ephrin receptor.

Ephrin receptors are a family of tyrosine kinase receptors involved in neuronal connectivity, blood vessel development, and cell-cell interactions. EphA2 was identified in 1990 and is expressed in the majority of epithelial cells. In cancer cells, EphA2 is highly overexpressed and encourages communication not only between individual cancer cells, but also between cancer cells and surrounding stromal or vascular cells. EphA2 overexpression also correlates with poor prognosis in patients. Despite EphA2 overexpression, expression of EphrinA1, its ligand, often remains normal even in a cancerous state. This can lead to accumulation of unactivated EphA2 and subsequent oncogenic activity (135).

Peptides have been created that, similar to the natural ligand for this receptor, selectively bind EphA2 and cause receptor activation and internalization. These peptides are linked to commonly used chemotherapeutic drugs and act as a specific delivery strategy for these drugs to tumor cells. Once the receptor is activated, the peptide and its attached drug are internalized into a lysosome, where the peptide is degraded and the drug is free to exert its toxic effects on the cell (136). Previous studies have shown that Paclitaxel conjugated with these peptides shows increased efficacy in prostate and renal cancers (137).

Gemcitabine, though the current first-line treatment for pancreatic cancer, does not offer a great therapeutic benefit to patients. This study aims to study a modified version of Gemcitabine as an alternate to the traditional drug. This modified drug, YNH-Gemcitabine, consists of the drug with a peptide attached (YNH). This peptide was designed to specifically bind to the EphrinA2 receptor, which is overexpressed on pancreatic cancer cells. The result of this is that the attached Gemcitabine gets



internalized into the cell via EphA2, bypassing its normal mechanism of cellular entry. We believe that this will allow a greater amount of Gemcitabine to enter the pancreatic cancer cell and, ultimately, show greater efficacy *in vivo* as compared to traditional Gemcitabine alone.

To expand these studies, we also evaluated 123B9, a newer derivative of the previously developed YNH family of compounds. Though the YNH compounds showed good efficacy, the terminal tyrosine of YNH could be degraded by aminopeptidases in the blood, which limited its half-life. 123B9 contains a synthetic tyrosine that is resistant to aminopeptidase degradation, leading to a significantly longer half-life in blood and, hopefully, greater efficacy as well. Due to the recent approval of Gemcitabine and Abraxane as first-line therapy for metastatic pancreatic cancer, we evaluated 123B9-Paclitaxel and Gemcitabine. Additional studies evaluating 123B9-Gemcitabine versus Gemcitabine in pancreatic cancer are currently in progress.

## **Materials and Methods:**

### ***Human Cell Lines***

MIA PaCa-2, PANC-1, BxPC-3, and AsPC-1 cells were all obtained from the American Type Culture Collection (ATCC). LT2 cells were purchased from Millipore. MIA PaCa-2 and PANC-1 were maintained in DMEM plus 10% FBS. BxPC-3 and AsPC-1 cells were maintained in RPMI plus 10% FBS. LT2 cells were maintained with media according to distributor's instructions. Cell lines were expanded and cryopreserved at early passages and new vials were thawed out and used for experiments approximately every 3 months.

### ***Drugs and Drug Administration***

Gemcitabine, YDH-Gemcitabine, YNH-Gemcitabine, Paclitaxel, 123B9, 123B9-Paclitaxel and 123B9-Gemcitabine were produced by Dr. Maurizio Pellecchia (Sanford-Burnham Institute, La Jolla, CA). For biological studies, all drugs were diluted in 10% Tween80, 10% DMSO, and 80% PBS.

### ***Western Blotting***

$5 \times 10^5$  cells were plated in 6-cm dishes and treated as described. After 48 hours, whole cell lysates were prepared and western blotting analysis was carried out as previously described (120). Primary antibodies used for these studies were EphrinA2 (1:1,000, Cell Signaling) and EF1- $\alpha$  (1:5,000, Sigma).

### ***Subcutaneous Xenograft Studies***

$5 \times 10^6$  MIA PaCa-2-luciferase cells were used to establish bilateral subcutaneous tumors on the flanks of 8-10 week old male athymic nude mice. Studies were done as previously described (109). Treatment began when tumors reached  $\sim 100\text{-mm}^3$ . All drugs were administered by tail vein injection twice per week for 4 weeks, a total of 8 injections. Gemcitabine was given at a dose of 10 mg/kg and all Gemcitabine derivatives were given at equimolar doses to 10mg/kg Gemcitabine, also via tail vein injection. PTX was given at a dose of 2.5mg/kg. All 123B9 compounds were given in equimolar doses to PTX. BLI was done at the beginning and end of the study. Tumors

were measured twice per week using calipers. Tumors were fixed in formalin, embedded in paraffin, and sectioned for staining.

### ***Survival Study***

After their last injection, mice were kept for 1 additional week to monitor tumor growth and imaged at the end of this week. The mice were then kept to monitor for the effects of treatment on survival. Mice were kept until reaching a moribund status or until tumors reached a combined volume of 2000mm<sup>3</sup>, whichever came first. They were then sacrificed at this time.

### ***BLI***

During imaging, mice were placed in the imaging chamber and maintained with 2% isoflurane gas anesthesia at a flow rate of approximately 0.5-1 L/min per mouse. Anesthetized mice were injected IP with 150 mg/kg body weight D-Luciferin (Xenogen Corporation, Alameda, CA). After approximately 10 min, mice were imaged using a charge-coupled-device (CCD) camera coupled to the Xenogen *in vivo* imaging (IVIS) imaging system (Caliper Life Sciences, Inc., Hopkinton, MA).

### ***Statistical Analysis***

For *in vivo* studies, data shown are the mean  $\pm$  95% confidence interval. Significance was determined using the Student's t-test.  $p < 0.05$  was considered statistically significant.

## **Results:**

### **YNH-Gemcitabine shows greater efficacy *in vivo* compared to Gemcitabine**

MIA-PaCa-2-luc cells were used to create bilateral subcutaneous xenografts in athymic mice. Western blot data shows that this pancreatic cancer cell line highly expresses EphA2 (Figure 31). Cells were injected into each flank and then allowed to grow for approximately 1 week. At this point, mice were imaged using BLI and treatment was subsequently initiated. Mice were divided into 4 groups (PBS, Gemcitabine, YDH-Gemcitabine, YNH-Gemcitabine) with 9 mice/group. YDH-Gemcitabine is a scrambled control, where the peptide attached to Gemcitabine should not be specific for EphA2 and, therefore, should not bind to the receptor. Animals were treated 2x/week via tail vein injection for 4 weeks. A dose of 10mg/kg Gemcitabine was used along with equimolar doses of YDH-Gemcitabine and YNH-Gemcitabine. At the end of 4 weeks, animals were again imaged and treatment was ended.

As expected, YDH-Gemcitabine did not have significant effects on tumor growth. Gemcitabine had a modest effect on tumor growth, though YNH-Gemcitabine showed the greatest inhibition of tumor growth of all groups evaluated (Fig. 32). This can be observed both through tumor measurement and by BLI (Fig. 33). No negative side effects of the drugs were observed and the mouse weight remained consistent

throughout the study (data not shown). 3 animals per group were sacrificed at the end of this study and tumors were excised and fixed in formalin for further study.

To determine whether YNH-Gemcitabine also gave a survival advantage, remaining mice were not sacrificed at the end of the experiment, but rather when their individual tumor burden approached 2000mm<sup>3</sup>. YNH-Gemcitabine gave mice a significant survival advantage over other treatment groups (Fig. 34).

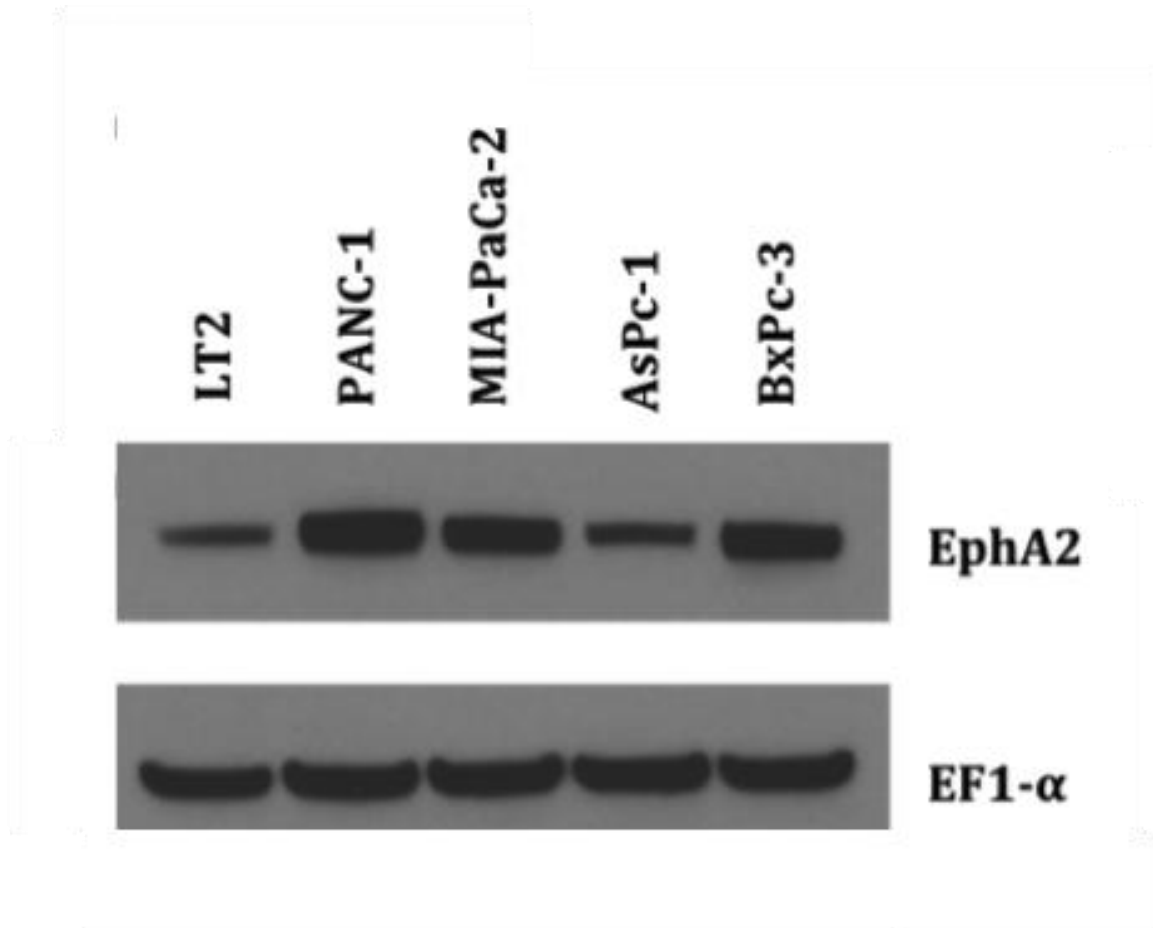


**Figure 31: Pancreatic Cancer cells express EphA2.** Western blotting of normal pancreatic fibroblasts and pancreatic cancer cells.

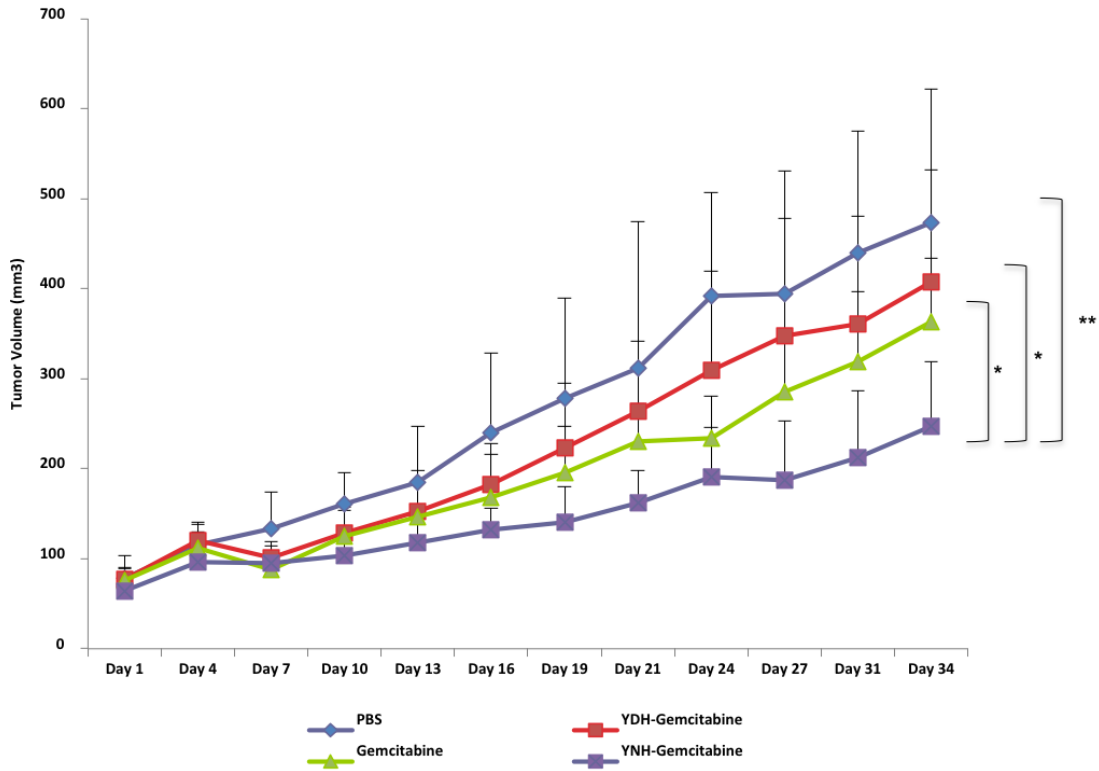


**Figure 32 : YNH-Gemcitabine inhibits tumor growth in vivo to a greater extent as compared to Gemcitabine.** Tumor volume as calculated by caliper tumor measurement. \* $p < 0.05$ ; \*\*  $p < 0.01$ .  $n = 9$  mice/group

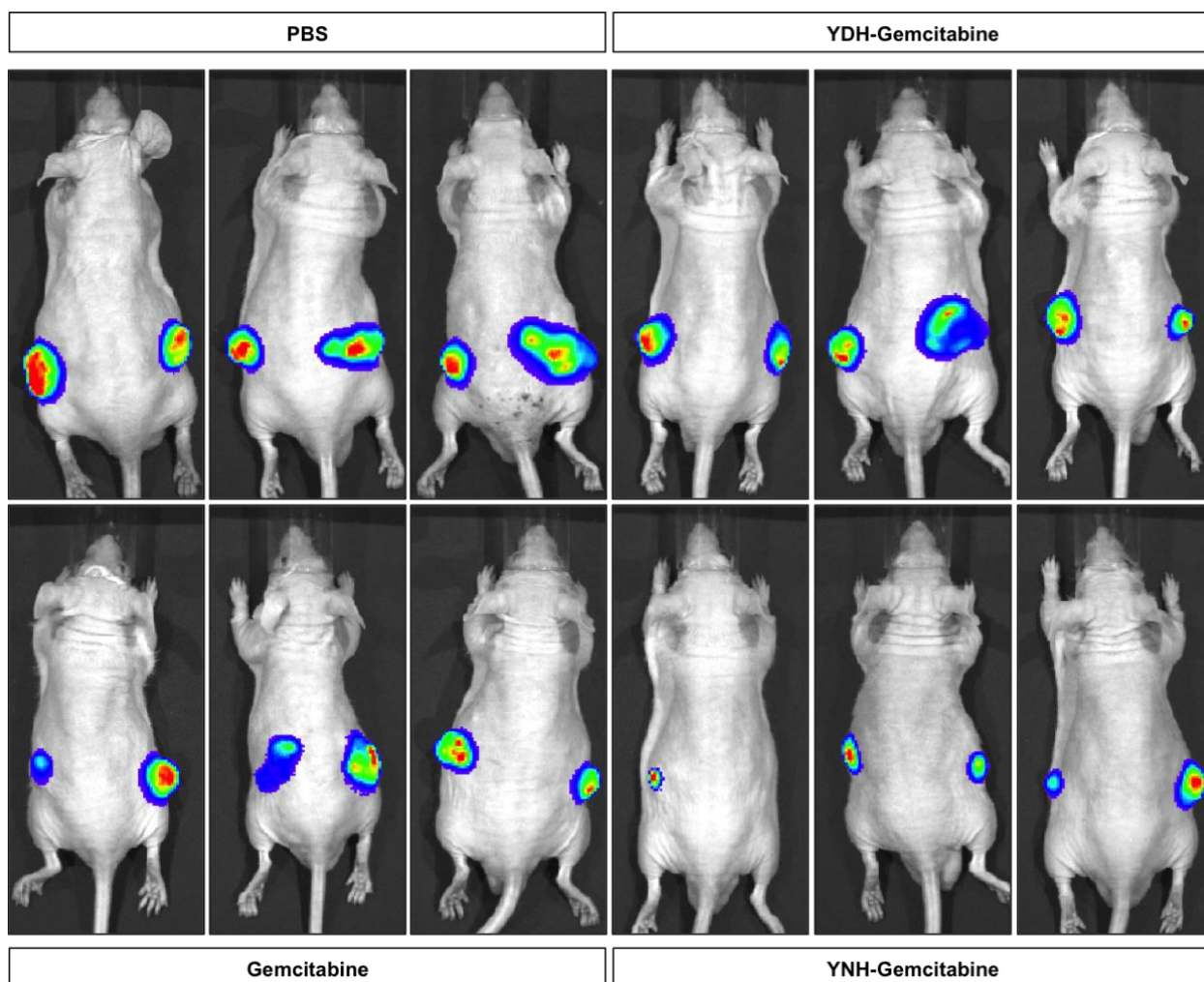


**Figure 33 : YNH-Gemcitabine inhibits tumor growth in vivo to a greater extent as compared to Gemcitabine. Bioluminescent tumor images at Day 34. Exposure time = 0.5 seconds**



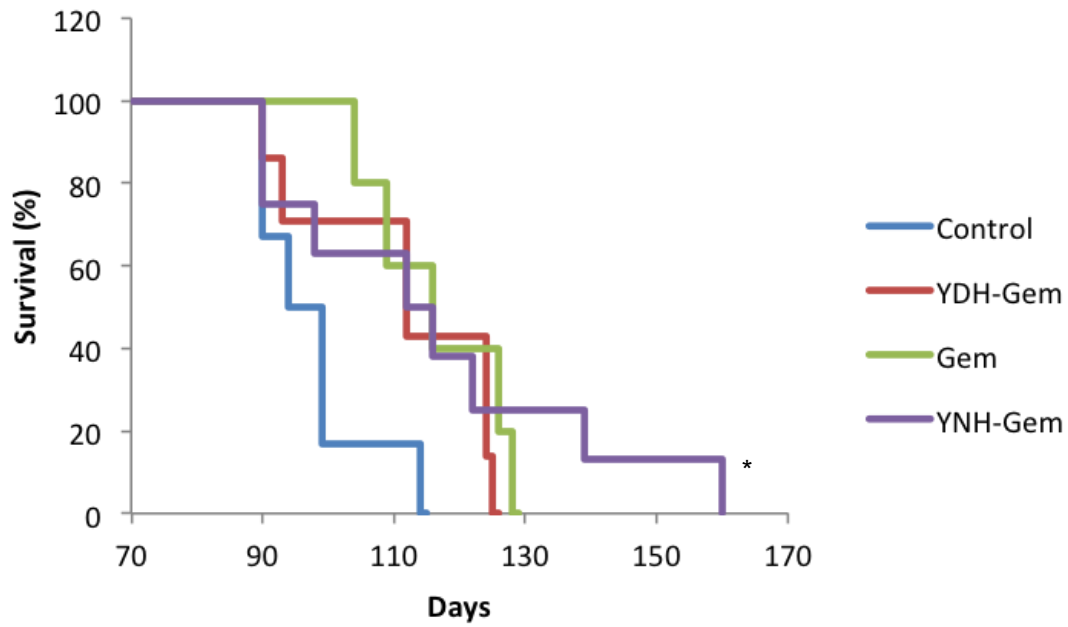


**Figure 34: YNH-Gemcitabine prolongs in a xenograft model of pancreatic cancer.** Kaplan-Meier curve showing survival in days. \*p < 0.05.

## **123B9-Paclitaxel and Gemcitabine show combination effects in pancreatic cancer *in vivo***

MIA-PaCa-2-luc cells were used to create bilateral subcutaneous xenografts in athymic mice. Cells were injected bilaterally into the flanks and then allowed to grow for approximately 1 week. At this point, mice were imaged using BLI and then treatment was initiated. Mice were divided into 8 groups (Control, Gemcitabine, PTX, Gem+PTX, 123B9-PTX, 123B9+PTX, 123B9-PTX+Gem, 123B9+PTX+Gem) with 5 mice/group. Animals were treated 2x/week via tail vein injection for 4 weeks. A dose of 10mg/kg Gemcitabine, 2.5mg/kg PTX, and an equimolar dose of the 123B9 compounds were used. Tumors were measured with calipers twice a week. At the end of 4 weeks, animals were again imaged and treatment was stopped. No negative side effects from any of the compounds used were observed and the mouse weight remained consistent throughout the study (data not shown).

As expected, Gemcitabine or PTX treatment alone did not have a significant effect on tumor growth, but the combination of these two drugs did significantly inhibit tumor growth (Fig. 35). Additionally, both 123B9-PTX and 123B9+PTX showed greater inhibition of tumor growth as compared to PTX (Fig. 36). The addition of Gemcitabine to these groups further suppressed tumor growth. Mice that were treated with 123B9+PTX+Gem showed the greatest inhibition of tumor growth (Fig. 37). Tumors in this group were significantly smaller as compared to 123B9+PTX, PTX, Gem, and Control groups.

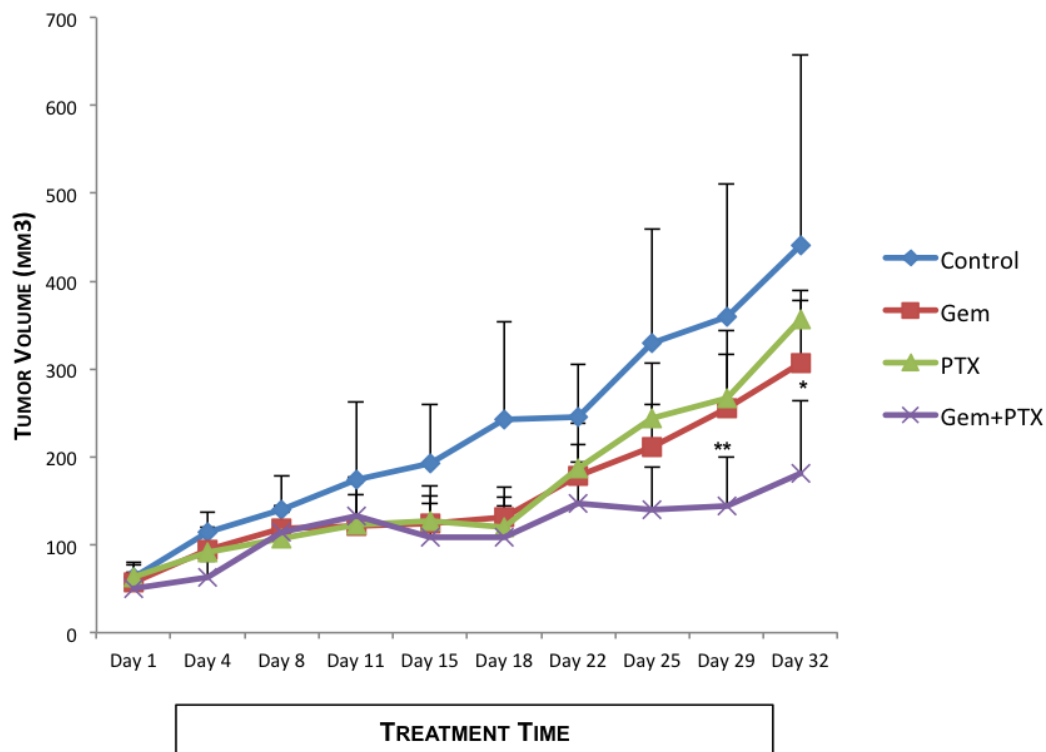


**Figure 35: Gemcitabine (Gem) and Paclitaxel (PTX) inhibit tumor growth in vivo to a greater extent than either single drug.** Tumor volume as calculated by caliper tumor measurement. Asterisks show significance between the Gem+PTX group and Control, Gem, and PTX groups. \* $p < 0.05$ ; \*\* $p < 0.01$ .  $n = 5$  mice/group

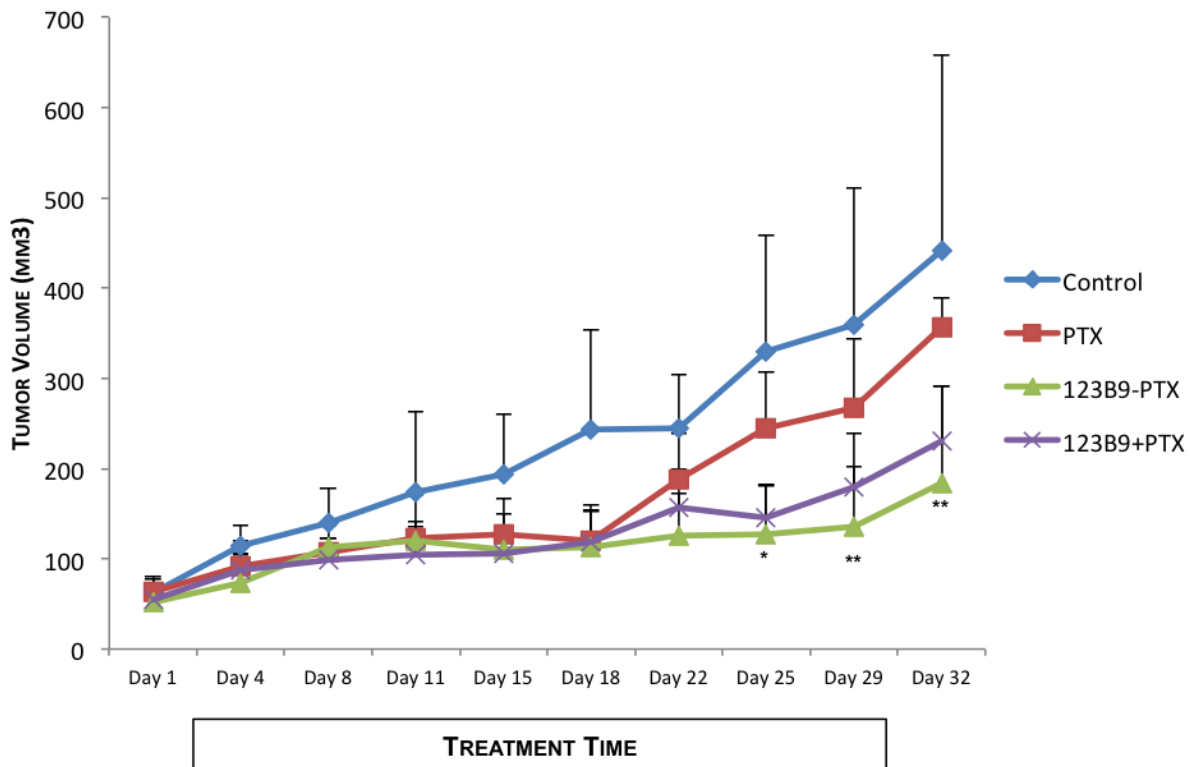


**Figure 36: 123B9-PTX inhibits tumor growth *in vivo* to a greater extent than PTX.** Tumor volume as calculated by caliper tumor measurement. Asterisks show significance between the 123B9-PTX group and both the PTX and Control groups. \* $p < 0.05$ ; \*\* $p < 0.01$   $n = 5$  mice/group

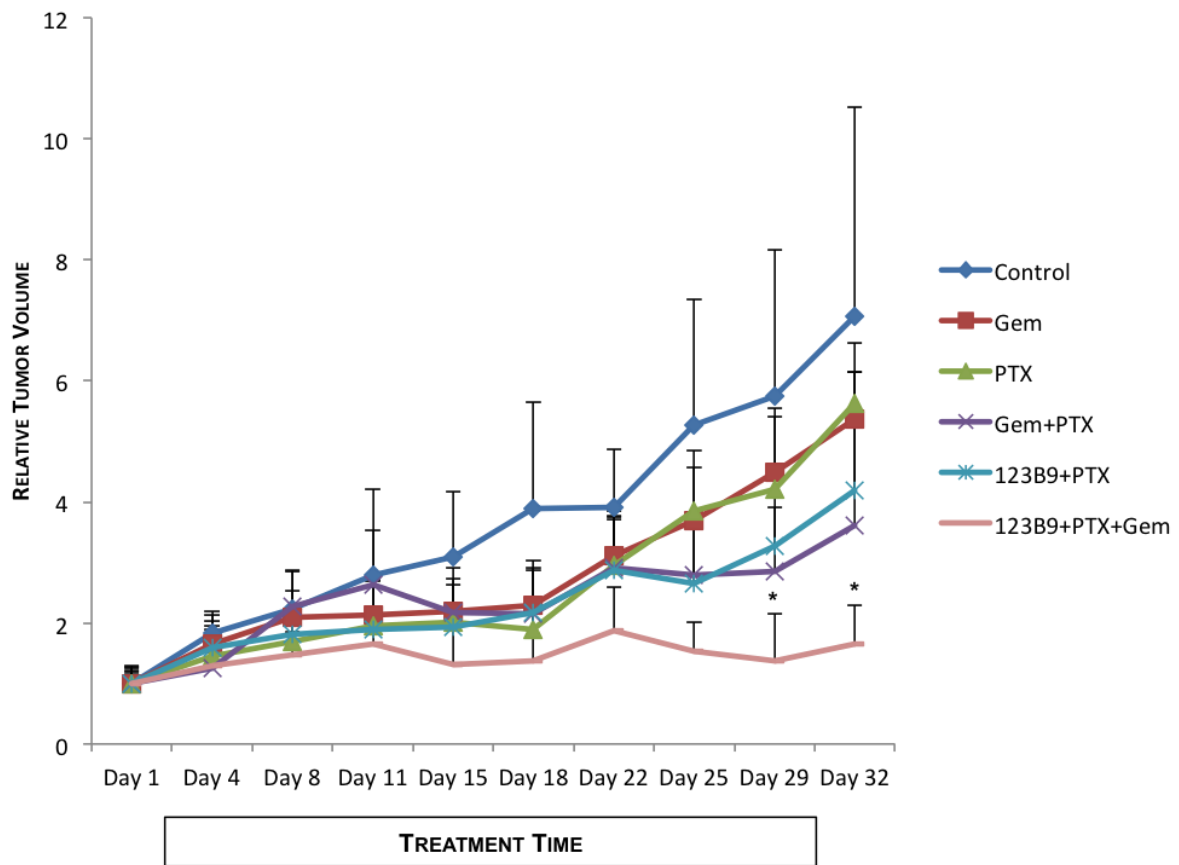


**Figure 37: 123B9+PTX+Gem inhibit tumor growth *in vivo* to a greater extent than other treatment combinations.** Tumor volume as calculated by caliper tumor measurement. Asterisks show significance between the 123B9+PTX+Gem group and Control, Gem, PTX, Gem+PTX, and 123B9+PTX groups. \* $p < 0.05$ .  $n = 5$  mice/group

## **Discussion**

Though not overly efficacious, chemotherapy remains the mainstay of pancreatic cancer therapy. There is a vital need to develop novel therapies that provide greater clinical benefit to patients. This study evaluated modifications of both Gemcitabine and Paclitaxel against pancreatic cancer. The strategy involved in these modifications revolved around developing conjugated drugs that are capable of specifically targeting the EphA2 receptor that is overexpressed on the surface of pancreatic cancer cells. Initial studies used Gemcitabine linked to the YNH peptide, which showed encouraging results. This modified drug show greater tumor growth inhibition and prolonged survival in a xenograft model of pancreatic cancer.

However, despite these results, the YNH was found to have less than optimal plasma stability. The terminal tyrosine of this peptide, which is essential to specific EphA2 binding, was shown to be susceptible to aminopeptidases in the blood, leading to degradation. This resulted in a half-life of only a few minutes. A new peptide was subsequently created, 123B9, which replaced the terminal tyrosine with a synthetic tyrosine. This new amino acid is resistant to aminopeptidase degradation while still retaining EphA2 specificity. This translates into an increased drug half-life of approximately 4 hours.

Paclitaxel is a commonly used chemotherapeutic drug most often used in breast, lung, ovarian, and AIDS-related sarcomas, though it is studied and sometimes used in combination in other cancer types as well. Paclitaxel is a microtubule inhibitor and acts to stabilize polymerized microtubules. Consequently, cells get stuck in the G2 and M phases of the cell cycle. Solubility is a major issue with this drug. It must be

administered in a solution with Cremophor and dehydrated ethanol. These vehicles can have toxic effects on their own and have led to the inability to use higher doses of this chemotherapeutic drug in patients. Furthermore, Cremophor-bound paclitaxel has a tendency to form micelles that trap the drug in the center, limiting its efficacy (138).

Recently a novel formulation of Paclitaxel has been developed in which the drug is bound to albumin (nab-Paclitaxel). High-pressure homogenization is used to combine albumin and paclitaxel. Once injected, the drug is free to bind/unbind albumin or other molecules in the blood freely. This results in more unbound drug in the circulation as compared to Cremophor-bound drug. However, the nab-paclitaxel that is bound tends to be bound to albumin, which helps to facilitate its entry into tumor cells. Nab-Paclitaxel can use normal albumin transport mechanisms to gain entry. Also, some albumin-binding proteins, such as SPARC, show high prevalence in the tumor microenvironment. Whether or not this has clinical significance is still unclear (138). In mouse studies, xenografted pancreatic tumors were found to have a 2.8 fold increase in intratumoral Gemcitabine concentration when the drug was administered in combination with nab-Paclitaxel. They hypothesized that this may be due to nab-Paclitaxel-induced disruption of the stroma (139).

A Phase 3 clinical study in patients with metastatic pancreatic cancer evaluated nab-Paclitaxel + Gemcitabine versus Gemcitabine alone in a total of 861 patients. The median survival was 8.5 months in the nab-paclitaxel + Gemcitabine group vs. 6.7 months in the Gemcitabine group. The survival rate at 1 year was 35% vs 22%; 9% vs 4% at 2 years. The response rate was 23% for combination group and 7% for Gemcitabine alone. Toxicities included neutropenia, fatigue, and neuropathy (140).

These results encouraged the FDA to approve the combination of Gemcitabine and nab-Paclitaxel (Gem-Abraxane) for metastatic pancreatic cancer.

In conclusion, these novel Ephrin-binding peptides represent an exciting new strategy in cancer drug development. Of significant interest is that this technique is not limited to a single drug, but rather can be adapted to almost any drug, either by linking the drug of interest to a peptide or by using it in combination with the peptide. We found in our studies with Paclitaxel that 123B9 showed greater tumor inhibition, presumably by helping to facilitate drug entry into cancer cells, even when it wasn't actually linked with Paclitaxel. In fact, when 123B9 was administered in conjunction with chemotherapy (Gemcitabine and Paclitaxel), but not actually as part of a modified drug, we saw the greatest efficacy. We believe that this may be due to 123B9 encouraging entry of both Paclitaxel and Gemcitabine. Overall, these studies provide encouraging evidence that modifications of standard chemotherapeutic agents have the potential to improve clinical outcome in pancreatic cancer patients.



## **Chapter 4: Characterization of a novel double transgenic pancreatic adenocarcinoma mouse, 'PanMetView (PMV) Mouse', to non-invasively monitor tumor development and progression.**

### **Introduction**

Pancreatic cancer is an extremely deadly disease that lacks efficacious therapeutic options (1). There is a dire need to develop novel therapies for targeting this cancer. Translational research has focused on many strategies to target this cancer (141-145), but the study of such strategies is often impeded by the lack of appropriate preclinical models to validate efficacy. The creation of effective drugs or therapeutic strategies is a rigorous process that requires not only an understanding of the mechanism of action of a new drug, but also the ability to stringently test compounds in appropriate *in vitro* and *in vivo* settings. *In vitro* studies are fairly straightforward, as a variety of human pancreatic cancer cell lines have been established and are available to test experimental drugs (146). Testing new drugs *in vivo*, however, can be a daunting challenge if one does not have an appropriate preclinical model that recapitulates pancreatic cancer development and disease progression. Currently, there are a number of transgenic mouse models of pancreatic cancer that have been developed. They vary in a variety of ways, including the histological subtype of tumor developed, tumor latency, and the absence or presence of metastases (147,148). However, one missing component of all of these models is an efficient and simple global method to temporally monitor tumor development and growth. To perform sophisticated preclinical animal studies, one must be able to monitor tumor kinetics in a quantifiable way and use this strategy to define efficacy of newly developed therapies. Doing so in a non-invasive manner without having to sacrifice the mouse is particularly difficult and defining

approaches to obviate this problem will be transformative for preclinical testing of therapies.

Bioluminescence imaging (BLI) is an optical imaging technique that is relatively inexpensive, user-friendly, and has wide-spectrum applicability. It is based on the ability of a cell that expresses luciferase to convert luciferin into oxyluciferin, which results in the release of photons that can be captured and processed into an image (149,150). Traditionally, this imaging modality has been used in xenograft studies, where cells that are engineered to express luciferase are injected subcutaneously or orthotopically into mice to create a tumor model with imaging capabilities. We are pioneering a strategy in which we can use BLI to image pancreatic tumors in the widely used pancreatic ductal adenocarcinoma (KPC) transgenic mouse model, or in principle any other solid tumor transgenic mouse model.

Bioluminescence imaging (BLI) has been transformative for animal tumor studies permitting live non-invasive *in vivo* imaging to monitor tumor growth and progression using xenograft, orthotopic and metastasis models (149-154). For optimizing this type of imaging for transgenic animals, cancerous cells in the transgenic animals need to express a reporter gene, such as luciferase, under the control of a cancer-specific (cancer-selective) promoter. In previous collaborative studies with Dr. Martin G. Pomper (Johns Hopkins University) we demonstrated the utility of a reporter gene expressed under the control of a cancer-specific promoter, progression elevated gene-3 (PEG-Prom), to image metastases (153) and study tumor progression.

CCN1 is a member of a large family of integrin-binding proteins that affects multiple signal transduction pathways in cells (155,156). In cancer, integrin-binding proteins are often dysregulated and can lead to changes in cell migration, adhesion, angiogenesis, and tumor growth. In pancreatic cancer, CCN1 mRNA and protein are elevated in tumor specimens and established pancreatic tumor cell lines (157). CCN1 is critical for EMT in this cancer type as well as for maintenance of stemness and aggressive behavior, with more aggressive cell lines expressing higher levels of CCN1 (158). These pro-tumorigenic properties result in part through signaling via the Sonic hedgehog pathway (159,160). Silencing of CCN1 has also been shown to mitigate some of CCN1's pro-cancer properties (158). Based on the cancer-selectivity of CCN1, we hypothesized that a CCN1-promoter-driven construct would be amenable for imaging tumors and metastases *in vivo*, similar to what we found with the PEG-Prom-Luc-PEI construct (154). This possibility was verified using a CCN1-Prom-Luc-PEI construct, which when administered intravenously to nude mice containing primary and metastatic tumors was able to image these tumors/metastases (data not shown).

The PDAC KPC transgenic mouse model, Pdx-1-Cre/*K-ras*<sup>LSL-G12D</sup>/*p53*<sup>flox<sup>wt</sup></sup>, has been used to study pancreatic cancer development and progression as well as therapeutic approaches for inhibiting these processes (128-132). As with all cancers, there is a multitude of genetic changes observed in PDAC that contribute to its development and progression. Activating *K-ras* mutations are found in over 90% of pancreatic cancers (1), making it a highly active contributor to the tumorigenic state. There is also a variety of tumor suppressors lost in high frequency in this disease, p53 being one of them. This important gene is either deleted or functionally inactivated in

approximately 50-75% of PDAC (1). The KPC model of PDAC, which is broadly used in the pancreatic cancer field, mimics these human genetic changes in the mouse. A mutated form of K-ras, rendering it constitutively active (*K-ras*<sup>G12D</sup>), is introduced into the mouse with a Lox-Stop-Lox sequence located transcriptionally upstream (*K-ras*<sup>LSL-G12D</sup>). p53 alleles are floxed in these animals as well, either one or both alleles (*p53*<sup>fl/wt</sup> or *p53*<sup>fl/fl</sup>). Cre-mediated recombination results in the removal of the stop codon preceding the mutant *K-ras* and expression of this new genetic element, giving the tissue continual *K-ras* signaling. Additionally, Cre will remove one or both alleles of p53, resulting in full or partial loss of function of this critical tumor suppressor. Cre is introduced into the pancreas through the transcriptional control of a pancreatic-specific promoter, Pdx-1. When both alleles of p53 are deleted, tumors develop very rapidly and most animals do not live past 2 months of age, with a tumor latency of around 6 weeks. Animals that still retain one functioning p53 allele show longer tumor latency of around 21 weeks. This longer survival permits additional time to therapeutically intervene. p53 null animals, however, have more aggressive disease and can be useful for certain studies. As seen in human PDAC, this disease initially develops as a series of pre-invasive lesions, or Pancreatic Intraepithelial Neoplasms (PanINs) before eventually becoming an invasive cancer. The tumors show both local invasion and micrometastasis (133).

We hypothesized that crossing these animals to a mouse that expresses luciferase under the control of a cancer-selective promoter, CCN1, would result in a mouse in which CCN1 would be transcriptionally activated in conjunction with tumor development in the pancreas and that the tumor cells would subsequently express luciferase, allowing them to be easily imaged via BLI (Fig. 38). We also aim to show that

this model is not only capable of detecting primary tumor development through BLI, but that metastatic lesions may also be visualized through this method. This is a significant advantage over traditional imaging methods, where the detection of metastasis is very difficult. These studies in general are highly significant, as they will provide a new platform for developing and using transgenic mice to study pancreatic, and theoretically other cancers, development and progression.

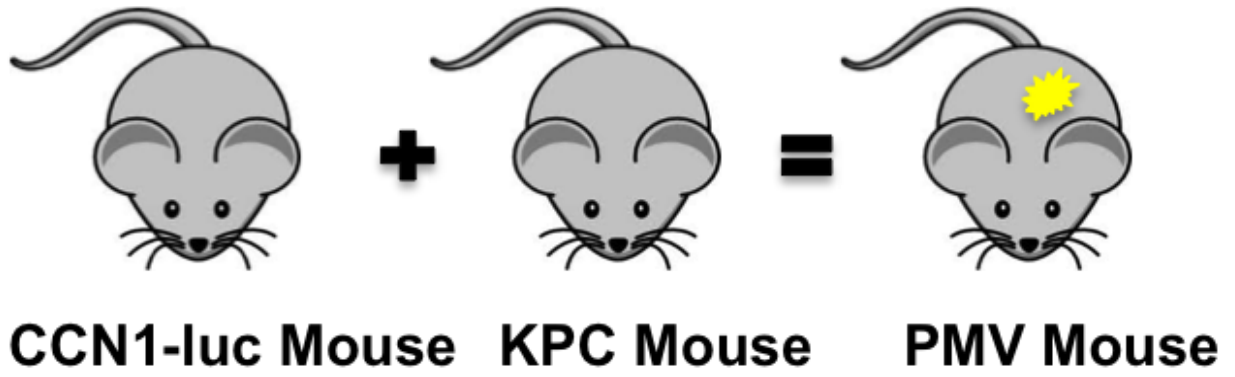


Figure 38: Development strategy for the PMV Mouse

## **Methods**

### ***Characterization of 'PanMetView' (PMV) Mice***

Useful progeny PMV mice with the following genotypes were followed temporally by BLI: animals positive for the activating K-*ras* mutation, having either one or both alleles of p53 lost, positive for Pdx-1-Cre (which is responsible for the appropriate K-*ras* and p53 genetic changes), and also expressing CCN1-luc. We evaluated approximately 15-20 mice. Mice were started on an imaging protocol beginning post-weaning, at around 4 weeks of age. Animals were imaged using BLI one time per week and any signal on these images was quantified using Living Image software. Weekly imaging was followed over time and tumor kinetic graphs for each mouse based on these imaging studies were created. These mice were followed by BLI until they reached a moribund status. At this point, the mice were sacrificed and imaging done at different points throughout the necropsy to determine the origin of any signal seen in the animal.

### ***BLI of PMV Mice***

During imaging, PMV mice were placed in the imaging chamber and maintained with 2% isoflurane gas anesthesia at a flow rate of approximately 0.5-1 L/min per mouse. Anesthetized mice were injected IP with 150 mg/kg body weight D-Luciferin (Xenogen Corporation, Alameda, CA). After approximately 10 min, mice were imaged using a charge-coupled-device (CCD) camera coupled to the Xenogen *in vivo* imaging (IVIS) imaging system (Caliper Life Sciences, Inc., Hopkinton, MA). The positive signal from

background-subtracted images was analyzed by Living Image software for integrated density.

### ***Analysis of tumor tissues***

Criteria for euthanasia included loss of body mass, abdominal bloating and/or lack of grooming behavior. Once mice reach a point where sacrifice is required, the animals were necropsied post-imaging. A second set of images was taken of individual organs to confirm the origin of the signal seen in the first set of images of the live animal. Tumor tissue was preserved in neutral buffered formalin and formalin fixed and sectioned for further evaluation.

### ***Immunohistochemistry***

Tumors were fixed in formalin, embedded in paraffin, and sectioned for staining. Staining was done as previously described (122) with anti-CCN1 (1:100, Abcam) per the manufacturer's instructions.

## **Results**

### **KPC mouse tumors express CCN1**

The KPC (Pdx-1-Cre/K-*ras*<sup>LSL-G12D</sup>/*p53*<sup>flox/wt</sup>) mouse is extensively used as a representative model for PDAC development and progression, and for therapeutic studies (128-132). This animal spontaneously develops precursor pancreatic lesions, PanINs, which progress and eventually develop into invasive disease. The model recapitulates the human condition, in which animals remain symptomatically unaffected by their disease until it is at a late stage of development. Tumors form as a result of



activated *K-ras* and functional loss of *p53* in the pancreas, genetic changes also seen in a high percentage of human tumors. Histological analysis shows extensive local invasion as well as metastasis in a subset of animals (133). Immunohistochemistry (IHC) was used to monitor CCN1 expression in KPC mouse pancreatic tissue from control, *p53*<sup>+/-</sup>, and *p53*<sup>-/-</sup> animals. Control animals had limited basal CCN1 expression, with the exception of the islets of Langerhans, which showed mild CCN1 expression. Mice with *p53*<sup>+/-</sup> tumors had increased CCN1 expression and mice with *p53*<sup>-/-</sup> tumors, which are more aggressive, showed very high CCN1 expression (Fig. 39). To summarize, CCN1 expression correlates with both PDAC development and aggressiveness in the KPC mouse model. This data supports double transgenic GEMs that incorporate the CCN1-Luc promoter to identify tumors and metastases in the KPC PDAC mouse.

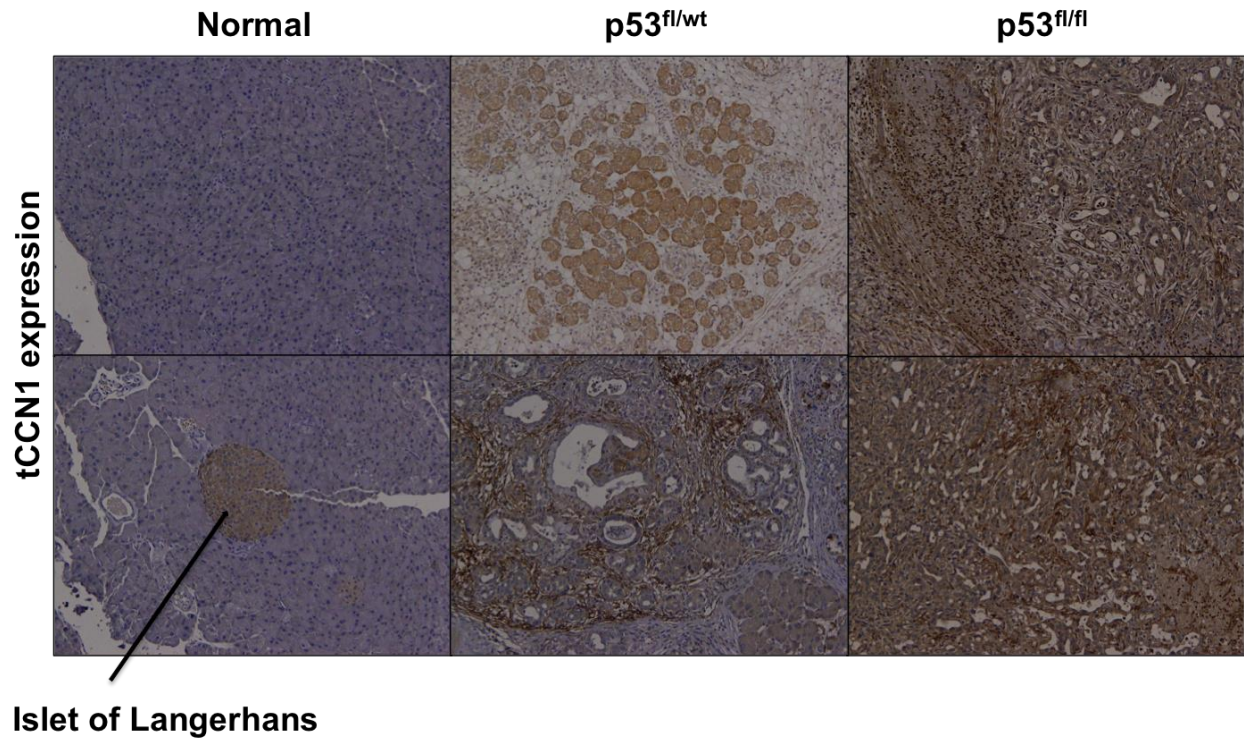


**Figure 39: KPC mouse tumors highly express CCN1.** CCN1 expression by IHC in sections of normal pancreas or pancreatic tumor from control and transgenic KPC mice.

## **CCN1-luc-KPC mice can monitor pancreatic tumor growth in vivo**

CCN1-luc mice were crossed with KPC mice to generate PanMetView (PMV) mice and several PMV mice have now been evaluated. After weaning, the mice were started on an imaging protocol, in which they were imaged by BLI one time per week. We evaluated both p53<sup>wt/fl</sup> and p53<sup>fl/fl</sup> mice. This allowed us to study a number of additional factors, such as metastases. As has been previously shown (133), a portion of p53<sup>wt/fl</sup> mice will show metastases as well as local invasion. Most p53<sup>fl/fl</sup> mice though, because of the aggressive nature of their disease and their short lifespan, do not show distant metastasis, though evidence of local invasion is still demonstrated (133).

**PMV Mouse #41 (p53<sup>fl/fl</sup>):** This mouse was imaged twice before it reached a moribund state requiring sacrifice. This animal showed strong abdominal signals, representing underlying tumor once the animal was necropsied. As CCN1 is expressed in the testes, a signal in the testes in this animal was evident (Fig. 40). The strong signal from the testes often masks the signal from the pancreas. To overcome this issue, we covered the testes with dark paper blocking the signal, thereby allowing any signal originating in the pancreas or other CCN1-expressing tumor cells to be identified (Fig. 40). During necropsy, individual organs were imaged to determine the signal source. As in the intact animal, the testes masked tumor expression, though when they were removed, the signal was clearly seen in the remaining organs. Most of the signal came from the pancreatic tumor, though signal was also detected in the spleen (which was encased in tumor upon opening the animal) and in the lung (Fig. 40B). Lung tissue will be analyzed to determine the presence of lung metastases.

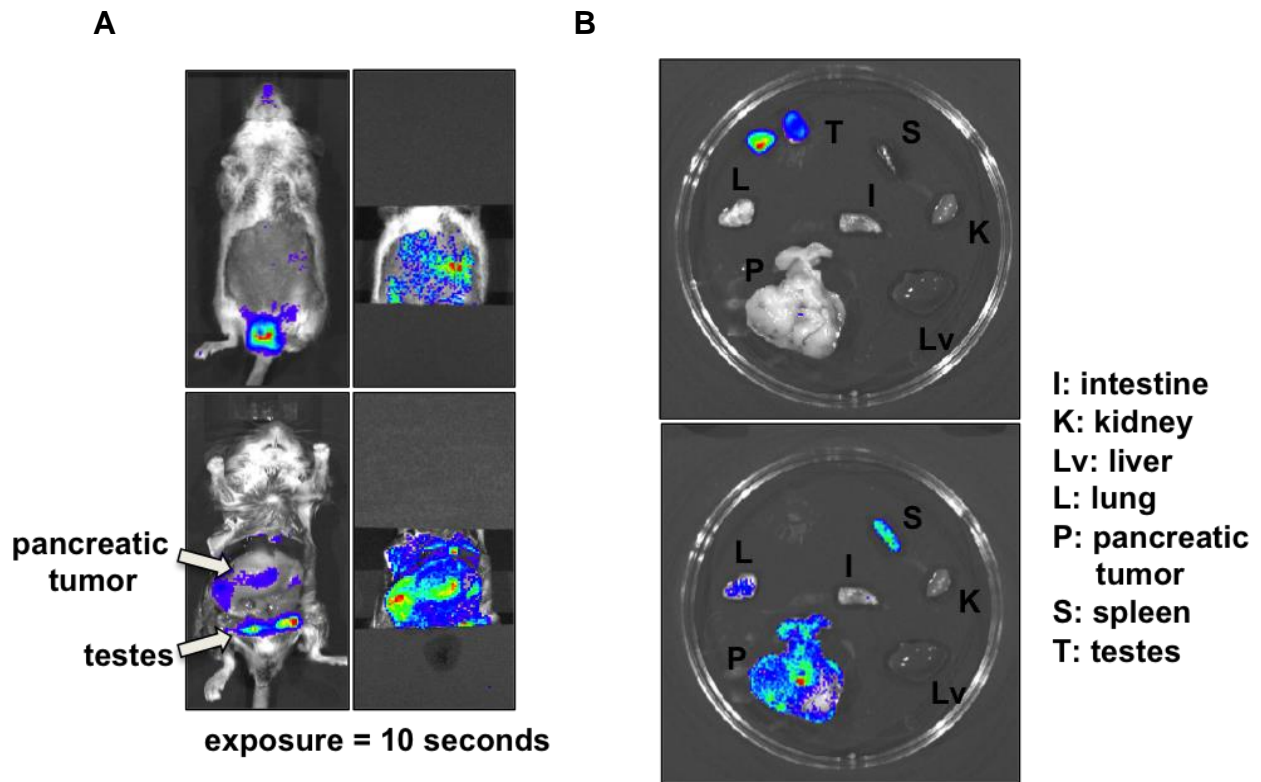


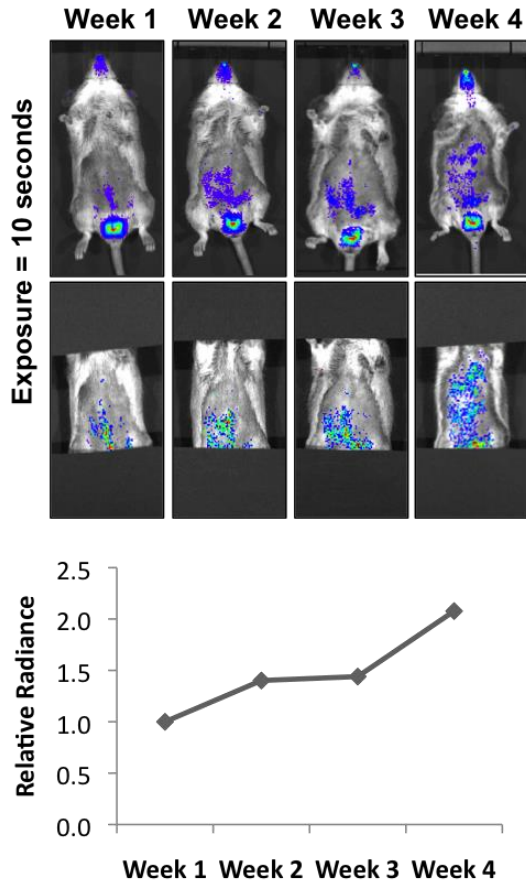
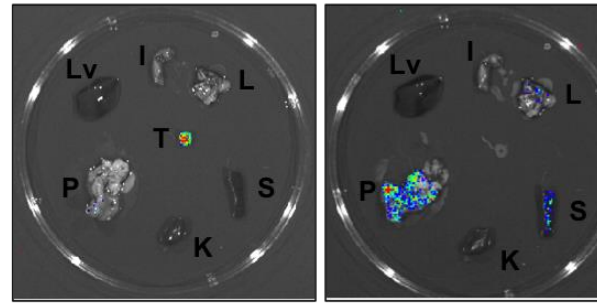
**Figure 40: Characterization of PMV Mouse #41 ( $p53^{fl/fl}$ ).** (A) Upper panel: intact mouse showing amplification of abdominal signal when testes are covered. Lower panel: exposed abdominal cavity showing actual pancreatic tumor and amplification of signal from that tumor following testes coverage. (B) Individual organ post necropsy of Mouse #41 showing specificity of signal

**PMV Mouse #51 (p53<sup>fl/fl</sup>):** This animal also showed strong abdominal signals, as well as signals from the testes (Fig. 41). This mouse was imaged for four weeks before sacrifice. Upon necropsy, a signal was also detected in the spleen and lung (Fig. 41B). This mouse had a large pancreatic tumor that displayed a strong and specific signal.

**PMV Mouse #48 (p53<sup>fl/wt</sup>):** This animal still has one functioning allele of p53, which results in a mouse with a longer tumor latency. Because of this, we were able to gather imaging data on this animal for approximately 2 months. The data show a clear increase in tumor growth that can be observed both through BLI and the quantification of these images (Fig. 42).

**PMV Mouse #225 (p53<sup>fl/fl</sup>):** Imaging of this mouse showed evidence of a pancreatic tumor as well as potential lung metastasis. Individual organ imaging supported this (Fig.43).

**PMV Mouse #247 (p53<sup>fl/fl</sup>):** Similar to previous mice evaluated, this mouse showed increasing signal over time, which paralleled its underlying tumor development. Evaluation of organs after sacrifice showed tumor specificity. This mouse also showed evidence of metastasis in the lung as well as in the area ventral to the esophagus/trachea. This latter region is atypical for this model (Fig 44).

**A****B**

I: intestine  
 K: kidney  
 Lv: liver  
 L: lung  
 P: pancreatic tumor  
 S: spleen  
 T: testes

**Figure 41: Characterization of PMV Mouse #51 ( $p53^{fl/fl}$ ).** (A) BLI images and quantification. (B) BLI of organs post necropsy. Exposure = 10 seconds

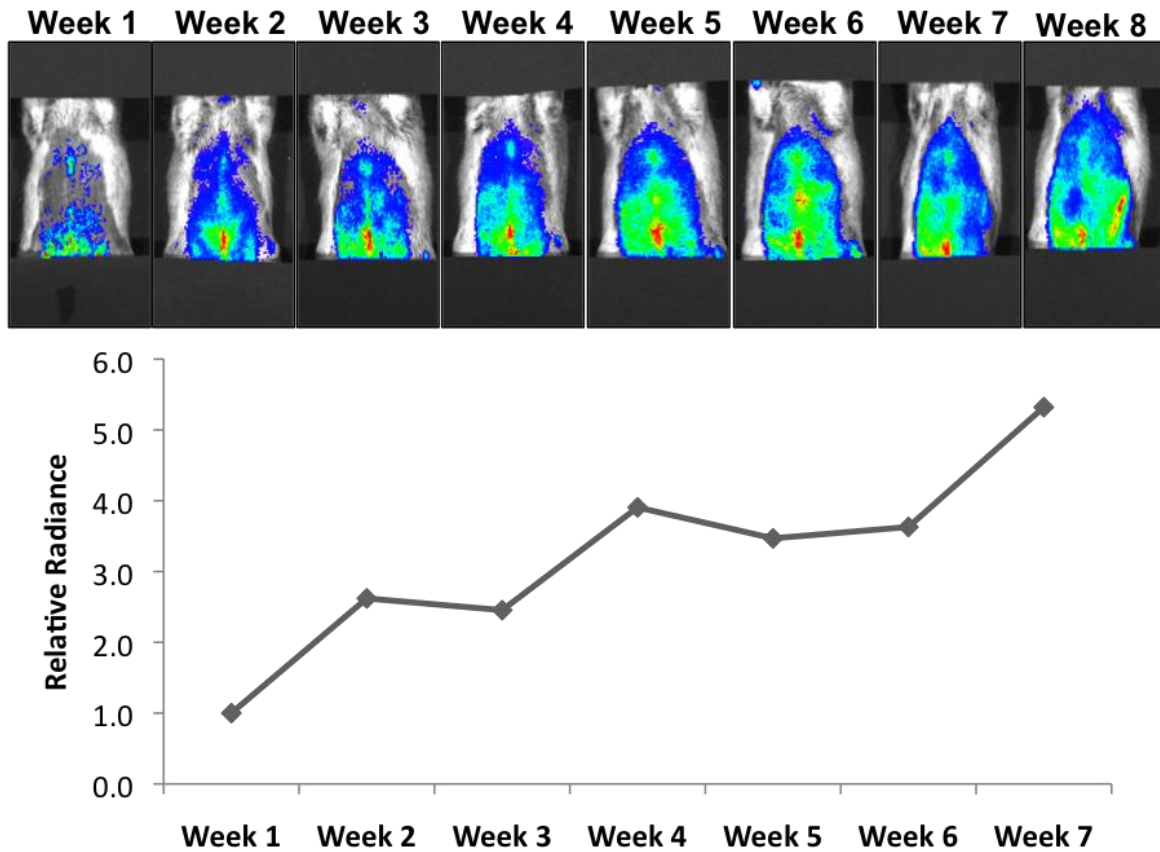
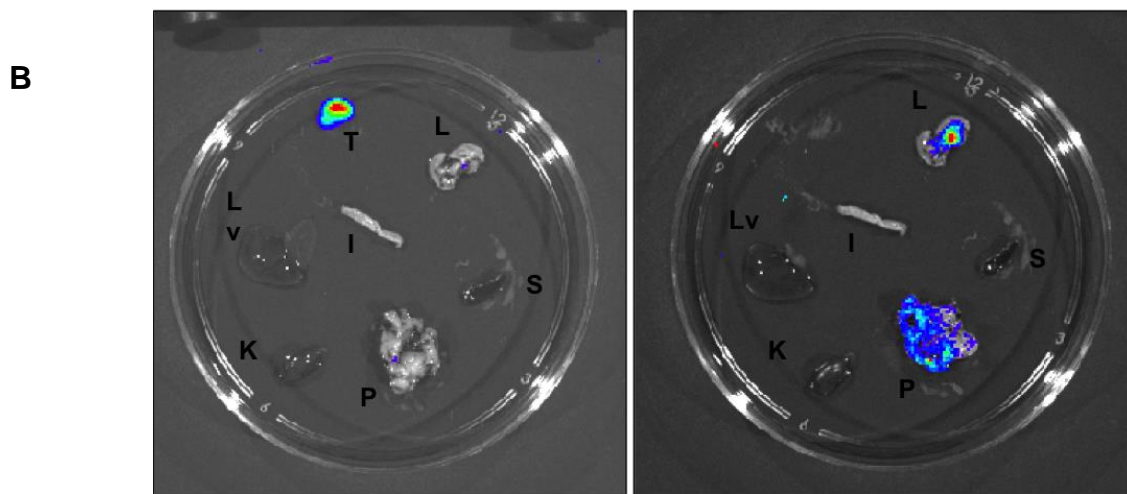
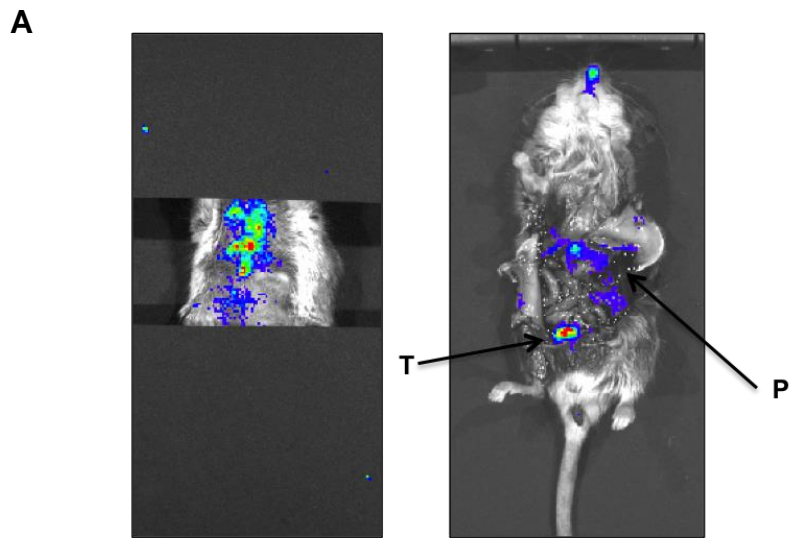


**Figure 42: Characterization of PMV Mouse #48 ( $p53^{fl/wt}$ ).** BLI images and quantification. Exposure = 15 seconds.



**P: pancreas/pancreatic tumor**    **I: intestine**  
**Lv: liver**                                **K: kidney**  
**L: lung**                                    **S: spleen**  
**T: testes**

**Figure 43: Characterization of PMV Mouse #225 ( $p53^{fl/fl}$ ).** (A) BLI images. (B) BLI images of organs post-necropsy.



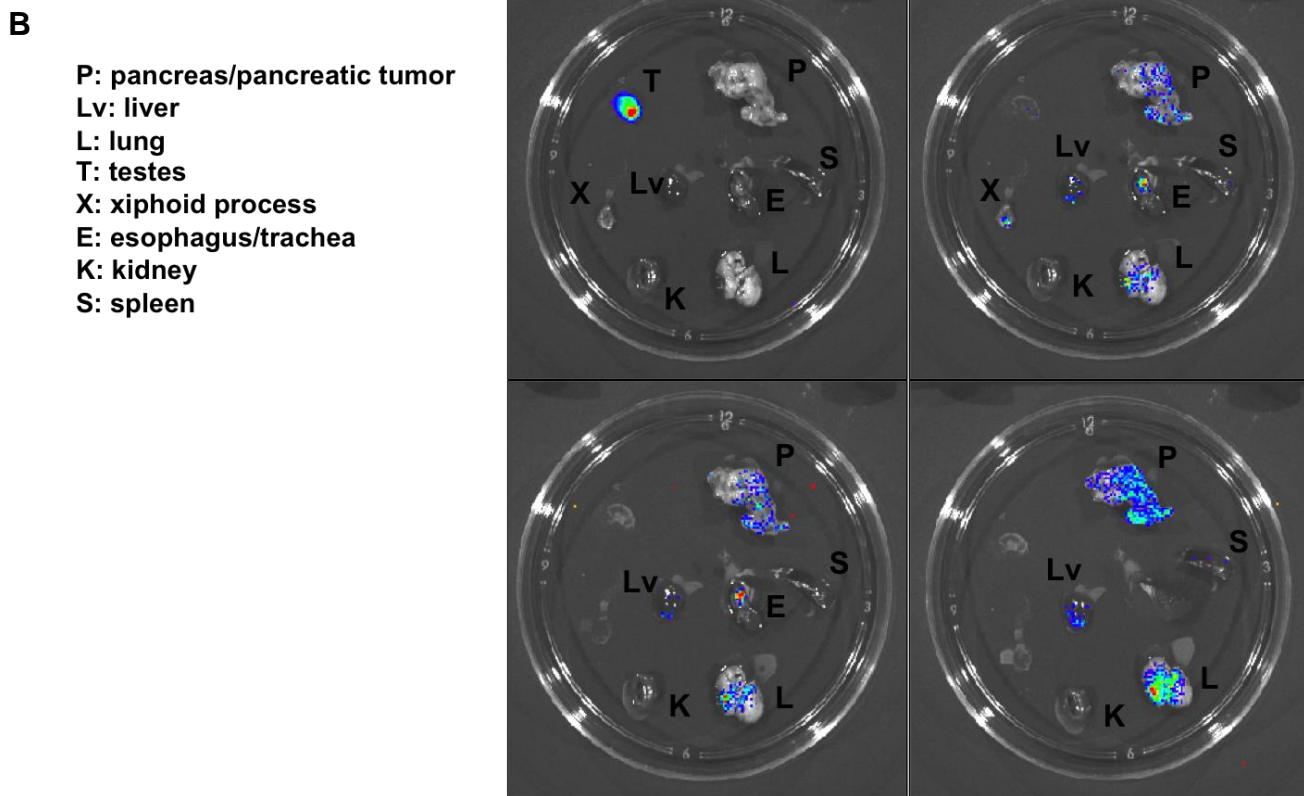
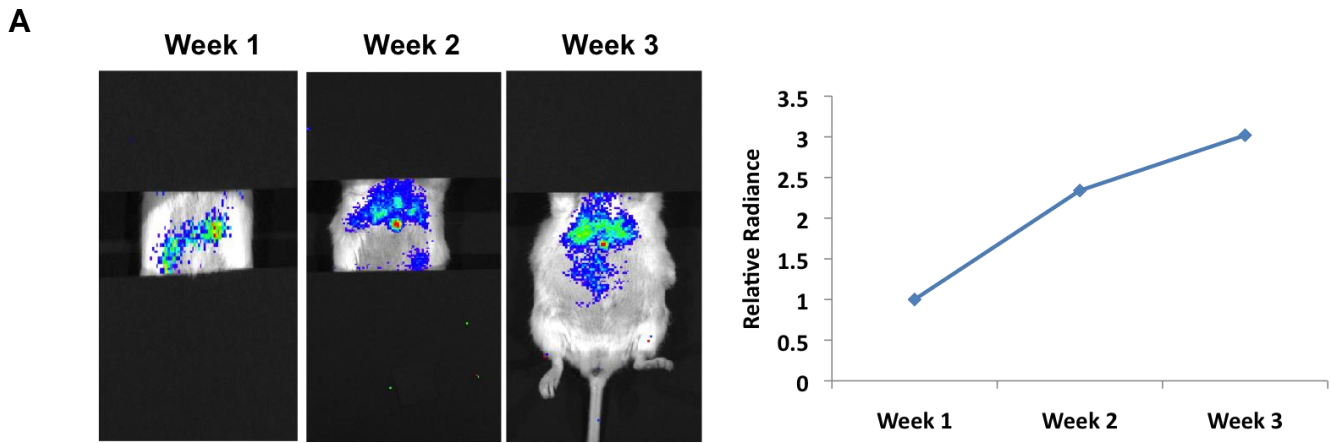


**Figure 44: Characterization of PMV Mouse #247 ( $p53^{fl/fl}$ ).** (A) BLI images and quantification. (B) BLI images of organs post-necropsy.

**PMV Mouse 271 (p53<sup>fl/fl</sup>) – female:** Unlike the testes of male mice, female PMV mice do not show any strong non-specific signal. The increasing signal seen is most likely indicative of underlying tumor (Fig. 45).

**PMV Mouse 261 (p53<sup>fl/fl</sup>) – female:** This mouse did not show significant non-specific signal throughout imaging. Upon necropsy, pancreatic tumor and lung showed expression, as well as minor expression in the reproductive tract. However, though there is some background signal in the reproductive tract, removing these organs do not significantly enhance the signal in the pancreas and lung, which supports that the signal is only mild and not affecting the ability to detect the pancreatic tumor (Fig. 46).

**PMV Mouse 249 (p53<sup>fl/fl</sup>) – female:** This mouse showed specific signal in the pancreas/pancreatic tumor. There does not appear to be any evidence of metastasis in this animal – the lungs were negative for expression (Fig. 47).

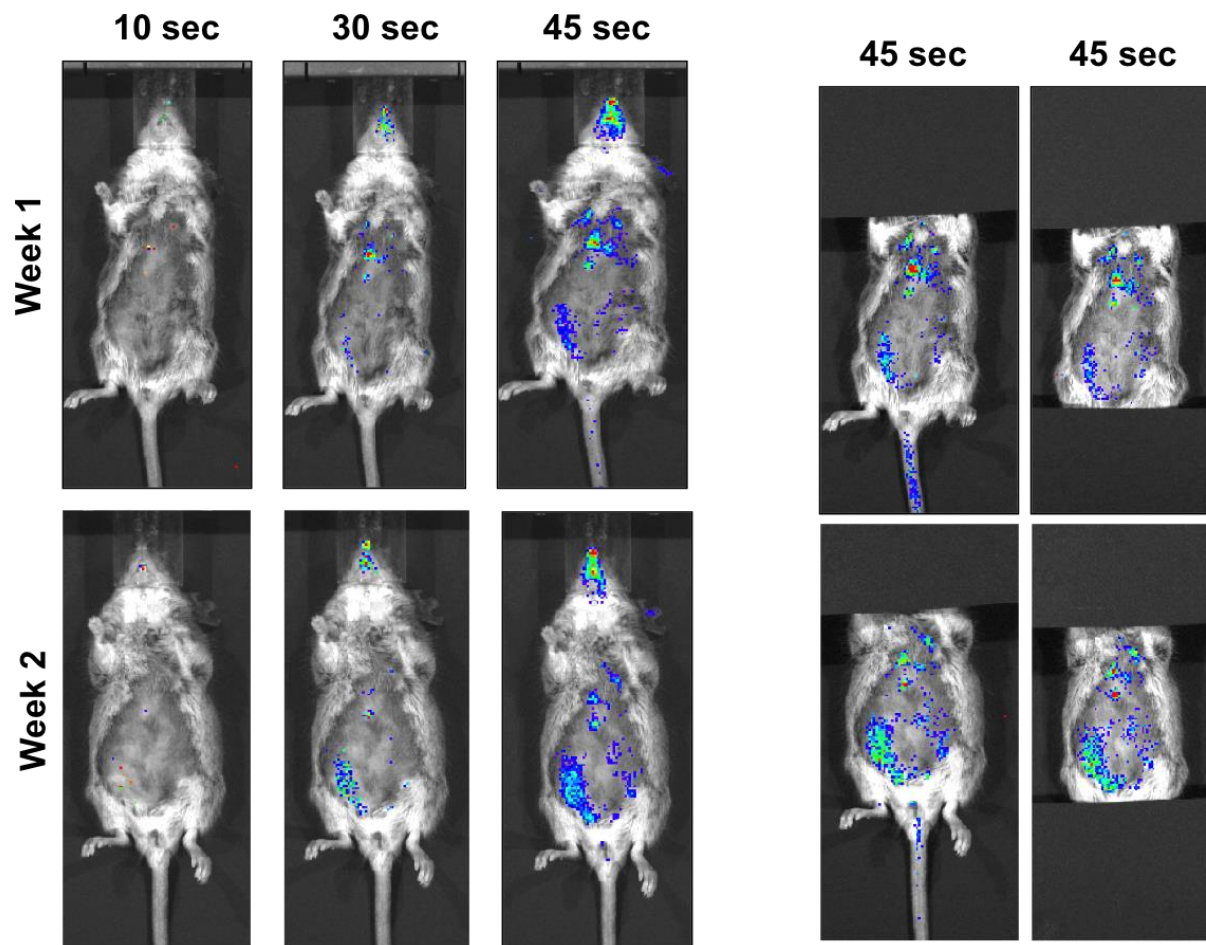
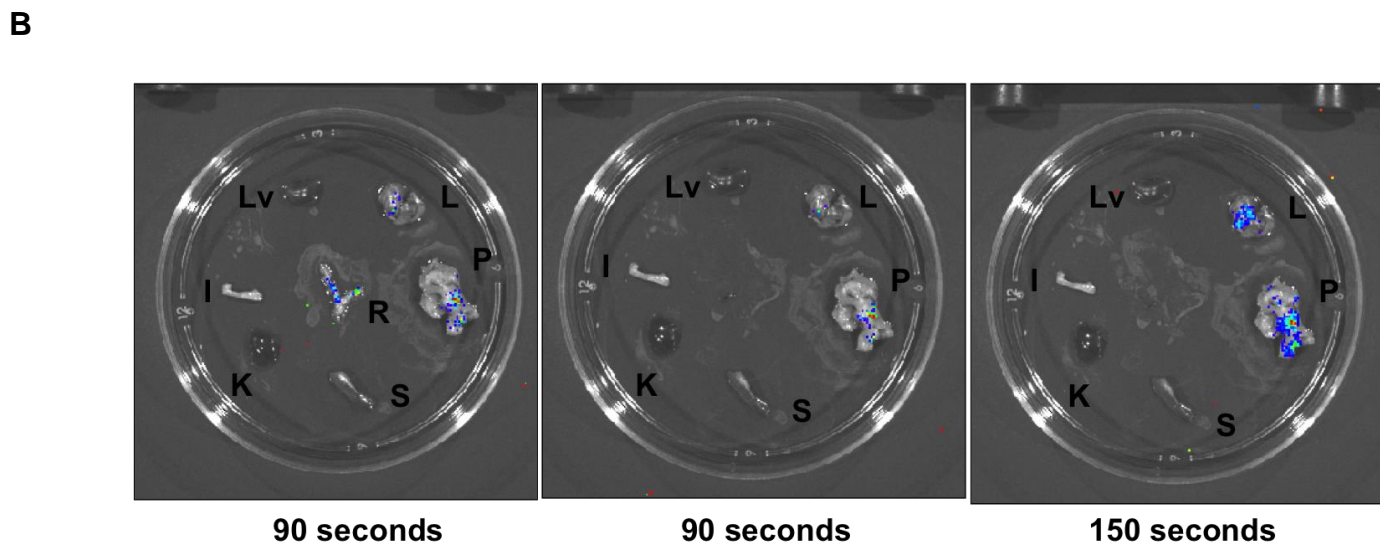
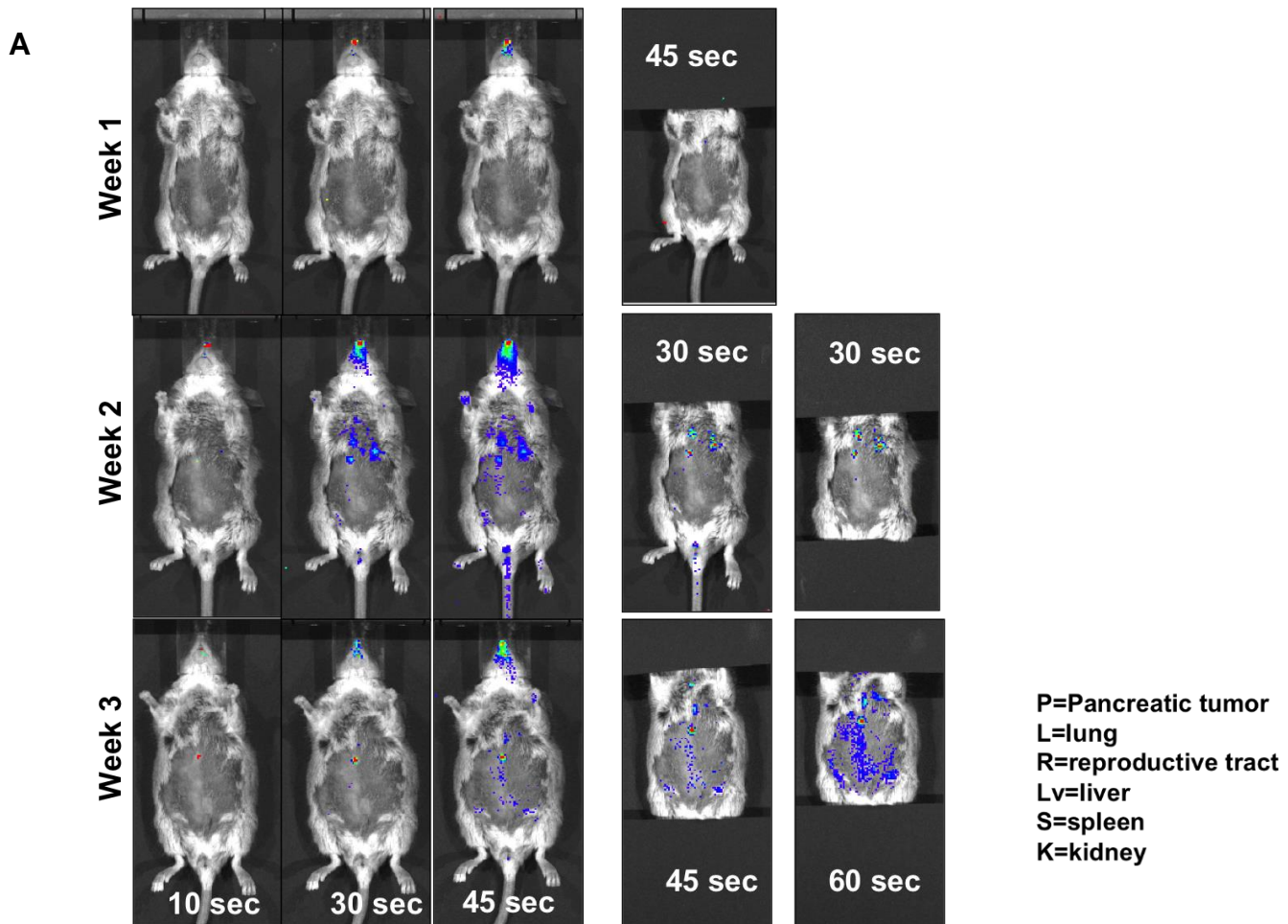
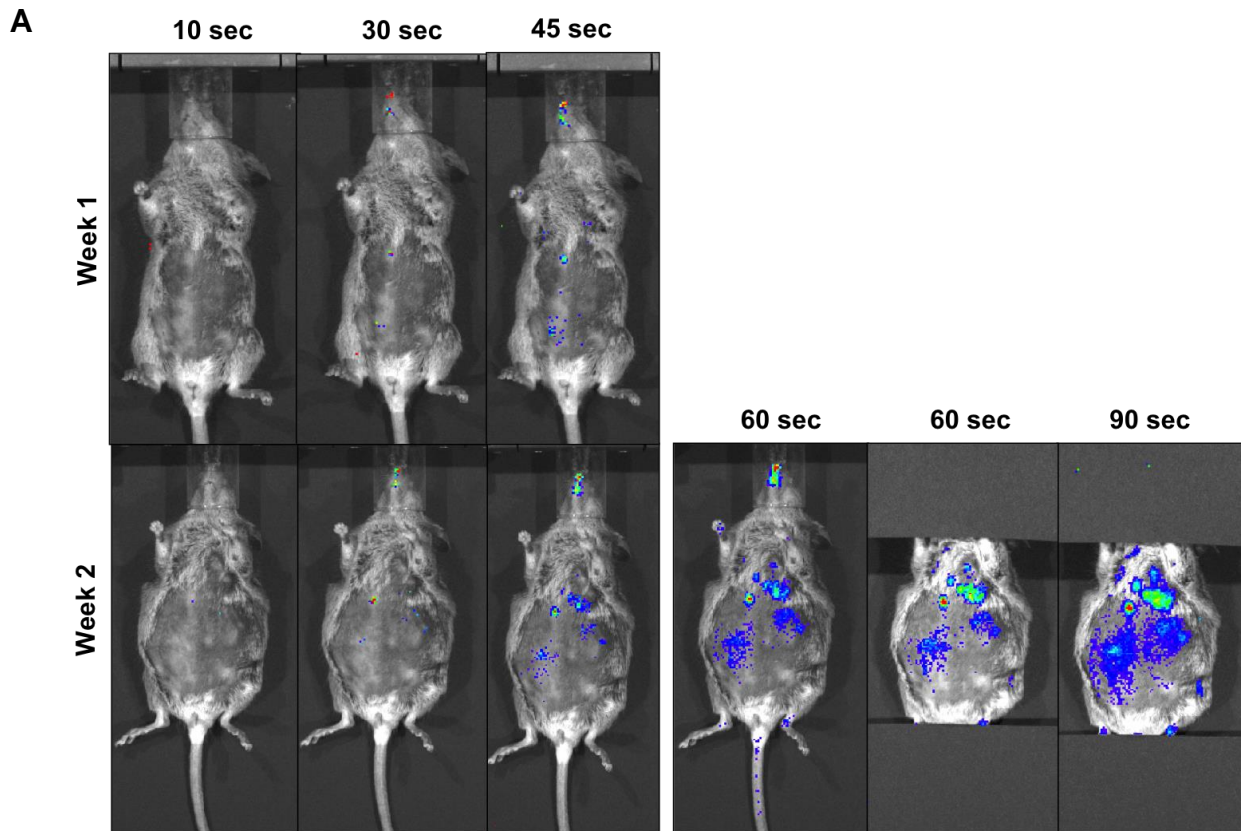


Figure 45: Characterization of PMV Mouse #271 (p53<sup>fl/fl</sup>)(female). BLI images.



**Figure 46: Characterization of PMV Mouse #261 ( $p53^{fl/fl}$ )(female). (A) BLI images. (B) BLI images of organs post-necropsy.**



**B**

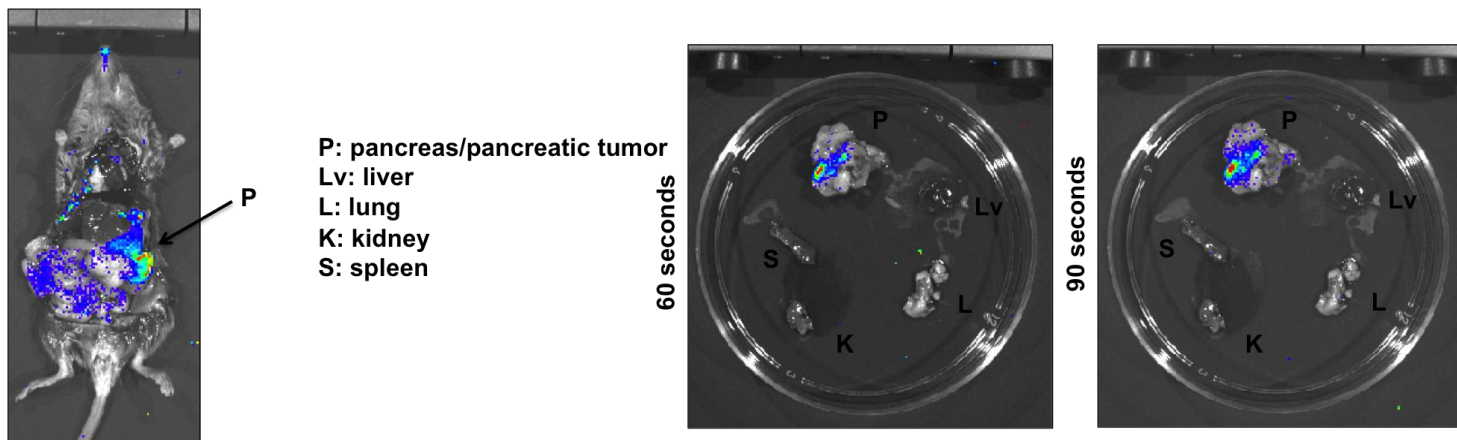


**Figure 47: Characterization of PMV Mouse #249 ( $p53^{fl/fl}$ )(female). (A) BLI images. (B) Imaging of opened abdominal cavity and organs post necropsy.**

### **A PMV pancreatic tumor-derived cell line retains luciferase expression *in vitro***

A cell line was established *in vitro* from a pancreatic tumor that developed in PMV Mouse #48. After being established in culture, cells ( $1 \times 10^6$ ) were injected bilaterally into the flanks of three athymic nude mice. Imaging at 10 days post-injection showed that these cells retained luciferase activity. Luciferase expression was detected by BLI in these tumors (Fig. 48). The tumors developed very rapidly and showed a more aggressive phenotype as compared to human pancreatic cancer cell lines similarly injected into nude mice (i.e., MIA-PaCa-2 and PANC-1 cells) (data not shown). These cells were also injected intraperitoneally into immune-competent Pdx-1-Cre-negative/*K-ras*<sup>LSL-G12D</sup>/*p53* mice, where they showed luciferase expression approximately 1 week after injection (Fig. 48). This last set of conditions was also repeated with bilateral flank injections. These mice form rapid tumors that can be imaged by BLI and make for a very useful syngeneic mouse model (Fig. 48).

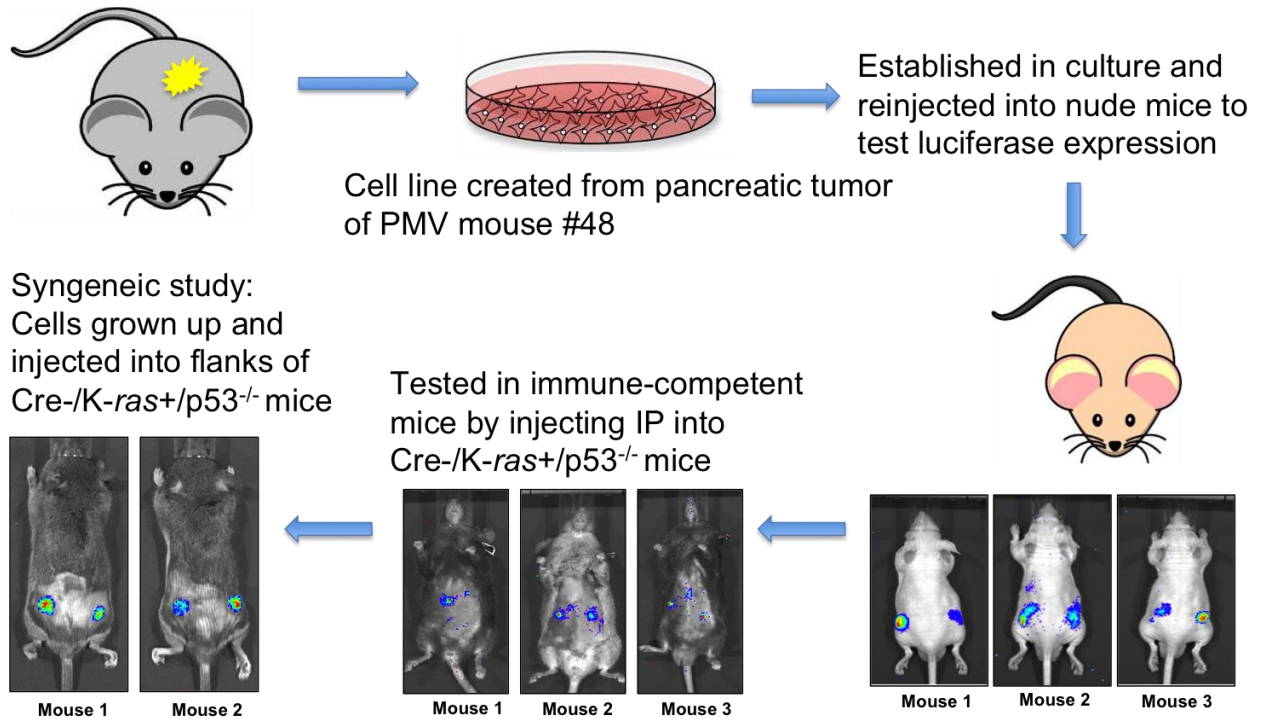


**Figure 48: PMV-derived cells retain luciferase activity *in vitro* and when reintroduced *in vivo***

## Discussion

The KPC model (Pdx-1-Cre/*K-ras*<sup>LSL-G12D</sup>/*p53*<sup>flox/wt</sup>) combines a mutated form of *K-ras* with loss of either one or both alleles of *p53* specifically in pancreatic tissue, which is accomplished through the use of a pancreatic specific promoter, Pdx-1. The result is a mouse that develops spontaneous pancreatic ductal adenocarcinoma (PDAC) at approximately 21 weeks of age (133).

Current studies utilizing the KPC model highlight the need for improved monitoring of tumors. Many studies either wait until an animal is sacrificed to collect data on therapeutic efficacy (130,132) or use more sophisticated imaging techniques that require additional training and cost (129,131). To enhance the utility of the KPC transgenic mouse model we developed CCN1-Prom-Luc (CCN1-Luc) transgenic mice, which display *de novo* Luciferase expression in the testes, but no other organ. Crossing CCN1-Luc mice with PDAC (KPC; Pdx-1-Cre/*K-ras*<sup>LSL-G12D</sup>/*p53*<sup>flox/wt</sup>) mice generated double transgenic mice (CCN1-luc/Pdx-1-Cre/*K-ras*<sup>LSL-G12D</sup>/*p53*<sup>flox/wt</sup> mice, *PanMetView* or PMV). Primary tumors and metastases in PMV mice display luciferase expression as pancreatic cancers develop and metastasize. Confirming the utility of PMV mice for detecting and monitoring progression and therapy of pancreatic cancer has the potential to transform how this PDAC animal model is used to study pancreatic cancer. Additionally, this approach also holds significant promise as a potentially universal strategy for converting any transgenic animal into a reporter-driven *PanMetView* (PMV) mouse by crossing it with CCN1-Prom-Luc transgenic mice.



All animals imaged thus far have shown expression in the testes, which was expected due to CCN1 expression in this organ. The signal in the testes is frequently strong enough that it overshadows any other signals, which can be problematic. However, because the anatomical location of this organ is distant from that of the pancreas, we can use black paper to physically cover parts of the mouse to block such signals. When one utilizes this approach, non-testes signals intensify. This has been a useful technique in identifying the presence of pancreatic tumors. Future studies will include alternate means of genetic and chemical modification to reduce or eliminate this signal in male animals. In the context of female animals, no non-specific signals are detected.

As with many transgenic models of human cancer, the KPC models shows great variability from animal to animal with respect to the precise time of tumor development, as well as the kinetics of tumor growth. This problem is also seen in the human disease state. PDAC is a particularly variable cancer, as some patients can survive for longer periods of time with a high tumor volume, while other patients die with relatively small tumors. The location of the tumor, as well as the growth parameters and invasive nature of the tumor, all of which can affect the normal functioning of surrounding organs and vessels, contributes to this end point. Because of this variability, one cannot make assumptions on the therapeutic efficacy of a drug based on a group of these mice. Rather, each mouse needs to be evaluated individually so as to be able to accurately assess the outcome of therapy on a particular tumor. The ability to generate individual tumor kinetic curves with the PMV mouse will be a great advantage to developing highly impactful preclinical studies.

Our PMV model provides a way of non-invasively monitoring KPC tumor progression that improves the quality of studies relying on survival and/or post-mortem evaluation for data. Additionally, our PMV model also provides an imaging strategy that is relatively inexpensive, easy to use, and has wide levels of applicability, which gives it advantages over other imaging modalities. Furthermore, the ability to detect metastasis is possible using the PMV system, which is not a possibility with imaging methods, such as ultrasound. The PMV model is transformative and can be rapidly used to test for effective therapies of PDAC in an immune-competent transgenic mouse. Showing the therapeutic efficacy of a novel drug or compound in immune-competent transgenic pre-clinical models of disease is critical for developing improved therapies for patients with PDAC. Our proposed studies will allow for a significant gain in utility of an accepted PDAC model for the study of pancreatic cancer development, progression and therapy.

## Chapter 5: Summary and Future Perspectives

Despite years of research, pancreatic cancer remains an extremely deadly disease with very few therapeutic options. The poor prognosis results from both a delay in diagnosis, due to a lack of telling symptoms, as well as a significant amount of diverse genetic changes, which contribute to its intrinsic aggressive nature and resistance to standard therapies. This body of work has focused on exploring novel avenues of therapeutic targeting in pancreatic cancer. This includes the identification and targeting of novel targets, the modification of current therapies to improve efficacy, and the creation of improved methods of studying potential therapies in preclinical work.

Chapter 2 describes this first technique, in which the anti-apoptotic Bcl-2 proteins were hypothesized to be a potential therapeutic target in pancreatic cancer. Sabutoclax, a small molecule BH3 mimetic, binds to and inhibits the function of the anti-apoptotic Bcl-2 proteins. In this study, we aimed to evaluate the efficacy of Sabutoclax and Minocycline, a synthetic tetracycline and understudied potential anti-cancer agent in the treatment of pancreatic cancer. We used a variety of *in vitro* techniques including proliferation and cell death assays, cell cycle analysis, and western blotting to accomplish this in multiple pancreatic cancer cell lines. Several mouse models were also used to scrutinize these drugs *in vivo*, including the commonly used KPC mouse model. Sabutoclax induced growth arrest and apoptosis in pancreatic cancer cells and synergized with Minocycline. Together, these two drugs showed profound cytotoxicity that was caspase-dependent and occurred through the mitochondrial pathway of apoptosis. Furthermore, the toxicity induced by Sabutoclax and Minocycline was reliant

upon loss of phosphorylated Stat3, with reintroduction of activated Stat3 capable of rescuing cells from toxicity. *In vivo* work showed that this combination inhibited tumor growth in immune-deficient and immune-competent models and prolonged survival in the KPC transgenic mouse. In conclusion, Sabutoclax and Minocycline promoted profound cytotoxicity in pancreatic cancer, both *in vitro* and in multiple *in vivo* animal models providing significant survival benefits. These drugs offer a novel and exciting direction for developing effective therapeutic options for patients with this devastating disease.

Chapter 3 introduced a novel strategy of taking a commonly used chemotherapeutic drug, Gemcitabine, and altering it in an attempt to increase efficacy. Despite being used extensively in the treatment of pancreatic cancer, Gemcitabine delivers minimal survival results at best. This is partly due to intrinsic cellular resistance mechanisms that lead to either decreased uptake of the drug, improper metabolism and utilization, or increased output of the drug. We showed that linking Gemcitabine to a peptide that specifically targets the EphrinA2 receptor, which is overexpressed on pancreatic cancer cell surfaces, leads to an increased uptake of the drug through an alternate delivery mechanism. More recent studies using a synthetic peptide, 123B9, tethered to Paclitaxel also showed encouraging results, with the drug conjugate demonstrating better efficacy as compared to Paclitaxel alone. This modified drug also showed exciting results when used in combination with Gemcitabine. These studies and this combination in particular are extremely clinically relevant due to the recent approval of Gemcitabine-Abraxane (nab-Paclitaxel) as the first line treatment for metastatic pancreatic cancer. 123B9 demonstrates increased plasma stability as

compared to YNH, which translates to greater clinical potential. We found that *in vivo*, these novel drug conjugates inhibit tumor growth and lead to a prolonged survival. Importantly, the addition of the peptide does not confer any additional toxicity to the drug and holds significant clinical potential. 123B9-Gemcitabine conjugates have been made as well and studies with this drug are in progress.

Finally, in Chapter 4 we introduce an exciting and novel preclinical mouse model that builds off of the existing and commonly used KPC transgenic mouse model of pancreatic cancer. Though this model accurately recapitulates the human disease, monitoring tumor development and growth remains a difficult obstacle and hinders the ability of researchers to perform sophisticated studies with this animal. Many imaging techniques, such as ultrasound or PET, though useful for monitoring tumor in these mice, can be expensive, require extensive training, and take significant time. Most importantly, these methods cannot detect tumor metastasis, an important feature of this disease. We hypothesized that crossing KPC mice to a mouse that expresses a Luciferase reporter gene under the control of a cancer specific promoter, CCN1, would allow us to create a mouse in which the promoter was turned on during cancer development in the pancreas and lead to luciferase expression in all transformed cells. Luciferase expression *in vivo* can be easily monitored via BLI and provides a rapid result image that can be easily quantified to follow tumor development. Of significance is the ability to monitor metastasis in this mouse. As tumor cells express luciferase, metastatic lesions that would otherwise be too small to see via other imaging modalities show expression using BLI and provide a novel technique of monitoring the metastatic process in the KPC model.

Moving forward, these studies provide important beginnings for novel avenues of therapeutic exploration in pancreatic cancer. The Bcl-2 family of proteins is understudied as a therapeutic target in pancreatic cancer and our data provide solid evidence that compounds such as Sabutoclax deserve further attention and study. From a clinical perspective, there is significant potential in targeting Mcl-1 for suppression. The Bcl-2 anti-apoptotic proteins continue to present roadblocks in the treatment of cancers when using conventional chemotherapeutics. Their overexpression becomes vital to the survival of many types of tumors. Mcl-1, in particular, plays a significant role in the ability of cancers not only to survive, but also to resist treatment with chemotherapy and radiation. *In vitro* experiments using Mcl-1 ASO emphasize the anti-tumor potential of targeting Mcl-1 both alone and in combination with other therapeutic agents.

Developing an optimal cancer therapeutic for any tumor indication is clearly an imprecise process and very difficult. To achieve this objective, a number of issues must be considered one of which is the best approach to use. What technique would be most appropriate to target Mcl-1? Since the ultimate aim is to develop a viable clinical therapy, it is important to consider the translational potential of any strategy. Some strategies, like those that employ ASO, may be very effective in *in vitro* and preclinical experimental settings, but are not easily translated into the clinic. In contrast, other methodologies, like the use of small molecule antagonists, may hold greater potential for clinical translation if an effective drug level can be attained without unacceptable toxicity. Ultimately, the real potential of these compounds may lie in combination therapies, as we have demonstrated with Sabutoclax and Minocycline.

Another important consideration in developing an appropriate cancer therapeutic is the target itself. There is abundant evidence in almost every cancer type that the Bcl-2 anti-apoptotic proteins play a significant role to some extent in that cancer's survival. Many studies provide evidence that targeting these anti-apoptotic proteins individually might be a promising treatment strategy. What is only recently becoming abundantly evident is the importance of interactions between these proteins in both normal and cancer cells. Protein:protein interactions are complex and the interplay between multiple proteins in these complexes and their consequences on cellular phenotype are active areas of investigation. It is also important that when targeting these proteins to block their interactions off-target toxicity in normal cells and tissues is not promoted.

Our studies with Sabutoclax and the combination of Sabutoclax and Minocycline may demonstrate the importance of such interactions through the potent loss of Stat3 activation observed with this treatment. Though the effect of Stat3 activation on Mcl-1 is clearly defined, the reverse situation is not. Why does targeting downstream proteins like Mcl-1 lead to such potent upstream signaling changes? Research into the literature on Stat3 regulation and potential feedback loops through Mcl-1 or Bcl-xL reveal very little. Known interactions between the anti-apoptotic Bcl-2 proteins with proteins outside of this family do not play any known role in Stat3 activation. However, due to the low dose of Sabutoclax that is being used, we feel strongly that these signaling changes are not reflective of off-target effects of the drug. Rather, we have hypothesized that Sabutoclax may be interrupting a protein:protein interaction between Mcl-1 or one of the other antiapoptotic proteins and a yet unidentified second protein. Our theory is that disruption of this interaction may release this second protein, which we hypothesize to

have either direct or indirect effects on Stat3 activation. Recent studies by Maurizio Pellecchia's group have provided evidence that may support this hypothesis (161). Using Sabutoclax as competition, they screened a 12-residue phage display library for peptides that bound Mcl-1, specifically the BH3 binding domain. Their studies resulted in the identification of a novel Mcl-1 protein-binding motif and subsequently, novel potential protein interaction partners that display this motif. This is significant, especially for our studies, as it sheds light on previously unknown Mcl-1 binding partners. As we have hypothesized that such an interaction may be mechanistically responsible for the effects we have observed with Sabutoclax and Minocycline, this new information provides a beneficial point from which to develop future studies.

In continuing efforts to develop new and better BH3 mimetics, understanding potential mechanisms of resistance is critical. Resistance remains a significant problem in cancer therapy in general, and understanding how it develops may be of great value in designing approaches to circumvent this major barrier to cure. Considering that the Bcl-2 family of anti-apoptotic proteins plays a critical role in cancer maintenance and resistance, these proteins represent high-priority targets for the next generation of combinatorial therapies for neoplastic diseases.

The development of novel targeted agents, however, is only as useful as the model with which you can test them. Our studies characterizing the PMV mouse are very exciting, as this strategy elevates the sophistication and utility of the KPC transgenic mouse model by adding a non-invasive imaging component. This mouse will soon be used in therapeutic studies that we hope will produce beneficial preclinical data. Future studies will focus not only on using these mice for preclinical work, but



also on improving the model even more. To enhance further the value of the PMV mouse we intend to create a transgenic mouse producing the human secreted embryonic alkaline phosphatase (SEAP) protein selectively in cancerous pancreatic tissue by regulation through a cancer-selective promoter, *CCN1-Prom*. Crossing tCCN1-SEAP animals with PMV animals will produce compound '*Pancreatic Biomarker Metastasis View*' (PBMV) mice. This model would not only have a built-in imaging system to non-invasively monitor tumor development and growth, but it would also have a built-in biomarker detection system to support and confirm imaging analyses non-invasively. Early detection of tumors can be integral in managing the life of a patient with cancer, but in most situations achieving this objective can be problematic. Although imaging and other modalities have been used for this purpose for subsets of cancers, developing a more direct approach would be of added benefit. The ability to detect cancer biomarkers in a patient's blood sample represents a valuable contribution to cancer detection. Unfortunately, there has been limited success to date clinically due to sensitivity and specificity issues related to a given biomarker.

*SEAP* transgenic mice have been previously engineered in which *SEAP* expression is under the control of an organ-specific promoter (162) and adenoviruses expressing *SEAP* under the control of cancer-specific promoters have been shown to be functional both *in vitro* and *in vivo* (163,164). However, a transgenic animal that expresses *SEAP* under the control of a cancer-specific promoter is a novel strategy that would further enhance the utility of our PMV mouse. Depending on the sensitivity of this system, it may even allow us to detect tumor initiation earlier than with BLI. This dual-monitoring compound transgenic model would be unique and would significantly

enhance a variety of chemoprevention and therapeutic studies in pancreatic cancer transgenic as well as in other cancer transgenic mouse models.

## References

1. Hezel AF, Kimmelman AC, Stanger BZ, Bardeesy N, Depinho RA. Genetics and biology of pancreatic ductal adenocarcinoma. *Genes & development* 2006;20(10):1218-49.
2. Ryan DP, Hong TS, Bardeesy N. Pancreatic adenocarcinoma. *The New England journal of medicine* 2014;371(11):1039-49.
3. Burris HA, 3rd, Moore MJ, Andersen J, Green MR, Rothenberg ML, Modiano MR, et al. Improvements in survival and clinical benefit with gemcitabine as first-line therapy for patients with advanced pancreas cancer: a randomized trial. *Journal of clinical oncology : official journal of the American Society of Clinical Oncology* 1997;15(6):2403-13.
4. Feldmann G, Beaty R, Hruban RH, Maitra A. Molecular genetics of pancreatic intraepithelial neoplasia. *Journal of hepato-biliary-pancreatic surgery* 2007;14(3):224-32.
5. Lohr M, Kloppel G, Maisonneuve P, Lowenfels AB, Luttges J. Frequency of K-ras mutations in pancreatic intraductal neoplasias associated with pancreatic ductal adenocarcinoma and chronic pancreatitis: a meta-analysis. *Neoplasia* 2005;7(1):17-23.
6. Aguirre AJ, Bardeesy N, Sinha M, Lopez L, Tuveson DA, Horner J, et al. Activated Kras and Ink4a/Arf deficiency cooperate to produce metastatic pancreatic ductal adenocarcinoma. *Genes & development* 2003;17(24):3112-26.

7. Klein AP, Beaty TH, Bailey-Wilson JE, Brune KA, Hruban RH, Petersen GM. Evidence for a major gene influencing risk of pancreatic cancer. *Genetic epidemiology* 2002;23(2):133-49.
8. Furukawa T. Molecular pathology of pancreatic cancer: implications for molecular targeting therapy. *Clinical gastroenterology and hepatology : the official clinical practice journal of the American Gastroenterological Association* 2009;7(11 Suppl):S35-9.
9. Hruban RH, Adsay NV, Albores-Saavedra J, Anver MR, Biankin AV, Boivin GP, et al. Pathology of genetically engineered mouse models of pancreatic exocrine cancer: consensus report and recommendations. *Cancer research* 2006;66(1):95-106.
10. Jing N, Tweardy DJ. Targeting Stat3 in cancer therapy. *Anti-cancer drugs* 2005;16(6):601-7.
11. Haftchenary S, Avadisian M, Gunning PT. Inhibiting aberrant Stat3 function with molecular therapeutics: a progress report. *Anti-cancer drugs* 2011;22(2):115-27.
12. Levy DE, Lee CK. What does Stat3 do? *The Journal of clinical investigation* 2002;109(9):1143-8.
13. Yang G, Huang C, Cao J, Huang KJ, Jiang T, Qiu ZJ. Lentivirus-mediated shRNA interference targeting STAT3 inhibits human pancreatic cancer cell invasion. *World journal of gastroenterology : WJG* 2009;15(30):3757-66.
14. Safran H, Steinhoff M, Mangray S, Rathore R, King TC, Chai L, et al. Overexpression of the HER-2/neu oncogene in pancreatic adenocarcinoma. *American journal of clinical oncology* 2001;24(5):496-9.

15. Hansel DE, Kern SE, Hruban RH. Molecular pathogenesis of pancreatic cancer. Annual review of genomics and human genetics 2003;4:237-56.
16. Gansauge S, Gansauge F, Ramadani M, Stobbe H, Rau B, Harada N, et al. Overexpression of cyclin D1 in human pancreatic carcinoma is associated with poor prognosis. Cancer research 1997;57(9):1634-7.
17. Hermanova M, Karasek P, Tomasek J, Lenz J, Jarkovsky J, Dite P. Comparative analysis of clinicopathological correlations of cyclooxygenase-2 expression in resectable pancreatic cancer. World journal of gastroenterology : WJG 2010;16(15):1879-84.
18. De La OJ, Murtaugh LC. Notch and Kras in pancreatic cancer: at the crossroads of mutation, differentiation and signaling. Cell cycle 2009;8(12):1860-4.
19. Mandelin AM, 2nd, Pope RM. Myeloid cell leukemia-1 as a therapeutic target. Expert opinion on therapeutic targets 2007;11(3):363-73.
20. Kang MH, Reynolds CP. Bcl-2 inhibitors: targeting mitochondrial apoptotic pathways in cancer therapy. Clinical cancer research : an official journal of the American Association for Cancer Research 2009;15(4):1126-32.
21. Danial NN. BCL-2 family proteins: critical checkpoints of apoptotic cell death. Clinical cancer research : an official journal of the American Association for Cancer Research 2007;13(24):7254-63.
22. Kozopas KM, Yang T, Buchan HL, Zhou P, Craig RW. MCL1, a gene expressed in programmed myeloid cell differentiation, has sequence similarity to BCL2. Proceedings of the National Academy of Sciences of the United States of America 1993;90(8):3516-20.

23. Reynolds JE, Yang T, Qian L, Jenkinson JD, Zhou P, Eastman A, et al. Mcl-1, a member of the Bcl-2 family, delays apoptosis induced by c-Myc overexpression in Chinese hamster ovary cells. *Cancer research* 1994;54(24):6348-52.
24. Thomas LW, Lam C, Edwards SW. Mcl-1; the molecular regulation of protein function. *FEBS letters* 2010;584(14):2981-9.
25. Germain M, Duronio V. The N terminus of the anti-apoptotic BCL-2 homologue MCL-1 regulates its localization and function. *The Journal of biological chemistry* 2007;282(44):32233-42.
26. Rechsteiner M, Rogers SW. PEST sequences and regulation by proteolysis. *Trends in biochemical sciences* 1996;21(7):267-71.
27. Day CL, Chen L, Richardson SJ, Harrison PJ, Huang DC, Hinds MG. Solution structure of prosurvival Mcl-1 and characterization of its binding by proapoptotic BH3-only ligands. *The Journal of biological chemistry* 2005;280(6):4738-44.
28. Akgul C. Mcl-1 is a potential therapeutic target in multiple types of cancer. *Cellular and molecular life sciences : CMLS* 2009;66(8):1326-36.
29. Bingle CD, Craig RW, Swales BM, Singleton V, Zhou P, Whyte MK. Exon skipping in Mcl-1 results in a bcl-2 homology domain 3 only gene product that promotes cell death. *The Journal of biological chemistry* 2000;275(29):22136-46.
30. Mott JL, Kobayashi S, Bronk SF, Gores GJ. mir-29 regulates Mcl-1 protein expression and apoptosis. *Oncogene* 2007;26(42):6133-40.
31. Steele R, Mott JL, Ray RB. MBP-1 upregulates miR-29b that represses Mcl-1, collagens, and matrix-metalloproteinase-2 in prostate cancer cells. *Genes & cancer* 2010;1(4):381-87.

32. Xiong Y, Fang JH, Yun JP, Yang J, Zhang Y, Jia WH, et al. Effects of microRNA-29 on apoptosis, tumorigenicity, and prognosis of hepatocellular carcinoma. *Hepatology* 2010;51(3):836-45.
33. Domina AM, Vrana JA, Gregory MA, Hann SR, Craig RW. MCL1 is phosphorylated in the PEST region and stabilized upon ERK activation in viable cells, and at additional sites with cytotoxic okadaic acid or taxol. *Oncogene* 2004;23(31):5301-15.
34. Maurer U, Charvet C, Wagman AS, Dejardin E, Green DR. Glycogen synthase kinase-3 regulates mitochondrial outer membrane permeabilization and apoptosis by destabilization of MCL-1. *Molecular cell* 2006;21(6):749-60.
35. Zhong Q, Gao W, Du F, Wang X. Mule/ARF-BP1, a BH3-only E3 ubiquitin ligase, catalyzes the polyubiquitination of Mcl-1 and regulates apoptosis. *Cell* 2005;121(7):1085-95.
36. Inuzuka H, Shaik S, Onoyama I, Gao D, Tseng A, Maser RS, et al. SCF(FBW7) regulates cellular apoptosis by targeting MCL1 for ubiquitylation and destruction. *Nature* 2011;471(7336):104-9.
37. Placzek WJ, Wei J, Kitada S, Zhai D, Reed JC, Pellecchia M. A survey of the anti-apoptotic Bcl-2 subfamily expression in cancer types provides a platform to predict the efficacy of Bcl-2 antagonists in cancer therapy. *Cell death & disease* 2010;1:e40.
38. Zhuang L, Lee CS, Scolyer RA, McCarthy SW, Zhang XD, Thompson JF, et al. Mcl-1, Bcl-XL and Stat3 expression are associated with progression of melanoma whereas Bcl-2, AP-2 and MITF levels decrease during progression of melanoma. *Modern pathology : an official journal of the United States and Canadian Academy of Pathology, Inc* 2007;20(4):416-26.

39. Selzer E, Schlagbauer-Wadl H, Okamoto I, Pehamberger H, Potter R, Jansen B. Expression of Bcl-2 family members in human melanocytes, in melanoma metastases and in melanoma cell lines. *Melanoma research* 1998;8(3):197-203.
40. Thallinger C, Wolschek MF, Wacheck V, Maierhofer H, Gunsberg P, Polterauer P, et al. Mcl-1 antisense therapy chemosensitizes human melanoma in a SCID mouse xenotransplantation model. *The Journal of investigative dermatology* 2003;120(6):1081-6.
41. Hotz MA, Bosq J, Zbaeren P, Reed J, Schwab G, Krajewski S, et al. Spontaneous apoptosis and the expression of p53 and Bcl-2 family proteins in locally advanced head and neck cancer. *Archives of otolaryngology--head & neck surgery* 1999;125(4):417-22.
42. Skoda C, Erovic BM, Wachek V, Vormittag L, Wrba F, Martinek H, et al. Down-regulation of Mcl-1 with antisense technology alters the effect of various cytotoxic agents used in treatment of squamous cell carcinoma of the head and neck. *Oncology reports* 2008;19(6):1499-503.
43. Sieghart W, Losert D, Strommer S, Cejka D, Schmid K, Rasoul-Rockenschaub S, et al. Mcl-1 overexpression in hepatocellular carcinoma: a potential target for antisense therapy. *Journal of hepatology* 2006;44(1):151-7.
44. Derenne S, Monia B, Dean NM, Taylor JK, Rapp MJ, Harousseau JL, et al. Antisense strategy shows that Mcl-1 rather than Bcl-2 or Bcl-x(L) is an essential survival protein of human myeloma cells. *Blood* 2002;100(1):194-9.
45. Wei SH, Dong K, Lin F, Wang X, Li B, Shen JJ, et al. Inducing apoptosis and enhancing chemosensitivity to gemcitabine via RNA interference targeting Mcl-1 gene in



- pancreatic carcinoma cell. *Cancer chemotherapy and pharmacology* 2008;62(6):1055-64.
46. Khoury JD, Medeiros LJ, Rassidakis GZ, McDonnell TJ, Abruzzo LV, Lai R. Expression of Mcl-1 in mantle cell lymphoma is associated with high-grade morphology, a high proliferative state, and p53 overexpression. *The Journal of pathology* 2003;199(1):90-7.
47. Zhou P, Levy NB, Xie H, Qian L, Lee CY, Gascoyne RD, et al. MCL1 transgenic mice exhibit a high incidence of B-cell lymphoma manifested as a spectrum of histologic subtypes. *Blood* 2001;97(12):3902-9.
48. Hussain SR, Cheney CM, Johnson AJ, Lin TS, Grever MR, Caligiuri MA, et al. Mcl-1 is a relevant therapeutic target in acute and chronic lymphoid malignancies: down-regulation enhances rituximab-mediated apoptosis and complement-dependent cytotoxicity. *Clinical cancer research : an official journal of the American Association for Cancer Research* 2007;13(7):2144-50.
49. Chen R, Keating MJ, Gandhi V, Plunkett W. Transcription inhibition by flavopiridol: mechanism of chronic lymphocytic leukemia cell death. *Blood* 2005;106(7):2513-9.
50. Bible KC, Lensing JL, Nelson SA, Lee YK, Reid JM, Ames MM, et al. Phase 1 trial of flavopiridol combined with cisplatin or carboplatin in patients with advanced malignancies with the assessment of pharmacokinetic and pharmacodynamic end points. *Clinical cancer research : an official journal of the American Association for Cancer Research* 2005;11(16):5935-41.

51. Kitada S, Zapata JM, Andreeff M, Reed JC. Protein kinase inhibitors flavopiridol and 7-hydroxy-staurosporine down-regulate antiapoptosis proteins in B-cell chronic lymphocytic leukemia. *Blood* 2000;96(2):393-7.
52. Byrd JC, Lin TS, Dalton JT, Wu D, Phelps MA, Fischer B, et al. Flavopiridol administered using a pharmacologically derived schedule is associated with marked clinical efficacy in refractory, genetically high-risk chronic lymphocytic leukemia. *Blood* 2007;109(2):399-404.
53. Mitchell C, Yacoub A, Hossein H, Martin AP, Bareford MD, Eulitt P, et al. Inhibition of MCL-1 in breast cancer cells promotes cell death in vitro and in vivo. *Cancer biology & therapy* 2010;10(9):903-17.
54. Rosato RR, Almenara JA, Kolla SS, Maggio SC, Coe S, Gimenez MS, et al. Mechanism and functional role of XIAP and Mcl-1 down-regulation in flavopiridol/vorinostat antileukemic interactions. *Molecular cancer therapeutics* 2007;6(2):692-702.
55. Tan AR, Yang X, Berman A, Zhai S, Sparreboom A, Parr AL, et al. Phase I trial of the cyclin-dependent kinase inhibitor flavopiridol in combination with docetaxel in patients with metastatic breast cancer. *Clinical cancer research : an official journal of the American Association for Cancer Research* 2004;10(15):5038-47.
56. Dai Y, Rahmani M, Grant S. Proteasome inhibitors potentiate leukemic cell apoptosis induced by the cyclin-dependent kinase inhibitor flavopiridol through a SAPK/JNK- and NF-kappaB-dependent process. *Oncogene* 2003;22(46):7108-22.
57. Holkova B, Perkins EB, Ramakrishnan V, Tombes MB, Shrader E, Talreja N, et al. Phase I trial of bortezomib (PS-341; NSC 681239) and alvocidib (flavopiridol; NSC 649890) in patients with recurrent or refractory B-cell neoplasms. *Clinical cancer*

research : an official journal of the American Association for Cancer Research  
2011;17(10):3388-97.

58. Chen R, Wierda WG, Chubb S, Hawtin RE, Fox JA, Keating MJ, et al. Mechanism of action of SNS-032, a novel cyclin-dependent kinase inhibitor, in chronic lymphocytic leukemia. *Blood* 2009;113(19):4637-45.
59. Tong WG, Chen R, Plunkett W, Siegel D, Sinha R, Harvey RD, et al. Phase I and pharmacologic study of SNS-032, a potent and selective Cdk2, 7, and 9 inhibitor, in patients with advanced chronic lymphocytic leukemia and multiple myeloma. *Journal of clinical oncology : official journal of the American Society of Clinical Oncology* 2010;28(18):3015-22.
60. Rahmani M, Davis EM, Crabtree TR, Habibi JR, Nguyen TK, Dent P, et al. The kinase inhibitor sorafenib induces cell death through a process involving induction of endoplasmic reticulum stress. *Molecular and cellular biology* 2007;27(15):5499-513.
61. Yu C, Bruzek LM, Meng XW, Gores GJ, Carter CA, Kaufmann SH, et al. The role of Mcl-1 downregulation in the proapoptotic activity of the multikinase inhibitor BAY 43-9006. *Oncogene* 2005;24(46):6861-9.
62. Rahmani M, Davis EM, Bauer C, Dent P, Grant S. Apoptosis induced by the kinase inhibitor BAY 43-9006 in human leukemia cells involves down-regulation of Mcl-1 through inhibition of translation. *The Journal of biological chemistry* 2005;280(42):35217-27.

63. Schwickart M, Huang X, Lill JR, Liu J, Ferrando R, French DM, et al. Deubiquitinase USP9X stabilizes MCL1 and promotes tumour cell survival. *Nature* 2010;463(7277):103-7.
64. Sun H, Kapuria V, Peterson LF, Fang D, Bornmann WG, Bartholomeusz G, et al. Bcr-Abl ubiquitination and Usp9x inhibition block kinase signaling and promote CML cell apoptosis. *Blood* 2011;117(11):3151-62.
65. Askari FK, McDonnell WM. Antisense-oligonucleotide therapy. *The New England journal of medicine* 1996;334(5):316-8.
66. Muchmore SW, Sattler M, Liang H, Meadows RP, Harlan JE, Yoon HS, et al. X-ray and NMR structure of human Bcl-xL, an inhibitor of programmed cell death. *Nature* 1996;381(6580):335-41.
67. Oltersdorf T, Elmore SW, Shoemaker AR, Armstrong RC, Augeri DJ, Belli BA, et al. An inhibitor of Bcl-2 family proteins induces regression of solid tumours. *Nature* 2005;435(7042):677-81.
68. Chauhan D, Velankar M, Brahmandam M, Hideshima T, Podar K, Richardson P, et al. A novel Bcl-2/Bcl-X(L)/Bcl-w inhibitor ABT-737 as therapy in multiple myeloma. *Oncogene* 2007;26(16):2374-80.
69. Tagscherer KE, Fassel A, Campos B, Farhadi M, Kraemer A, Bock BC, et al. Apoptosis-based treatment of glioblastomas with ABT-737, a novel small molecule inhibitor of Bcl-2 family proteins. *Oncogene* 2008;27(52):6646-56.
70. Hann CL, Daniel VC, Sugar EA, Dobromilskaya I, Murphy SC, Cope L, et al. Therapeutic efficacy of ABT-737, a selective inhibitor of BCL-2, in small cell lung cancer. *Cancer research* 2008;68(7):2321-8.

71. Mason KD, Vandenberg CJ, Scott CL, Wei AH, Cory S, Huang DC, et al. In vivo efficacy of the Bcl-2 antagonist ABT-737 against aggressive Myc-driven lymphomas. *Proceedings of the National Academy of Sciences of the United States of America* 2008;105(46):17961-6.
72. Ni Chonghaile T, Letai A. Mimicking the BH3 domain to kill cancer cells. *Oncogene* 2008;27 Suppl 1:S149-57.
73. van Delft MF, Wei AH, Mason KD, Vandenberg CJ, Chen L, Czabotar PE, et al. The BH3 mimetic ABT-737 targets selective Bcl-2 proteins and efficiently induces apoptosis via Bak/Bax if Mcl-1 is neutralized. *Cancer cell* 2006;10(5):389-99.
74. Okumura K, Huang S, Sinicrope FA. Induction of Noxa sensitizes human colorectal cancer cells expressing Mcl-1 to the small-molecule Bcl-2/Bcl-xL inhibitor, ABT-737. *Clinical cancer research : an official journal of the American Association for Cancer Research* 2008;14(24):8132-42.
75. Keuling AM, Felton KE, Parker AA, Akbari M, Andrew SE, Tron VA. RNA silencing of Mcl-1 enhances ABT-737-mediated apoptosis in melanoma: role for a caspase-8-dependent pathway. *PloS one* 2009;4(8):e6651.
76. Zall H, Weber A, Besch R, Zantl N, Hacker G. Chemotherapeutic drugs sensitize human renal cell carcinoma cells to ABT-737 by a mechanism involving the Noxa-dependent inactivation of Mcl-1 or A1. *Molecular cancer* 2010;9:164.
77. Chen S, Dai Y, Harada H, Dent P, Grant S. Mcl-1 down-regulation potentiates ABT-737 lethality by cooperatively inducing Bak activation and Bax translocation. *Cancer research* 2007;67(2):782-91.

78. Gandhi L, Camidge DR, Ribeiro de Oliveira M, Bonomi P, Gandara D, Khaira D, et al. Phase I study of Navitoclax (ABT-263), a novel Bcl-2 family inhibitor, in patients with small-cell lung cancer and other solid tumors. *Journal of clinical oncology : official journal of the American Society of Clinical Oncology* 2011;29(7):909-16.
79. Rudin CM, Hann CL, Garon EB, Ribeiro de Oliveira M, Bonomi PD, Camidge DR, et al. Phase II study of single-agent navitoclax (ABT-263) and biomarker correlates in patients with relapsed small cell lung cancer. *Clinical cancer research : an official journal of the American Association for Cancer Research* 2012;18(11):3163-9.
80. Konopleva M, Watt J, Contractor R, Tsao T, Harris D, Estrov Z, et al. Mechanisms of antileukemic activity of the novel Bcl-2 homology domain-3 mimetic GX15-070 (obatoclax). *Cancer research* 2008;68(9):3413-20.
81. Li J, Viallet J, Haura EB. A small molecule pan-Bcl-2 family inhibitor, GX15-070, induces apoptosis and enhances cisplatin-induced apoptosis in non-small cell lung cancer cells. *Cancer chemotherapy and pharmacology* 2008;61(3):525-34.
82. Pan J, Cheng C, Verstovsek S, Chen Q, Jin Y, Cao Q. The BH3-mimetic GX15-070 induces autophagy, potentiates the cytotoxicity of carboplatin and 5-fluorouracil in esophageal carcinoma cells. *Cancer letters* 2010;293(2):167-74.
83. Heidari N, Hicks MA, Harada H. GX15-070 (obatoclax) overcomes glucocorticoid resistance in acute lymphoblastic leukemia through induction of apoptosis and autophagy. *Cell death & disease* 2010;1:e76.
84. Nguyen M, Marcellus RC, Roulston A, Watson M, Serfass L, Murthy Madiraju SR, et al. Small molecule obatoclax (GX15-070) antagonizes MCL-1 and overcomes MCL-1-

- mediated resistance to apoptosis. *Proceedings of the National Academy of Sciences of the United States of America* 2007;104(49):19512-7.
85. Schimmer AD, O'Brien S, Kantarjian H, Brandwein J, Cheson BD, Minden MD, et al. A phase I study of the pan bcl-2 family inhibitor obatoclax mesylate in patients with advanced hematologic malignancies. *Clinical cancer research : an official journal of the American Association for Cancer Research* 2008;14(24):8295-301.
  86. Paik PK, Rudin CM, Brown A, Rizvi NA, Takebe N, Travis W, et al. A phase I study of obatoclax mesylate, a Bcl-2 antagonist, plus topotecan in solid tumor malignancies. *Cancer chemotherapy and pharmacology* 2010;66(6):1079-85.
  87. Hwang JJ, Kuruvilla J, Mendelson D, Pishvaian MJ, Deeken JF, Siu LL, et al. Phase I dose finding studies of obatoclax (GX15-070), a small molecule pan-BCL-2 family antagonist, in patients with advanced solid tumors or lymphoma. *Clinical cancer research : an official journal of the American Association for Cancer Research* 2010;16(15):4038-45.
  88. Gilbert NE, O'Reilly JE, Chang CJ, Lin YC, Brueggemeier RW. Antiproliferative activity of gossypol and gossypolone on human breast cancer cells. *Life sciences* 1995;57(1):61-7.
  89. Wei J, Kitada S, Rega MF, Emdadi A, Yuan H, Cellitti J, et al. Apogossypol derivatives as antagonists of antiapoptotic Bcl-2 family proteins. *Molecular cancer therapeutics* 2009;8(4):904-13.
  90. Meng Y, Tang W, Dai Y, Wu X, Liu M, Ji Q, et al. Natural BH3 mimetic (-)-gossypol chemosensitizes human prostate cancer via Bcl-xL inhibition accompanied by increase of Puma and Noxa. *Molecular cancer therapeutics* 2008;7(7):2192-202.

91. Voss V, Senft C, Lang V, Ronellenfitsch MW, Steinbach JP, Seifert V, et al. The pan-Bcl-2 inhibitor (-)-gossypol triggers autophagic cell death in malignant glioma. *Molecular cancer research : MCR* 2010;8(7):1002-16.
92. Sung B, Ravindran J, Prasad S, Pandey MK, Aggarwal BB. Gossypol induces death receptor-5 through activation of the ROS-ERK-CHOP pathway and sensitizes colon cancer cells to TRAIL. *The Journal of biological chemistry* 2010;285(46):35418-27.
93. Pang X, Wu Y, Wu Y, Lu B, Chen J, Wang J, et al. (-)-Gossypol suppresses the growth of human prostate cancer xenografts via modulating VEGF signaling-mediated angiogenesis. *Molecular cancer therapeutics* 2011;10(5):795-805.
94. Le Blanc M, Russo J, Kudelka AP, Smith JA. An in vitro study of inhibitory activity of gossypol, a cottonseed extract, in human carcinoma cell lines. *Pharmacological research : the official journal of the Italian Pharmacological Society* 2002;46(6):551-5.
95. Heist RS, Fain J, Chinnasami B, Khan W, Molina JR, Sequist LV, et al. Phase I/II study of AT-101 with topotecan in relapsed and refractory small cell lung cancer. *Journal of thoracic oncology : official publication of the International Association for the Study of Lung Cancer* 2010;5(10):1637-43.
96. Ready N, Karaseva NA, Orlov SV, Luft AV, Popovych O, Holmlund JT, et al. Double-blind, placebo-controlled, randomized phase 2 study of the proapoptotic agent AT-101 plus docetaxel, in second-line non-small cell lung cancer. *Journal of thoracic oncology : official publication of the International Association for the Study of Lung Cancer* 2011;6(4):781-5.



97. Bagstrom MQ, Qi Y, Koczywas M, Argiris A, Johnson EA, Millward MJ, et al. A phase II study of AT-101 (Gossypol) in chemotherapy-sensitive recurrent extensive-stage small cell lung cancer. *Journal of thoracic oncology : official publication of the International Association for the Study of Lung Cancer* 2011;6(10):1757-60.
98. Sonpavde G, Matveev V, Burke JM, Caton JR, Fleming MT, Hutson TE, et al. Randomized phase II trial of docetaxel plus prednisone in combination with placebo or AT-101, an oral small molecule Bcl-2 family antagonist, as first-line therapy for metastatic castration-resistant prostate cancer. *Annals of oncology : official journal of the European Society for Medical Oncology / ESMO* 2012;23(7):1803-8.
99. Kitada S, Kress CL, Krajewska M, Jia L, Pellecchia M, Reed JC. Bcl-2 antagonist apogossypol (NSC736630) displays single-agent activity in Bcl-2-transgenic mice and has superior efficacy with less toxicity compared with gossypol (NSC19048). *Blood* 2008;111(6):3211-9.
100. Wei J, Stebbins JL, Kitada S, Dash R, Placzek W, Rega MF, et al. BI-97C1, an optically pure Apogossypol derivative as pan-active inhibitor of antiapoptotic B-cell lymphoma/leukemia-2 (Bcl-2) family proteins. *Journal of medicinal chemistry* 2010;53(10):4166-76.
101. Kazi A, Sun J, Doi K, Sung SS, Takahashi Y, Yin H, et al. The BH3 alpha-helical mimic BH3-M6 disrupts Bcl-X(L), Bcl-2, and MCL-1 protein-protein interactions with Bax, Bak, Bad, or Bim and induces apoptosis in a Bax- and Bim-dependent manner. *The Journal of biological chemistry* 2011;286(11):9382-92.
102. Yecies D, Carlson NE, Deng J, Letai A. Acquired resistance to ABT-737 in lymphoma cells that up-regulate MCL-1 and BFL-1. *Blood* 2010;115(16):3304-13.

103. Evans JD, Cornford PA, Dodson A, Greenhalf W, Foster CS, Neoptolemos JP. Detailed tissue expression of bcl-2, bax, bak and bcl-x in the normal human pancreas and in chronic pancreatitis, ampullary and pancreatic ductal adenocarcinomas. *Pancreatology : official journal of the International Association of Pancreatology* 2001;1(3):254-62.
104. Guoan X, Hanning W, Kaiyun C, Hao L. Adenovirus-mediated siRNA targeting Mcl-1 gene increases radiosensitivity of pancreatic carcinoma cells in vitro and in vivo. *Surgery* 2010;147(4):553-61.
105. Miyamoto Y, Hosotani R, Wada M, Lee JU, Koshiba T, Fujimoto K, et al. Immunohistochemical analysis of Bcl-2, Bax, Bcl-X, and Mcl-1 expression in pancreatic cancers. *Oncology* 1999;56(1):73-82.
106. Takahashi H, Chen MC, Pham H, Matsuo Y, Ishiguro H, Reber HA, et al. Simultaneous knock-down of Bcl-xL and Mcl-1 induces apoptosis through Bax activation in pancreatic cancer cells. *Biochimica et biophysica acta* 2013;1833(12):2980-7.
107. Quinn BA, Dash R, Azab B, Sarkar S, Das SK, Kumar S, et al. Targeting Mcl-1 for the therapy of cancer. *Expert opinion on investigational drugs* 2011;20(10):1397-411.
108. Wei J, Stebbins JL, Kitada S, Dash R, Zhai D, Placzek WJ, et al. An optically pure apogossypolone derivative as potent pan-active inhibitor of anti-apoptotic bcl-2 family proteins. *Frontiers in oncology* 2011;1:28.
109. Azab B, Dash R, Das SK, Bhutia SK, Shen XN, Quinn BA, et al. Enhanced delivery of mda-7/IL-24 using a serotype chimeric adenovirus (Ad.5/3) in combination with the Apogossypol derivative BI-97C1 (Sabutoclax) improves therapeutic efficacy in low CAR colorectal cancer cells. *Journal of cellular physiology* 2012;227(5):2145-53.

110. Dash R, Azab B, Quinn BA, Shen X, Wang XY, Das SK, et al. Apogossypol derivative BI-97C1 (Sabutoclax) targeting Mcl-1 sensitizes prostate cancer cells to mda-7/IL-24-mediated toxicity. *Proceedings of the National Academy of Sciences of the United States of America* 2011;108(21):8785-90.
111. Liu WT, Lin CH, Hsiao M, Gean PW. Minocycline inhibits the growth of glioma by inducing autophagy. *Autophagy* 2011;7(2):166-75.
112. Pourgholami MH, Ataie-Kachoei P, Badar S, Morris DL. Minocycline inhibits malignant ascites of ovarian cancer through targeting multiple signaling pathways. *Gynecologic oncology* 2013;129(1):113-9.
113. Pourgholami MH, Mekkawy AH, Badar S, Morris DL. Minocycline inhibits growth of epithelial ovarian cancer. *Gynecologic oncology* 2012;125(2):433-40.
114. Regen F, Heuser I, Herzog I, Hellmann-Regen J. Striking growth-inhibitory effects of minocycline on human prostate cancer cell lines. *Urology* 2014;83(2):509 e1-6.
115. Tang C, Yang L, Jiang X, Xu C, Wang M, Wang Q, et al. Antibiotic drug tigecycline inhibited cell proliferation and induced autophagy in gastric cancer cells. *Biochemical and biophysical research communications* 2014;446(1):105-12.
116. Kernt M, Neubauer AS, Eibl KH, Wolf A, Ulbig MW, Kampik A, et al. Minocycline is cytoprotective in human trabecular meshwork cells and optic nerve head astrocytes by increasing expression of XIAP, survivin, and Bcl-2. *Clinical ophthalmology* 2010;4:591-604.
117. Wang J, Wei Q, Wang CY, Hill WD, Hess DC, Dong Z. Minocycline up-regulates Bcl-2 and protects against cell death in mitochondria. *The Journal of biological chemistry* 2004;279(19):19948-54.

118. Zhu S, Stavrovskaya IG, Drozda M, Kim BY, Ona V, Li M, et al. Minocycline inhibits cytochrome c release and delays progression of amyotrophic lateral sclerosis in mice. *Nature* 2002;417(6884):74-8.
119. Lebedeva IV, Sarkar D, Su ZZ, Kitada S, Dent P, Stein CA, et al. Bcl-2 and Bcl-x(L) differentially protect human prostate cancer cells from induction of apoptosis by melanoma differentiation associated gene-7, mda-7/IL-24. *Oncogene* 2003;22(54):8758-73.
120. Dash R, Richards JE, Su ZZ, Bhutia SK, Azab B, Rahmani M, et al. Mechanism by which Mcl-1 regulates cancer-specific apoptosis triggered by mda-7/IL-24, an IL-10-related cytokine. *Cancer research* 2010;70(12):5034-45.
121. Venkatesan P, Puvvada N, Dash R, Prashanth Kumar BN, Sarkar D, Azab B, et al. The potential of celecoxib-loaded hydroxyapatite-chitosan nanocomposite for the treatment of colon cancer. *Biomaterials* 2011;32(15):3794-806.
122. Das SK, Bhutia SK, Azab B, Kegelman TP, Peachy L, Santhekadur PK, et al. MDA-9/syntenin and IGFBP-2 promote angiogenesis in human melanoma. *Cancer research* 2013;73(2):844-54.
123. Bissonnette N, Hunting DJ. p21-induced cycle arrest in G1 protects cells from apoptosis induced by UV-irradiation or RNA polymerase II blockage. *Oncogene* 1998;16(26):3461-9.
124. Canfield SE, Zhu K, Williams SA, McConkey DJ. Bortezomib inhibits docetaxel-induced apoptosis via a p21-dependent mechanism in human prostate cancer cells. *Molecular cancer therapeutics* 2006;5(8):2043-50.

125. Corcoran RB, Contino G, Deshpande V, Tzatsos A, Conrad C, Benes CH, et al. STAT3 plays a critical role in KRAS-induced pancreatic tumorigenesis. *Cancer research* 2011;71(14):5020-9.
126. Cowling V, Downward J. Caspase-6 is the direct activator of caspase-8 in the cytochrome c-induced apoptosis pathway: absolute requirement for removal of caspase-6 prodomain. *Cell death and differentiation* 2002;9(10):1046-56.
127. Lebedeva IV, Su ZZ, Vozhilla N, Chatman L, Sarkar D, Dent P, et al. Chemoprevention by perillyl alcohol coupled with viral gene therapy reduces pancreatic cancer pathogenesis. *Molecular cancer therapeutics* 2008;7(7):2042-50.
128. Bailey JM, Alsina J, Rasheed ZA, McAllister FM, Fu YY, Plentz R, et al. DCLK1 marks a morphologically distinct subpopulation of cells with stem cell properties in preinvasive pancreatic cancer. *Gastroenterology* 2014;146(1):245-56.
129. Courtin A, Richards FM, Bapiro TE, Bramhall JL, Neesse A, Cook N, et al. Anti-tumour efficacy of capecitabine in a genetically engineered mouse model of pancreatic cancer. *PloS one* 2013;8(6):e67330.
130. Li H, Yang AL, Chung YT, Zhang W, Liao J, Yang GY. Sulindac inhibits pancreatic carcinogenesis in LSL-KrasG12D-LSL-Trp53R172H-Pdx-1-Cre mice via suppressing aldo-keto reductase family 1B10 (AKR1B10). *Carcinogenesis* 2013;34(9):2090-8.
131. Rao CV, Mohammed A, Janakiram NB, Li Q, Ritchie RL, Lightfoot S, et al. Inhibition of pancreatic intraepithelial neoplasia progression to carcinoma by nitric oxide-releasing aspirin in p48(Cre/+)-LSL-Kras(G12D/+) mice. *Neoplasia* 2012;14(9):778-87.

132. Yip-Schneider MT, Wu H, Hruban RH, Lowy AM, Crooks PA, Schmidt CM. Efficacy of dimethylaminoparthenolide and sulindac in combination with gemcitabine in a genetically engineered mouse model of pancreatic cancer. *Pancreas* 2013;42(1):160-7.
133. Bardeesy N, Aguirre AJ, Chu GC, Cheng KH, Lopez LV, Hezel AF, et al. Both p16(Ink4a) and the p19(Arf)-p53 pathway constrain progression of pancreatic adenocarcinoma in the mouse. *Proceedings of the National Academy of Sciences of the United States of America* 2006;103(15):5947-52.
134. Moysan E, Bastiat G, Benoit JP. Gemcitabine versus Modified Gemcitabine: a review of several promising chemical modifications. *Molecular pharmaceutics* 2013;10(2):430-44.
135. Tandon M, Vemula SV, Mittal SK. Emerging strategies for EphA2 receptor targeting for cancer therapeutics. *Expert opinion on therapeutic targets* 2011;15(1):31-51.
136. Wang S, Placzek WJ, Stebbins JL, Mitra S, Noberini R, Koolpe M, et al. Novel targeted system to deliver chemotherapeutic drugs to EphA2-expressing cancer cells. *Journal of medicinal chemistry* 2012;55(5):2427-36.
137. Wang S, Noberini R, Stebbins JL, Das S, Zhang Z, Wu B, et al. Targeted delivery of paclitaxel to EphA2-expressing cancer cells. *Clinical cancer research : an official journal of the American Association for Cancer Research* 2013;19(1):128-37.
138. Hoy SM. Albumin-bound Paclitaxel: a review of its use for the first-line combination treatment of metastatic pancreatic cancer. *Drugs* 2014;74(15):1757-68.

139. Alvarez R, Musteanu M, Garcia-Garcia E, Lopez-Casas PP, Megias D, Guerra C, et al. Stromal disrupting effects of nab-paclitaxel in pancreatic cancer. *British journal of cancer* 2013;109(4):926-33.
140. Von Hoff DD, Ervin T, Arena FP, Chiorean EG, Infante J, Moore M, et al. Increased survival in pancreatic cancer with nab-paclitaxel plus gemcitabine. *The New England journal of medicine* 2013;369(18):1691-703.
141. Lebedeva IV, Sarkar D, Su ZZ, Gopalkrishnan RV, Athar M, Randolph A, et al. Molecular target-based therapy of pancreatic cancer. *Cancer research* 2006;66(4):2403-13.
142. Lebedeva IV, Washington I, Sarkar D, Clark JA, Fine RL, Dent P, et al. Strategy for reversing resistance to a single anticancer agent in human prostate and pancreatic carcinomas. *Proceedings of the National Academy of Sciences of the United States of America* 2007;104(9):3484-9.
143. Lebedeva IV, Su ZZ, Vozhilla N, Chatman L, Sarkar D, Dent P, et al. Mechanism of in vitro pancreatic cancer cell growth inhibition by melanoma differentiation-associated gene-7/interleukin-24 and perillyl alcohol. *Cancer research* 2008;68(18):7439-47.
144. Sarkar S, Azab BM, Das SK, Quinn BA, Shen X, Dash R, et al. Chemoprevention gene therapy (CGT): novel combinatorial approach for preventing and treating pancreatic cancer. *Current molecular medicine* 2013;13(7):1140-59.
145. Sarkar S, Azab B, Quinn BA, Shen X, Dent P, Klivanov AL, et al. Chemoprevention gene therapy (CGT) of pancreatic cancer using perillyl alcohol and a novel chimeric serotype cancer terminator virus. *Current molecular medicine* 2014;14(1):125-40.

146. Deer EL, Gonzalez-Hernandez J, Coursen JD, Shea JE, Ngatia J, Scaife CL, et al. Phenotype and genotype of pancreatic cancer cell lines. *Pancreas* 2010;39(4):425-35.
147. Guerra C, Barbacid M. Genetically engineered mouse models of pancreatic adenocarcinoma. *Molecular oncology* 2013;7(2):232-47.
148. Westphalen CB, Olive KP. Genetically engineered mouse models of pancreatic cancer. *Cancer journal* 2012;18(6):502-10.
149. Brader P, Serganova I, Blasberg RG. Noninvasive molecular imaging using reporter genes. *Journal of nuclear medicine : official publication, Society of Nuclear Medicine* 2013;54(2):167-72.
150. O'Farrell AC, Shnyder SD, Marston G, Coletta PL, Gill JH. Non-invasive molecular imaging for preclinical cancer therapeutic development. *British journal of pharmacology* 2013;169(4):719-35.
151. Klerk CP, Overmeer RM, Niers TM, Versteeg HH, Richel DJ, Buckle T, et al. Validity of bioluminescence measurements for noninvasive in vivo imaging of tumor load in small animals. *BioTechniques* 2007;43(1 Suppl):7-13, 30.
152. Kang JH, Chung JK. Molecular-genetic imaging based on reporter gene expression. *Journal of nuclear medicine : official publication, Society of Nuclear Medicine* 2008;49 Suppl 2:164S-79S.
153. Bhang HE, Gabrielson KL, Laterra J, Fisher PB, Pomper MG. Tumor-specific imaging through progression elevated gene-3 promoter-driven gene expression. *Nature medicine* 2011;17(1):123-9.



154. Bhatnagar A, Wang Y, Mease RC, Gabrielson M, Sysa P, Minn I, et al. AEG-1 Promoter-Mediated Imaging of Prostate Cancer. *Cancer research* 2014;74(20):5772-81.
155. Chen Y, Du XY. Functional properties and intracellular signaling of CCN1/Cyr61. *Journal of cellular biochemistry* 2007;100(6):1337-45.
156. Minn I, Menezes ME, Sarkar S, Yarlagadda K, Das SK, Emdad L, et al. Molecular-genetic imaging of cancer. *Advances in cancer research* 2014;124:131-69.
157. Lau LF. CCN1/CYR61: the very model of a modern matricellular protein. *Cellular and molecular life sciences : CMLS* 2011;68(19):3149-63.
158. Zuo GW, Kohls CD, He BC, Chen L, Zhang W, Shi Q, et al. The CCN proteins: important signaling mediators in stem cell differentiation and tumorigenesis. *Histology and histopathology* 2010;25(6):795-806.
159. Leask A. CCN1: a novel target for pancreatic cancer. *Journal of cell communication and signaling* 2011;5(2):123-4.
160. Haque I, Mehta S, Majumder M, Dhar K, De A, McGregor D, et al. Cyr61/CCN1 signaling is critical for epithelial-mesenchymal transition and stemness and promotes pancreatic carcinogenesis. *Molecular cancer* 2011;10:8.
161. Placzek WJ, Sturlese M, Wu B, Cellitti JF, Wei J, Pellecchia M. Identification of a novel Mcl-1 protein binding motif. *The Journal of biological chemistry* 2011;286(46):39829-35.
162. Shiraiwa T, Kaneto H, Miyatsuka T, Kato K, Yamamoto K, Kawashima A, et al. Establishment of a non-invasive mouse reporter model for monitoring in vivo pdx-1 promoter activity. *Biochemical and biophysical research communications* 2007;361(3):739-44.

163. Richter JR, Mahoney M, Warram JM, Samuel S, Zinn KR. A dual-reporter, diagnostic vector for prostate cancer detection and tumor imaging. *Gene therapy* 2014;21(10):897-902.
164. Warram JM, Borovjagin AV, Zinn KR. A genetic strategy for combined screening and localized imaging of breast cancer. *Molecular imaging and biology : MIB : the official publication of the Academy of Molecular Imaging* 2011;13(3):452-61.